REGULATION OF DRUG DELIVERY FROM POROUS POLYMER MATRICES USING OSCILLATING MAGNETIC FIELDS

by

ELAZER REUVEN EDELMAN

S.B. Massachusetts Institute of Technology (1978)

S.M. Massachusetts Institute of Technology (1979)

M.D. Harvard Medical School (1983)

SUBMITTED IN PARTIAL FULFILLMENT
OF THE REQUIREMENTS FOR THE
DEGREE OF

DOCTOR OF PHILOSOPHY
in
MEDICAL ENGINEERING AND MEDICAL PHYSICS

at the
MASSACHUSETTS INSTITUTE OF TECHNOLOGY

September 1984

Signature of Author: _____
Department of Medical Engineering and Medical Physics
15 June 1984

Certified by: _____
Robert S. Langer
Thesis Supervisor

Certified by: _____
Ernest G. Cravahlo
Chairman, Division Committee on Graduate Thesis

This doctoral thesis has been examined by a committee of the Department of Medical Engineering and Medical Physics as follows:

Professor Robert Langer

Professor Judah Folkman

Professor Alan Grodzinsky

Professor Joel Habener

ELAZER R. EDELMAN

Medical Engineering and Medical Physics Program:
Harvard-MIT Division of Health, Sciences and Technology

REGULATION OF DRUG DELIVERY FROM POLYMER MATRICES USING OSCILLATING MAGNETIC FIELDS

A demand responsive polymer matrix based drug delivery system was developed. Small magnets were embedded within a matrix of ethylene - vinyl acetate copolymer and drug. When oscillating magnetic fields were applied the rate of drug release could be increased 15 fold. The critical parameters that governed release were examined, and the following conclusions were obtained.

(1) The response to the magnetic field was instantaneous, remained stable for as long as the field was applied, and returned exactly to baseline immediately after the field was withdrawn.

(2) The increase in release was directly proportional to the field amplitude, from 200 to 600 G, and to the frequency of field oscillation, from 0.5 to 60 Hz.

(3) Modulation increased with increasing size and strength of the embedded magnets.

(4) The matrix embedded magnet could be seen in magnified video taped images to move, apparently alternatingly compressing and dilating ajacent matrix material. At a distance 1.5 mm from the magnet surface no movement of the matrix could be detected.

(5) Modulation from a cylindrically shaped matrix was a function of the size of the matrix and there appeared to be a critical size, above and below which the enhanced release was lessened. The radius of this critical volume was on the order of 1.5 mm plus the radius of the magnet.

(6) Microtome sections of matrices (30-33% by weight bovine serum albumin, 150-180 micron particle size) embedded with magnets and exposed to oscillating magnetic fields, reveal that the pores adjacent to the magnet were broken open, with a greater porosity (43%) than peripheral areas of the matrix (31%). In addition, after release had been terminated pockets of drug could be found far from the magnet, while, the areas around the magnet were completely cleared of drug.

Models were developed to explain the modulated release on both a macroscopic and microscopic level. The macroscopic model established a sphere of influence of the magnet on the matrix, corresponding to the decrease in effect with increasing distance from the magnet. When the volume of the matrix and this sphere coincided, modulation ability was optimized. If there was insufficient matrix around the magnet or substantially more matrix than could be acted on by the magnet, modulation was attenuated. The data obtained from matrices embedded with two types of magnets fit this theory (R^2 = 0.98, 0.94). The second model, incorporated Taylor diffusion to explain enhanced flow through small channels subjected to pulsatile pressure. This theory predicted the relationship between field frequency and the extent of modulation and was statistically indistinquishable from the actual data ($p>0.05$).

Thesis committee: Prof. Robert Langer, chairman
Prof. Judah Folkman
Prof. Alan Grodzinsky
Prof. Joel Habener

ACKNOWLEDGMENTS

The completion of this thesis was possible only because of the guidance, patience and love extended to me by many people.

Professor Robert Langer was an inspirational force in the research. He granted me a great deal of freedom, but never let me stray too far from relevance and reality. He taught me to think and communicate. Professor Judah Folkman not only supported my work in his Department of Surgical Research at Children's Hospital, but also took special interest in my research and my career. I shall be forever indebted to him. Professor Alan Grodzinsky taught me the basics of semiconductor physics, the rigor of electromagnetics and transport phenomena, and the 'joy of continuum dynamics'. He has been unselfish with his time and the facilities in his laboratory. Professor Joel Habener has had the patience and tolerance to review and guide this research from its crudest forms. His critique and insight were always sought out. Professors James Melcher and Ioannis Yannas served on my qualifying committee, and offered valuable advice. Professor Ernest Cravahlo's foresight and advice made these past two years feasible, and his insightful questions on the fluid dynamics problems in this work prompted the development of a good part of the model. Dr. Larry Brown was my closest friend and colleague, and I consistently drew on his talents and expertise in all fields of science and research.

I have been blessed with the aid of many talented coworkers. Heidi Bobeck was at times my hands and my voice. Her diligence and ingenuity contributed to the success of many experiments. John Taylor approached every problem with calm and creativity. Scott Bercelli, Dan Flores, Stephen Scaringe, Raj Aggarwal and Wayne Rubenstein all devoted great time and effort. Drs. William Rhine, Rajan Bawa, Ron Siegel and Andrew Braunstein helped me get started and were always available to discuss any aspect of the work. Dr. Yosi Kost performed the electronmicroscopy, and offered valuable advice in experimental design and analysis. Dr. Howard Bernstein help me to solve integrals, review papers, and with Drs. Margaret Wheately, Judy Sudhalter, Joanne Murray, Joachim Kohn and Ross Feldberg maintain my sanity. Dr. Terry Hsu, Enora Kunica, and Jackie Wolfram were constantly called on for help with issues of polymer and material science. Eliot Frank gave a great deal of time and patience in demonstrating and trouble shooting the DYNASTAT. Drs. Michael McCarthy and David Soong first proposed the form of the microscopic model of enhanced release, and collaborated on further work along those lines.

Drs. Will Gilbert and Frank Kulash made the computer system less of a mystery. Drs. Chuck Rosenblatt, Richard Frankel, and Roshan Aggarwal provided acess to important equipment, and clarified some of the more difficult concepts in magnetism. Pam Phillips and the entire animal facility staff helped with the *in vivo* experiments, and Stella Hetelekidis repeatedly demonstrated surgical techniques. Pam Brown, Polly Breen, Anna Piccolo, Virginia Safford and Ron Johns smoothed out the administrative details and headaches.

I cannot finish my formal education at MIT without thanking Professor Laurence Young, Dr. Chuck Oman, Dr. Alan Natapoff, Bob Renshaw, Earl Wassmouth, and Al Shaw. They helped a wide-eyed freshman become a wide-eyed graduate student, and have provided continuous support through my decade at the Institute. I must also thank Dr. Irving London for answering the phone call of an interested 15 year old, and telling him to learn to work and think, and graduate high school before applying to HST. He has always had the time and the perspective.

I am especially obliged to Dr. Karl Skorecki, who has had the greatest impact on my medical education and who persuaded me to finish this work. I cannot adequately thank him for his patience and concern, for sharing his knowledge and philosophy of medicine, and above all his friendship.

Finally, my parents and brothers, Teddy, Raphael and Daniel, put up with all the crises and catastrophes, imaginary and real, from little league to medical and graduate school.

The National Institute of Health, the Juvenile Diabetes Foundation, and the Surdna Fellowship Foundation supported this research.

To my wife Cheryl, for everything.

page

TABLE OF CONTENTS

page

LIST OF FIGURES

page

LIST OF TABLES

CHAPTER I: POLYMER-BASED DRUG DELIVERY SYSTEMS

I.1 SUSTAINED RELEASE

I.1.1 Introduction Periodic ingestion or administration of drugs is an inefficient and potentially dangerous mode of therapy. Metabolic and degradative processes may lower drug concentrations into the ineffective, subtherapeutic range, while boluses of drug may elevate titers to toxic levels. To achieve more desirable patterns of drug administration, various means of sustaining drug release have been explored. One approach has been the incorporation of drug in solid polymers. In the initial studies, drugs were placed inside the lumen of dialysis [1] or silicone rubber tubing [2]. This type of device is known as a reservoir system because a saturated solution of drug is encapsulated by a polymeric membrane (figure 1.a). Since the coefficient of diffusion of drugs through the polymer material is much lower than through water the release of drugs from reservoir devices is prolonged. As long as the interior drug solution is held at the saturation concentration a constant rate of drug release is observed [3]. Devices are available for the sustained administration of such low molecular weight drugs as nitroglycerin, scopolamine, progesterone and pilocarpine[4,5]. However, reservoir devices are difficult to make and potentially dangerous. If the containing polymer membrane ruptures, the entire contents of the system will be released with great potential toxicity. More importantly, the surrounding membrane is only permeable to those macromolecules whose radii are smaller than the characteristic distance between polymer strands in

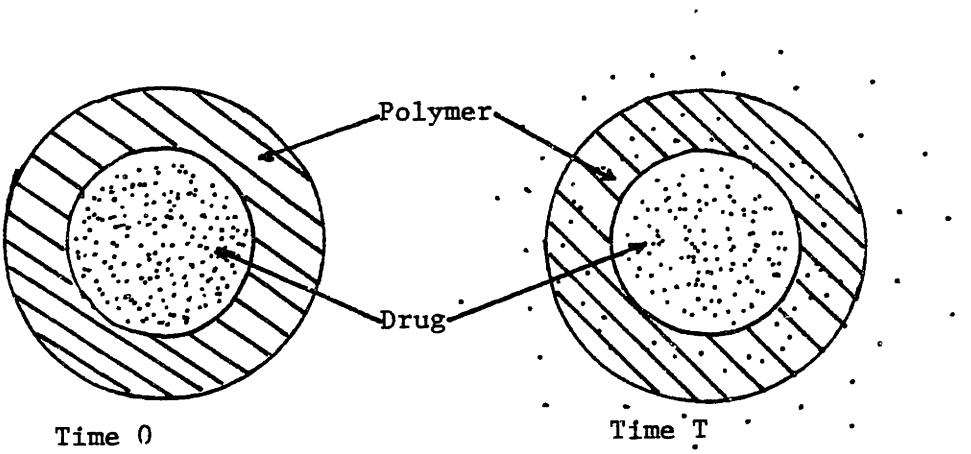

Figure 1.a Schematic diagram of diffusion-controlled reservoir type polymer based drug delivery system [32].

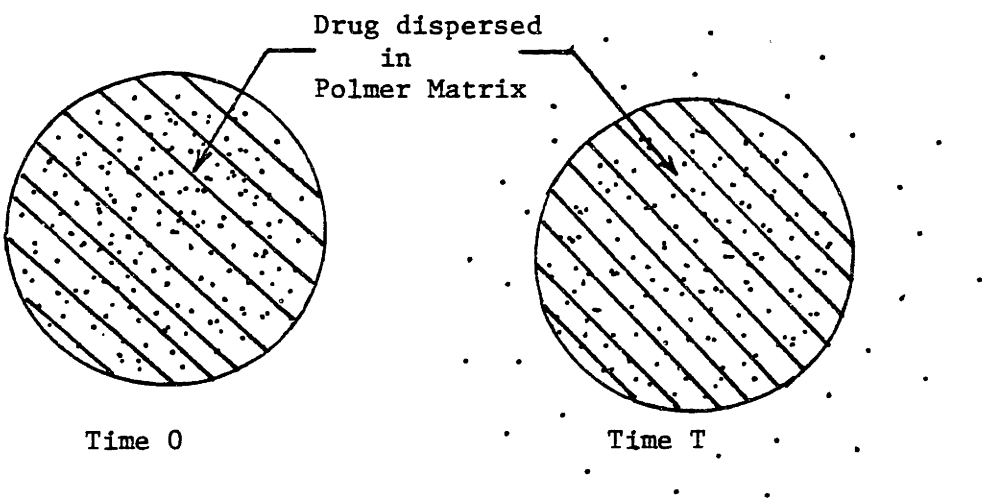

Figure 1.b Schematic diagram of a diffusion-controlled matrix type polymer based drug delivery system [32].

the surrounding membrane. This constrains the use of reservoir systems to a small class of drugs with low molecular weights.

In the 1970's Langer and Folkman incorporated the drug to be delivered within the membrane that was in communication with the environment [6]. This monolithic or matrix device can be used with virtually any size macromolecule (figure 1.b). The polymer material was dissolved by an organic solvent and the drugs or macromolecules added to this solution in their dry, powdered form(figure 2). The drugs were insoluble in the organic solvent and remained intact in the suspension. The suspension was poured into a glass mold that had been resting on dry ice. This created a matrix of polymer and homogeneously dispersed drug(figure 3).

I.1.2 Particle Size and Loading The size of the dry particles determined the size of the pores in which the drug resided and through which it had to pass to be released from the matrix. If the drug powder was seived to narrow ranges of particle sizes, a narrow range of pore sizes were created. This contributed to reproducible release kinetics [7].

The drug loading was defined as the weight of the drug relative to the weight of the entire polymer and drug matrix. The higher the loading the greater the number of pores. Figures 4.a and 4.b illustrate the effects of particle size and loading on the release kinetics of BSA. The abcissa is the square root of time and the ordinate is the cumulative fraction of drug released. This fraction was obtained by dividing the amount of drug released up to a point in time by the total amount of drug

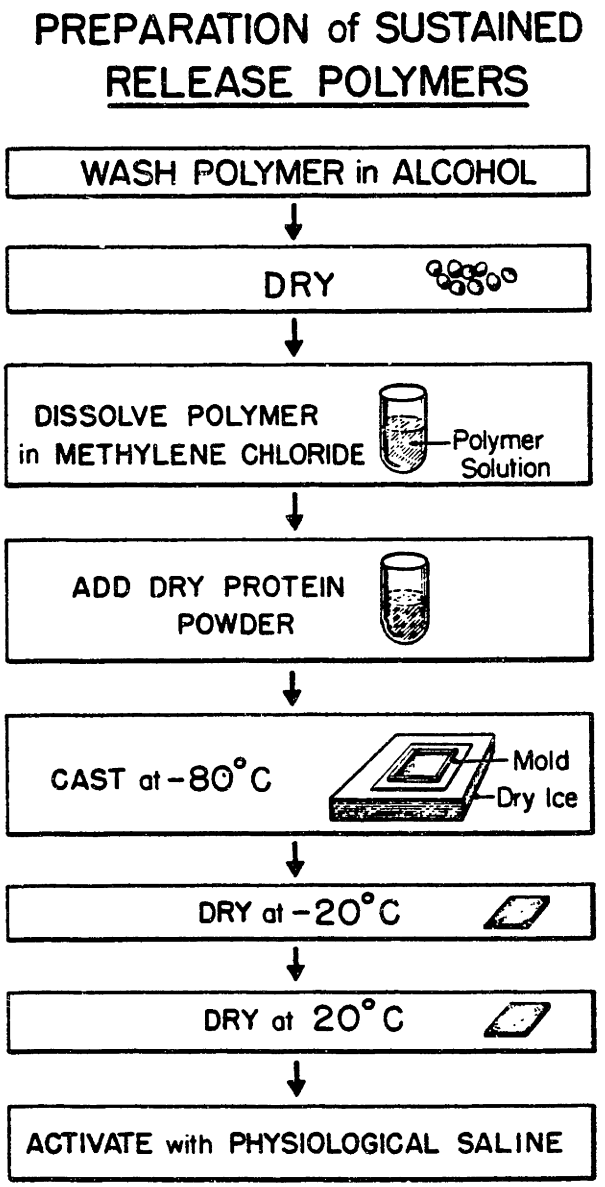

Figure 2: Flow diagram summary of the procedure for fabricating polymer matrices uniformly dispersed with a macromolecular substance [7].

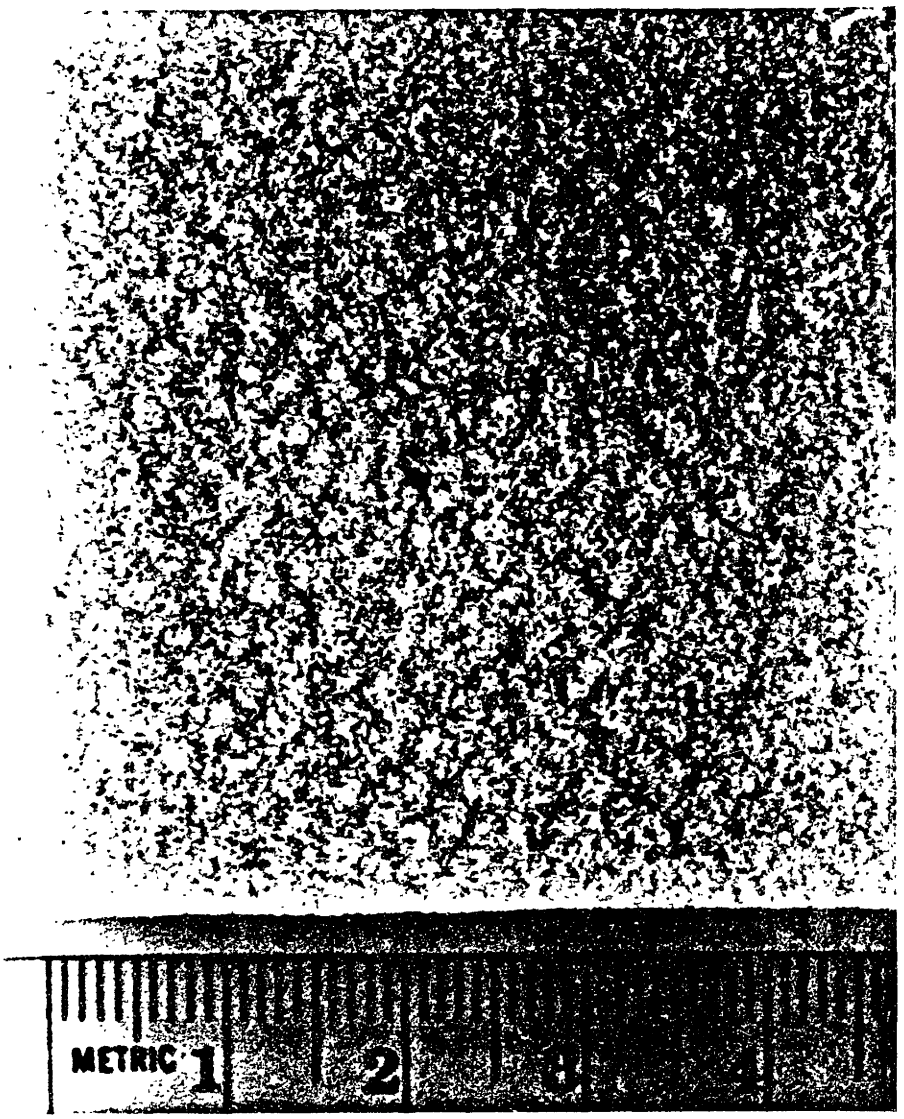

Figure 3: Typical slab matrix of ethylene - vinyl acetate with homogeneously dispersed bovine serum albumin [7].

intially incorporated into the matrix. As the particle size increased so did the amount released from the matrix. The amount of drug released and the rate at which it is released increased as the loading increased. At lower loadings and particle sizes some of the drug was never released from the matrix.

I.1.3 pH and Temperature Release kinetics from the matrices were sensitive to the pH of the media in which the matrix was releasing [7]. At or near the isoionic point of BSA, 5.2 [8], release rates were at a minimum. On either side of pH 5 the release rates increased.

They also found that long term exposure to different temperatures led to differences in kinetics. If matrices were kept at different temperatures for the duration of a release experiment, higher release rates were observed at the higher temperatures. It is noteworthy that only prolonged exposure to the elevated temperatures produced this difference; periodic exposures to different temperature did not change release rates (see section II.3.2).

An activation energy of 4.5 kcal/mole was derived from an Arrhenius plot of the log of the slope of the release curves versus the inverse of the temperature. This was almost identical for the activation energy derived from the same type of plot for BSA in water [9], and it was therefore concluded that the release of BSA from the matrices is diffusion controlled.

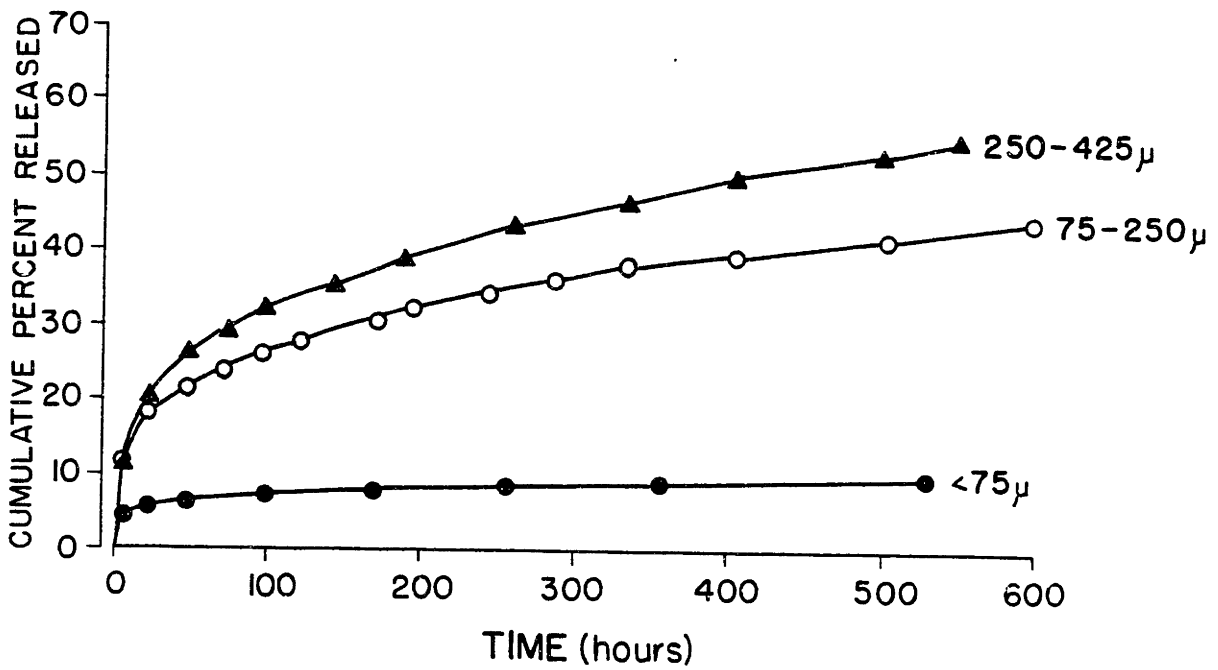

Figure 4.a: The amount of drug released relative to the amount initially dispersed in an EVAc matrix is plotted versus the square root of time [7]. The three curves represent the results obtained from matrices made with BSA sieved to three ranges of particle sizes.

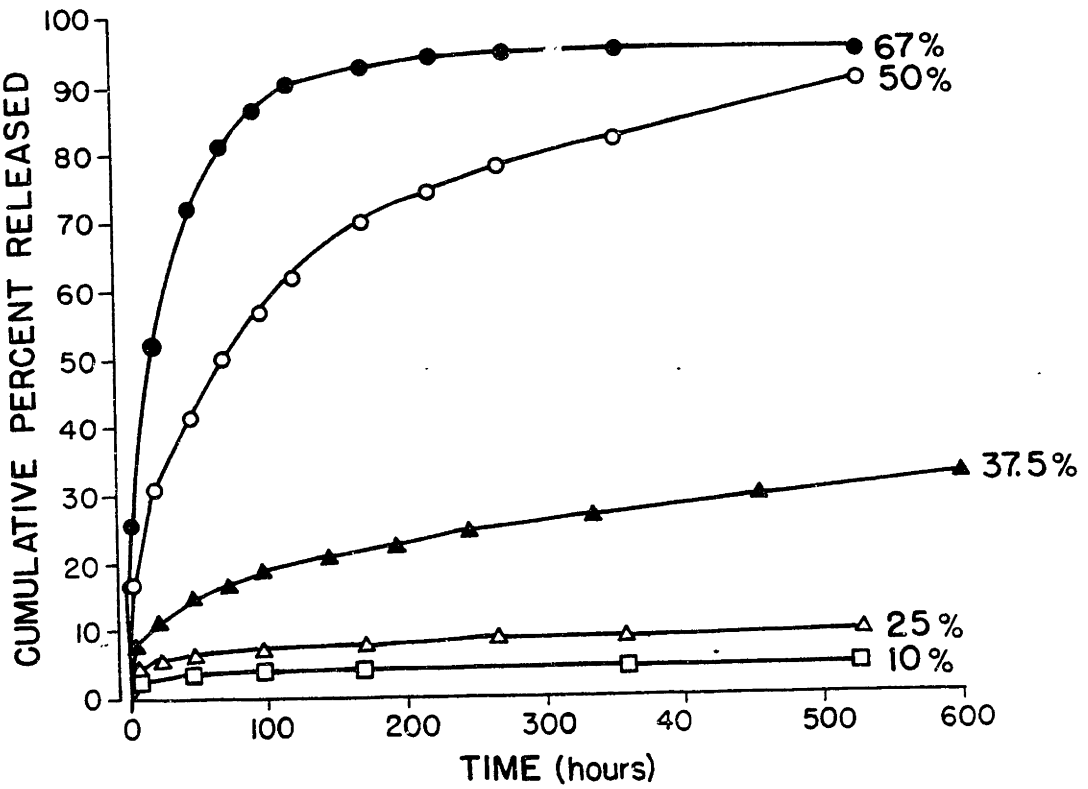

Figure 4.b: The amount of drug released relative to the amount initially dispersed in an EVAc matrix is plotted versus the square root of time [7]. The five curves represent the results obtained from matrices fabricated with five different ratios of BSA to EVAc.

I.2 Sustained Release of Macromolecules in vivo

Numerous potential applications for sustained release exist in all fields of science and technology. Indeed, there are already over 100 papers published describing the use of the EVAc for macromolecule delivery in some form. Table I below lists a number of *in vivo* applications of this technology in organisms ranging from cells to large animals. Murray and her associates studied the effect of sustained release of epidermal growth factor on cell growth [10] and Bergman *et. al.* used these systems as the source of a variety of chemoactive agents in one arm of a maze. Planaria and Dugesia dortocephala worms and the bacterium, Escheria Coli, placed in this maze consistently migrated to the arm with the matrix[11] . An EVAc matrix releasing bovine serum albumin induced an immune reponse that was superior to or better than the conventional method of immunization; two injections of BSA emulsified in complete Freund's adjuvant [12]. Moskowitz used these polymer matrices to release the marker enzyme horseradish peroxidase for histochemical localization of sensory nerve pathways surrounding large cerebral arteries in cats [13]. A series of studies were conducted to isolate both a factor that stimulates the growth of nutrient vessels to vascular tumors and an inhibitor to this factor [14-15]. After various isolates were obtained they were embedded in a matrix and placed adjacent to tumors *in vivo*. If the substances had been injected instead, they would have diffused away from the injection site. Anderson has already reported on the constant infusion of antibiotics from a silicon rubber ring surrounding an artificial heart valve [16]. Levy has recently embedded

TABLE I: *IN VIVO* APPLICATIONS OF CONTROLLED RELEASE

organism	macromolecule	ref.	purpose
cells	EGF	10	cell culture
bacteria	chemoatxis	11	bacteriology
C57 mice	antigens	12	immuniziation
cats	horseradish peroxidase	13	histological staining
rabbits	tumor angiogensis factor & inhibitor	14,15	tumor inhibition
rats	diphosphonate	17	inhibit calcification prosthetic heart valves
rats	inulin	20	monitor release from delivery devices
rats	insulin	21	diabetes mellitus

ethane-1-hydroxy-1,1 diphosphonate (EHDP), a calcium crystallization inhibitor, to prevent calcification of bioprosthetic heart valves. Systemic administration of EHDP is associated with hypercalcemia and its asscoiated side effects. Sustained release from EVAc matrices, on the other hand, has kept implanted heterologous heart valves free of calcifications for more than 84 days without altering serum calcium from normal values [17]. The monitoring of the sustained release of macromolecules *in vivo* is now made possible through the use of tracer quantities of [^{3}H]inulin. Inulin is a polysacharride that is neither metabolized or excreted by renal tubules. Once absorbed into the bloodstream it is completely excreted in the urine [18]. Furthermore, when embedded in matrices in tracer quantities along with other macromolecules the rate of inulin release matches the release of the other macromolecule identically [19]. Thus, the collection and quantitation of inulin in the urine of animals implanted with an EVAc matrix can be used to study the *in vivo* release kinetics from this device [20]. Diabetes mellitus has long been the focus of intense research in this field. Brown has studied many of the important factors that influence the sustained release of insulin and has been able to maintain normoglycemia in diabetic rats for over 4 months with a single 0.06 cm diameter matrix [21]. Figure 5 presents the data he obtained in three groups of rats. The first, normal rats, had blood sugars that stayed about 117 $\pm$ 5 mg/dl for the duration of the 120 day experiment. The group of rats that were made diabetic with the injection of streptozotocin had persistently elevated blood sugars to about 500 mg/dl. In contrast, the blood sugars of those rats that were 'treated' with EVAc matrices containing insulin were

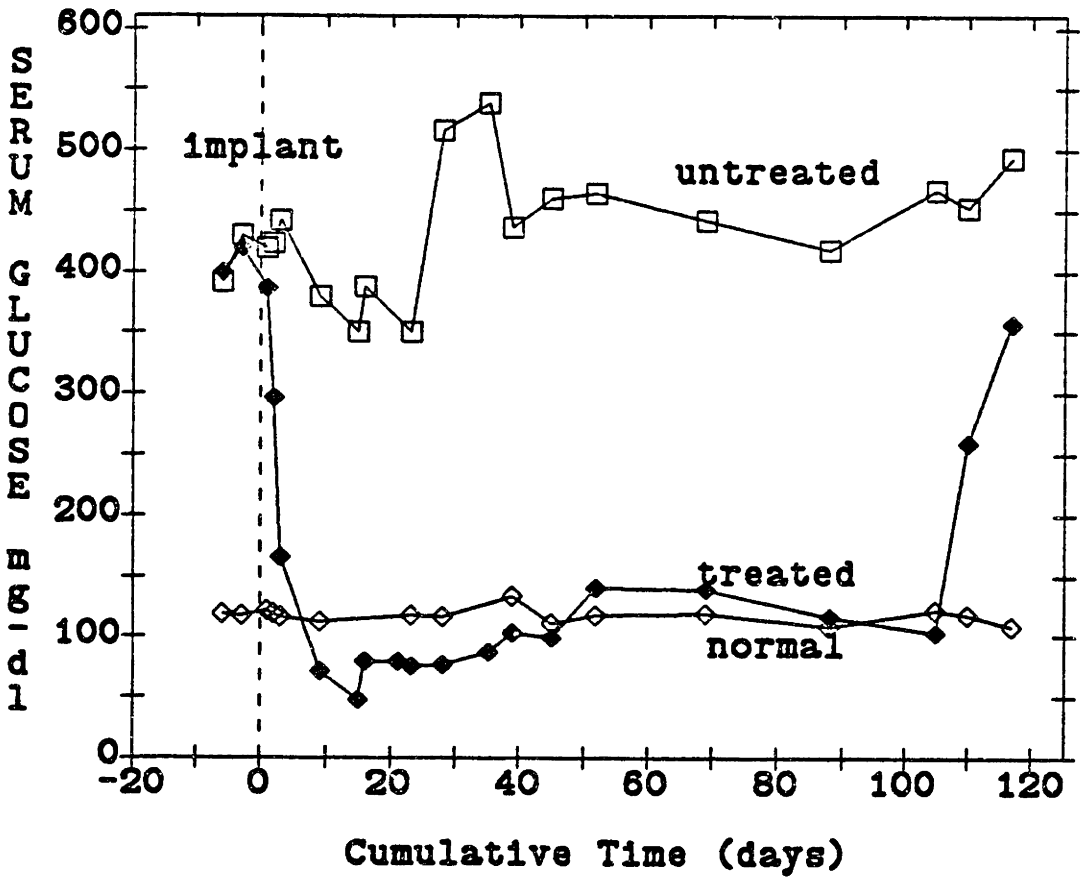

Figure 5: Plasma glucose levels in mg/dl for three groups of rats. The normal rats maintained a stable plasma glucose of 117 mg/dl. Two groups were made diabetic with streptozotocin and both exhibited elevated blood sugars. The group that received polymer matrices containing insulin had their serum glucose levels brought into or below the normal range [21].

maintained between 50 and 100 mg/dl for over 120 days. At that time the release of the drug from the matrices started to decrease below metabolic requirements and blood sugars rose accordingly. Just as multiple daily injections of insulin and pump delivery of the hormone have failed to suppress all the adverse effects of diabetes mellitus, examination of the diurinal variation in blood sugars reveals that these polymers did not achieve the ultimate in diabetic care. When blood was drawn from the normal and treated groups of rats every 2 hours throughout a day the daily pattern of serum glucose was revealed. The normal rats had fairly stable levels, but the treated ones did not. As depicted in figure 6 their blood sugars before meals were lower than normal, and were higher than normal following meals. This arose because the polymer matrices were excreting insulin at constant or decreasing release rates. When the carbohydrate load decreased an abundance of insulin existed and blood sugars fell below normal. In contrast, after the rats ate their lights out meal they required additional insulin, but the rate of release was constant and their blood sugars rose. This is but one instance where sustained release is necessary but not sufficient and where a more ideal drug delivery system would be one that responded to physiologic or metabolic demand.

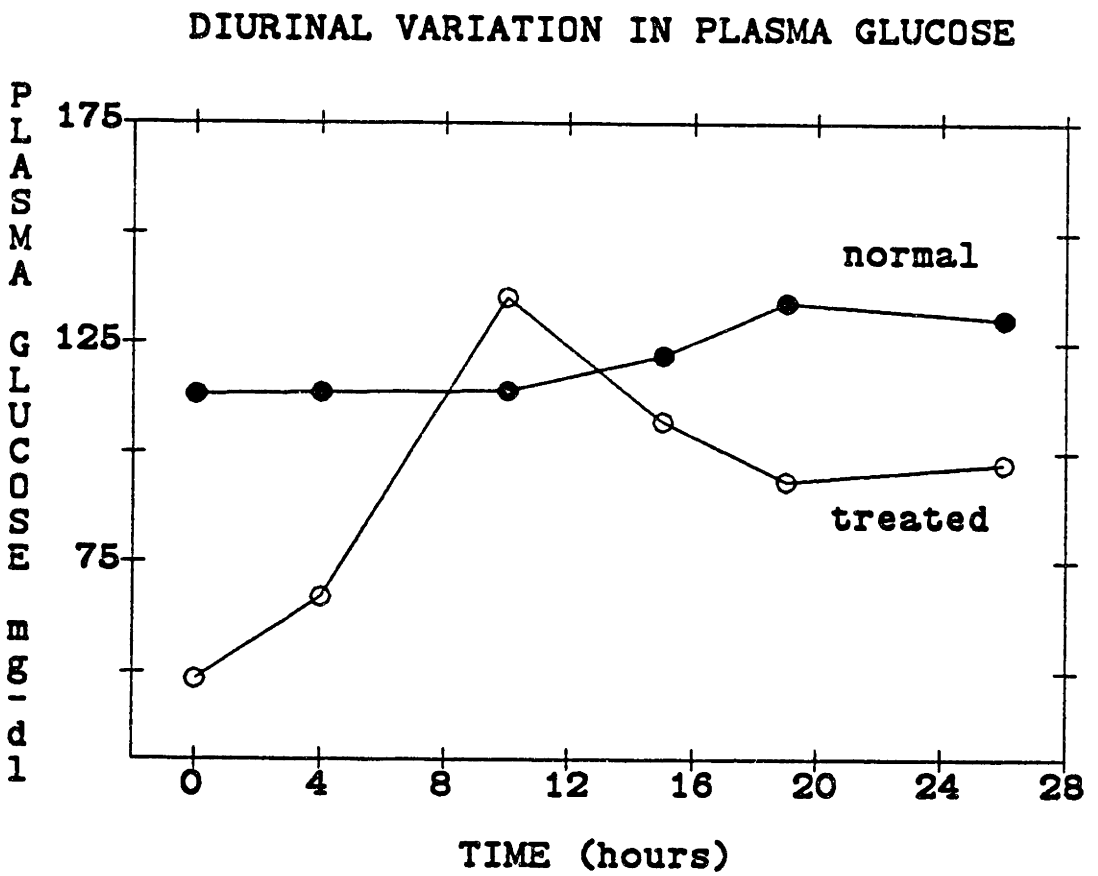

Figure 6: Diurinal variation on plasma glucose for the normal group of rats and a group of rats that was made diabetic with streptozotocin injection. Both groups of animals started to feed at about the time that the lights were turned off. In the normals blood glucoses rose very slightly. The diabetic group showed a wide swing throughout the day [21].

I.3 Demand Delivery

Diabetes mellitus is far from the only disease state where the delivery of drugs upon demand might be beneficial. A list of some potential clinical scenarios where such release would be desirable is provided in table II. Parathormone(PTH) and calcitonin act in a push-pull fashion to control calcium levels much like the carbohydrate regulatory system. A matrix delivery system might release PTH in a sustained fashion and calcitonin upon demand. Gastric acid inhibitors for ulcer control and pancreatic enzyme supplementation are required at times of stress and meals and though they are given on a chronic basis, should not be administered continuously. The synchronization of chemotherapy with other modes of cancer treatment might be provided by a polymer based demand delivery system and drugs for the control of chronic pain or seizures provided in the same fashion. Finally, there are times when the therapy for one disease may aggravate another. Careful selective administration of drugs is required, for example, in the case of asthmatics suffering from heart disease. A polymer matrix or a series of matrices containing anti-anginal, antiarrythmic and anti-asthmatic drugs might be implanted *in vivo* and release turned on and off as required.

The bulk of the systems now being considered for demand release utilize a mechanical pump, not polymer membranes. The pumps are large and costly, but offer precise control of the rate of drug release and can release drug directly into the bloodstream. In addition, some pumps are refillable.

TABLE II: CLINICAL SCENARIOS REQUIRING DEMAND DELIVERY

Metabolic-Endocrine:	insulin
	PTH - calcitonin
Gastrointestinal:	gastric acid inhibitors
	pancreatic enzymes
Oncology:	synchronized therapy
Neurology:	seizure disorders
	chronic pain
Cardiovascular:	anti-anginals
	anti-arrythmics
	selective
	blockade
Respiratory:	asthma

Externally worn and internally implanted pumps have been developed to generate a pressure gradient that leads to bulk flow of a solution through a small orifice. This pressure difference can be established by pressurizing a drug reservoir, by osmotic action, or by direct mechanical actuation. Alterations in the driving pressure difference leads to alterations in drug release. In the simplest case, this involves resetting the velocity of a driver that propels the plunger of a syringe pump and, in the most complex, includes sophisticated telemetry originally developed for satellite communication.

Despite the anticipated precision there remains a number of disadvantages to pump devices. Reports of increased incidence of sudden death in diabetic patients on insulin pumps[22] have been attributed to chance [23], but concern regarding the potential danger of these devices remains. The presence of complex 'moving parts' dictates a great deal of quality control, and make the pumps bulky, costly, unsightly and annoying to wear. Polymer based systems are safer and smaller but have been difficult to make sensitive to demand. Once release has commenced it cannot be externally controlled.

Recently there have been a number of proposals for the increase in release from polymer matrices upon demand by the alteration of the internal energy of these membranes by an external energy source. Three types of energy have been employed: electric, magnetic and ultrasonic. These thesis describes the development of the second of these systems.

I.3.1. Electric Grodzinsky and associates have proposed modulation of drug permeation through a charged polymer membrane by alteration of the electric charge on the membrane [24]. They have theorized that the membrane equilibrium morphology is dictated by two opposing forces. Electrical charges on crosslinked polymer strands tend to cause the strands to repel each other, while the crosslinking establishes a mechanical restraining force. When the charge on the strands is altered by the application of an electric field to the membrane, or by changinging the pH of the solution surrounding the membrane the equilibrium between the two forces is disturbed. If the electrical charge is increased the strands will be repelled farther apart, the membrane will swell and the

permeability will increase. On the other hand, just the opposite should occur if the net charge is diminshed. In this case the restraining force will predominate and the membrane will shrink, becoming less permeable. Using membranes made of poly-methyl acrylic acid they have been able to increase the permeability of compounds such as dextrans (mw 1000) by as much as 30 fold [25].

I.3.2 Magnetic In a series of reports Hsieh and associates demonstrated that when small magnetic spheres or cylinders were embedded within polymer matrices impregnated with bovine serum albumin (BSA), rates of BSA release could be increased by the application of an oscillating magnetic field to these samples [26,27]. However, the net increase above baseline was about 60 % and the standard errors about the mean were almost 100% (figure 6). Furthermore, there was no clear understanding of the mechanism of the control.

I.3.3 Ultrasonic Based on this work with magnetic fields and the improvements that followed, Kost and Leong developed a technique for controlling the rate of erosion of a PCPP polymer matrix with the application of ultrasonic fields [28].

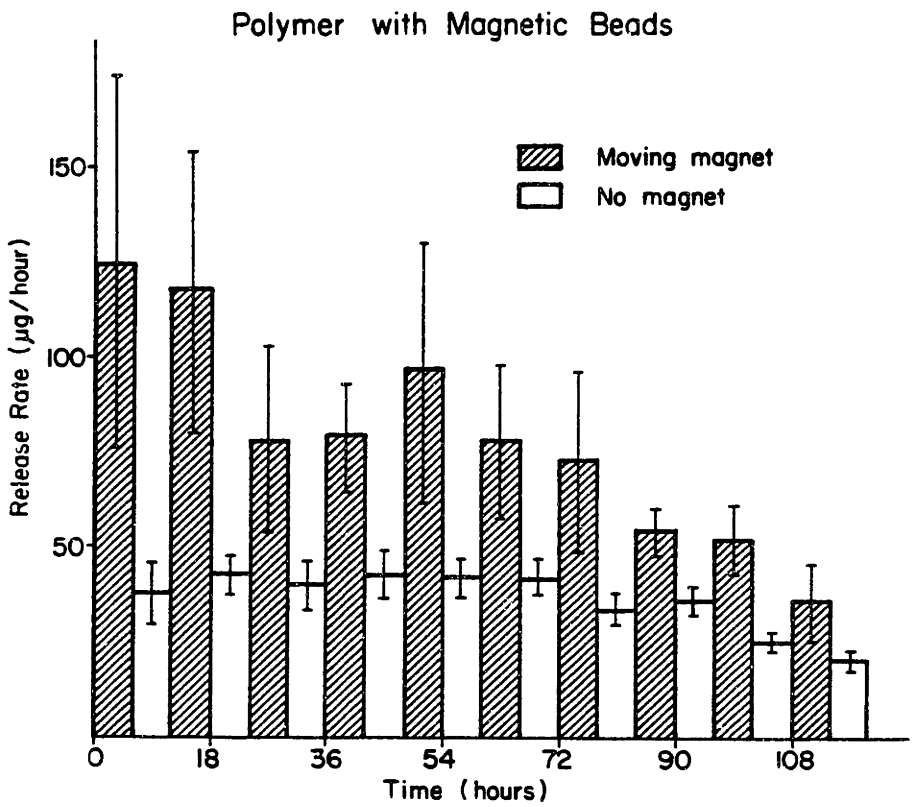

Figure 7: Data from feasibility study showing that BSA release from EVAc matrices embedded with magnetic spheres and subjected to oscillating magnetic fields could increased [26]. The matrices were exposed to the magnetic fields for six hours (hatched bars) and rested for six hours (clear bars). The net effect was small and the irreproducibility significant.

I.4 Closed Loop Systems

While controlled delivery of drugs is an important goal, the ultimate drug delivery system would have a built-in closed loop. This would provide for feedback, where the factor to be delivered would regulate its own release. Heller and Trescony [29] have developed a urea sensitive hydroxycortisone releasing biodegradable matrix. Hydroxycortisone incorporated into a matrix of methyl vinyl ether-maleic anhydride copolymer was coated with a hydrogel containing immobilized urease. When this enzyme reacted with external urea, ammonia bicarbonate and ammonium hydroxide were generated, accelerating polymer erosion and drug releasse. The enzyme reaction was proportional to the urea level.

Two types of insulin closed loop systems have been reported. In the first, insulin was bound to a sugar and this structure was then attached to the lectin concanavilin-A (Con-A). The Con-A was immobilized to agarose beads [30] or encapsulated in a polymer membrane permeable to both glucose and insulin. When sugars were used that had a lesser affinity for Con-A than glucose, glucose could displace the sugar-insulin moeity for release into the bloodstream. This displacement would be sensitive to the level of glucose and might establish a glucose senstive insulin delivery system.

Glucose senstive membranes have been studied by a number of groups. Soeldner[31] and Horbett[32] have proposed systems that take advantage of the reaction between glucose and glucose oxidase to establish a system

where the amount of glucose regulates the reponse of an implanted pump or the permeability or swelling of a membrane encasing insulin.

The transplantation of a part or the whole pancreas may ultimately be perfected. One possible scenario would have the beta cells or plasmid contolled insulin producing bacteria encased within a polymer membrane. If the cells or bacteria could remain or be made sensitive to physiologic need, then hormone replacement could take place in the presence of limited exposure to host immune system.

I.5 Scope of Thesis

This thesis will concentrate on the use of oscillating magnetic fields in augmenting release of drugs and macromolecules from polymer matrices embedded with small magnets. Initial reports demonstrated a weak and irreproducible effect [25], thus, a substantial focus of this work will be directed towards examining the parameters that control the system and make it reproducible. Chapter 2 details the techniques involved in fabricating these devices and the materials and methods used throughout this thesis. In addition, a demonstration of the modulation of BSA release from EVAc matrices is presented and issues surrounding the reproducibility of release kinetics examined. Control experiments are also described there. In the chapters that follow, characteristics of the matrices and the magnetic fields that might be used to control the system are studied. Chapter 3 presents investigations into the dynamics of modulated release and how the duration, amplitude and frequency of the applied field could be used to control this release. The properties of the matrices and embedded magnets that were important determinants in regulated release are presented in chapter 4. A model based on the volume of matrix acted on by the embedded magnet is also developed there. Mechanical deformation of the EVAc-BSA matrices confirmed the data and theory, and these studies are presented in chapter 5. A model of the events on a microscopic scale, involving enhanced flow through small channels under the influence of a pulsatile pressure source, is discussed in chapter 6. A demonstration of the use of this system *in vivo* is presented in chapter 7, along with an examination of how the parameters that provided control *in vitro* could

control release *in vivo*. Chapter 8 contains a discussion of pertinent issues related to the biocompatibility of the system. A summary of past work on EVAc drug delivery systems and suggestions for further research in this field are presented in chapter 9.

Relevant information regarding the EVA copolymer material and the device used to perform dynamic strength of materials testing, are included in appendix A. Data on the macromolecule BSA and the rare earth metal samarium cobalt are presented in appendix B. The derivations of the equations used in the analysis of the data are detailed in appendecies C-E, and the computer programs used to collect and analyze the data are listed in appendix F. The experimental data is listed in tabular form in appendix G.

REFERENCES

[1] Waitz, J.A., B.J. Olszewski and P.E.Thompson, Dialysis studies in rats on long-acting antimalarial Cl-105, Science 141:723-725 (1963)

[2] Folkman, J. and D.M. Long, The use of Silicon Rubber as a Carrier for Prolonged Drug Therapy, J. Surg. Res., 4,139 (1964)

[3] Baker, R.W. and H.K Lonsdale, Controlled release mechanisms and rates in Controlled Release of Bioactive Agents, vol 43 of Advances in Experimental Biology and Medicine, A.C. Tanquary and R.E. Lacey, eds., Plenum Press Pub., New York, p. 15 (1974)

[4] Robinson, J.R. ed., Sustained and Controlled Release Drug Delivery Systems, Marcel Dekker, Inc., New York (1978)

[5] Szycher, M. ed., Biocompatible Polymers, Metals and Composites, Technomic Pub. Co., Inc. (1983)

[6] Langer,R. and J. Folkman, Polymers for the Sustained Release of Proteins and Other Macromolecules, Nature, 263:797-800 (1976)

[7] Rhine W., D.S.T. Hsieh and R. Langer, Polymers for Sustained Macrmolecule Release: Procedures to Fabricate Reproducible Delivery Systems and Control Release Kinetics, J. Pharm. Sci., (69)265-270 (1980)

[8] Phillies, G.D.J., G.B. Benedek, and N.A. Mazer, Diffusion in Protein Solutions at High Concentrations: A Study of Quasielatic Light Scattering Spectroscopy, J. Chem. Phys. 65,1883 (1976)

[9] Longsworth, L.G., Temperature Dependence of Diffusion in Aquaeous Solutions, J. Phys. Chem., 58:770 (1954)

[10] Murray,J.B., L. Brown, R. Langer, and M. Klagsburn, A Micro Sustained Release System for Epidermal Growth Factor, In Vitro, 19(10):743-748 (1983)

[11] Langer, R., M. Fefferman, P. Gryska and K. Bergman, A Simple Method for Studying Chemotaxis Using Sustained RElease of Attractants from Inert Polymers, Can. J. Micro., 26(2)274-278 (1980)

[12] Preis, I. and R. Langer, A Single Step Immunization by Sustained Antigen Release, J. Immunol. Meth., 28:193-197 (1979)

[13] Moskowitz, M.A., Mayberg, M., and R. Langer, Controlled Release of Horseradish Peroxidase from Polymers: A Method to Improve Histochemical Localization and Sensitivity, Brain Research, 212:460-465 (1981)

[14] Langer, R., H. Brem, K. Falterman, M. Klein, and J. Folkman, Isolation of a Cartilage Factor that Inhibits Tumor Neovascularization, Science, 192,70-72 (1976)

[15] Brem, S., I. Preis, R. Langer, H. Brem, and J. Folkman, Inhibition of Neovascularization by an Extract Derived from the Vitreous, Am. J. Opth., 84, 323-328 (1977)

[16] Jones, R.D., L.S. Olanoff, J.M. Anderson and F.S. Cross, Host Response to Prosthetic Mitral Valves in Dogs at 20 Minutes to Four Years Post Implantation, chapter 52 in "Evaluation of Biomaterials", G.D. Winter, J.C. Kercy, and K. de Groot, John Wiley and Sons, Ltd., pps. 487-495 (1980)

[17] Levy, R., J. Wolfram, and R. Langer, unpublished data

[18] Guttman, Y., C.W. Gattschalk, and W.T. Lassiter, Micropuncture study of Inulin Adsorption in the Rat Kidney, Science 147:753-754 (1965)

[19] Murray, J., L. Brown and R. Langer, Controlled Release of Microquantities of Macromolecules, Cancer Drug Delivery, (1)2:119-123 (1984)

[20] Brown, L., C. Wei, and R. Langer, In Vitro and In Vivo Release of Macromolecules from Polymeric Drug Delivery Systems, J. Pharm. Sci., 72:1181-1185 (1983)

[21] Brown, L., C. Munoz, L. Seimer, E. Edelman, and R. Langer,Sustained Release of Insulin from Polymer Matrices:Control of Diabetes for 120 Days, Diabetes (1984)

[22] Gatling, R. et. al., Deaths Among Patients Using Subcutaneous Insulin Infusion Pumps-United States, Center for Disease Control - Morbidity and Mortality Weekly Report, (31)7:80-87, (1982)

[23] Teutsch, S.M., W.H. Herman, and D.W. Dwyer, Risk Factors for Death, Causes of Death, and Mortatlity Rates among Diabetic Patients using Continuous Subcutaneous Infusion Pumps, Diabetes 32, suppl 1, 36A (1983)

[24] Eisenberg,S. and A. Grodzinsky, Electrically Modulated Membrane Permeability, J. Mem. Sci., 19:173-194 (1984)

[25] Weiss,A. and A. Grodzinsky, Electric Field Control of Membrane Permeability, J. Sep. Pur. Met., in preparation, (1984)

[26] Hsieh, D.S.T, R. Langer and J. Folkman, Magnetic Modulation of Release of Macromolecules from Polymers, Proc. Natl. Acad. Sci. USA, 78:1863-1867 (1981)

[27] Langer, R., E. Edelman, and D.S.T. Hsieh, Magnetically Controlled Polymeric Delivery Systems, Chapter 25, pp 585-596 in ref. 2

[28] Leong, K., J. Kost and R. Langer, unpublished results

[29] Heller, J., and P.V. Trescony, J. Pharm. Sci., (68)7:919-921 (1979)

[30] Brownlee, M., and A. Cerami, Science, 206:1190-1191 (1979)

[31] Soeldner, J.S, K.W Chang, et. al., "Diabetes Mellitus", chapter 20 in Fogarty International, cnt. series on Preventive Medicine, vol. 4, S.S. Fajans, ed., pps. 267-677, Dept. DHEW-NIH publication no. 76-854 (1976)

[32] Horbett, T.A, J. Kost and B. Ratner, Swelling Behavior of Glucose sensitive membranes, Polymer Preprints (24)1:34-35 (1983)

[33] Langer, R. and N. Peppas, Present and Future applications of Biomaterials in Controlled Drug Delivery Systems, Biomaterials, 2(4) pps. 202, 205 (1981)

CHAPTER II: MATERIALS, METHODS DEMONSTRATION AND CONTROLS

II.1 INTRODUCTION

Early studies of the EVAc drug delivery system revealed that the method of fabrication was a great source of irreproducibility. Once the steps for producing these devices was perfected sustained release of macromolecules could be attained within confidence intervals of 5%, and the kinetics of release adjusted over a wide range as desired [1]. The same goals are desirable for a demand delivery system. Initial reports of modulated release from EVAc matrices embedded with magnetic objects showed standard errors about the mean that were on the order of the modulated effect [2]. In that study the means of generating the oscillating magnetic field, the method of matrix fabrication, and the mode by which the matrices were placed in the experimental set up, all contributed to problems with reproducibility. The modifications that were made to this original study and the investigation into the important determinants of reproducibility are presented in this chapter. The methods and materials discussed here apply for all of the experiments in this thesis. Control experiments are presented here as well.

II.2 MATERIALS AND METHODS

II.2.1 Fabrication techniques

The procedure for fabricating polymer matrices for magnetic modulation was modified from methods described earlier [3,4]. Ethylene-vinyl acetate copolymer (EVAc), (40% vinyl acetate) manufactured by DuPont Chemical Co. Wilmington, Delaware under the product name ELVAX-40P, was washed in distilled water and 95% alcohol to remove impurities [5] and then dissolved in methylene chloride to form a 10% (wt/vol) solution. Powdered bovine serum albumin (BSA, Sigma Chemical Co., St. Louis, Missouri, m.w. 68,800) was seived to particle sizes of 150-180 microns using standard U.S.A. testing sieves (A.S.T.M.E. specifications, Dual Manufacturing Co., Chicago Illinois). In separate experiments, different types of magnetic particles were embedded within the polymer matrices. At first, magnetic spheres were studied (type 440 C, Ultraspherics Inc., Marie, Michigan). These beads were 1.4 mm in diameter and made of a magnetic alloy of stainless steel containing 79.17% iron, 17% chromium, 1% carbon, 1% manganese, 1% silicon, 0.75% molybdenum, 0.04% phosphorus, and 0.04% sulfur. The iron provided the magnetic susceptibility and the chromium prevented rusting. In a second set of experiments permanent magnets composed of samarium cobalt, $SmCo_5$, coated with a layer of nickel to protect against corrosion were used. They were magnetized to 1100 Gauss (G) with their pole vectors oriented across the diameter (Permag Northeast, Waltham, Massachusetts). Two different geometries were examined. Cylinders 1.4 mm in diameter and 1.4 mm long were contrasted to

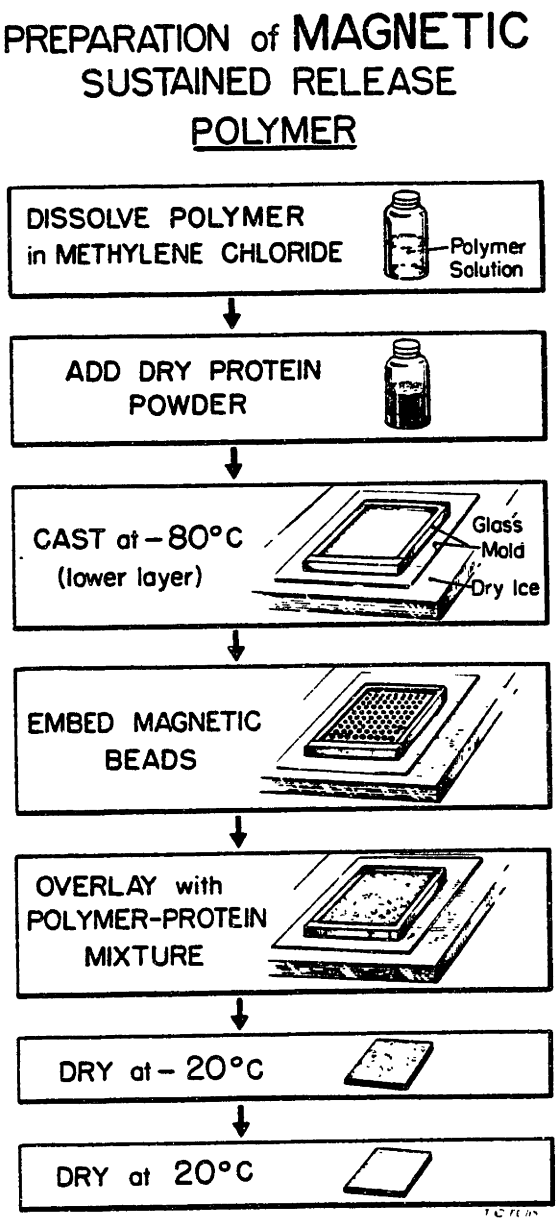

Figure 1.a: Flow diagram summary of the procedure for fabricating ethylene-vinyl acetate matrices homogeneously dispersed with a macromolecular substance and uniformly embedded with magnetic spheres.

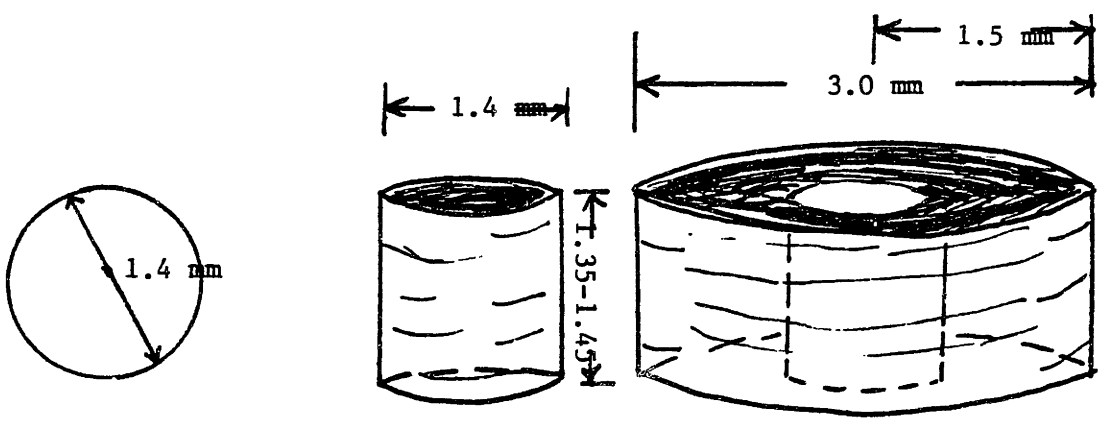

Figure 1.b: Photograph and drawing of the three different objects embedded in the matrices. The magnetic spheres were 1.4 mm in diameter and weighed 10 mg. The two samarium cobalt magnets were magnetized to 1100 G, and were 1.35-1.45 mm high. The cylinders were 1.4 mm in diameter and weighed 15 mg. The torroids had an inner diameter of 1.5 mm and an outer diameter of 3mm, and they weighed 60 mg.

torroids or rings, with an inner diameter of 1.5 mm, an outer diameter of 3.0 mm and height of 1.3-1.45 mm (figure 1.b).

Matrices were fabricated by low temperature casting of suspensions which contained 600 mg of BSA in 12 ml of a 10% solution of EVAc. The final drug loading was then 33% by weight BSA. All of the matrices examined in this thesis used BSA seived to 150-180 micron particle size at this loading. The step-by-step procedure is illustrated in figure 1.a. The copolymer-BSA suspension was vortexed for 45 seconds and then poured into a precooled glass mold that rested on dry ice and had been precooled for 10 minutes. This made the first layer of the system. The mold was 5.0 x 5.0 x 1.0 cm and made from window glass cemented in place with Silastic adhesive (Dow Chemical, Midland, Michigan). Fifteen seconds after the first layer was poured into the mold, magnetic particles were arrayed on top of it and then immediately covered with a second layer of the BSA-EVAc suspension, identical to the first. The magnetic spheres were arrayed within the polymer matrix by a specially constructed device consisting of two sheets of plexiglass in which an identical arrangement of 131 holes, 1.8 mm in diameter, had been drilled (figure 1.c) [2]. This replaced a similar device used in the early studies that was consrutced from the top and bottom of a standard lab petri dish. With the plates arranged so that the upper and lower holes were offset, the spheres rested in the upper holes. When the plates were shifted and the holes aligned, the magnets fell through the bottom holes in a set pattern. This pattern is displayed in figure 2.b next to the array that was achieved with the petri dish device (figure 2.a). The entire slab, containing the magnets, was allowed to harden in the mold for another ten minutes as it rested on

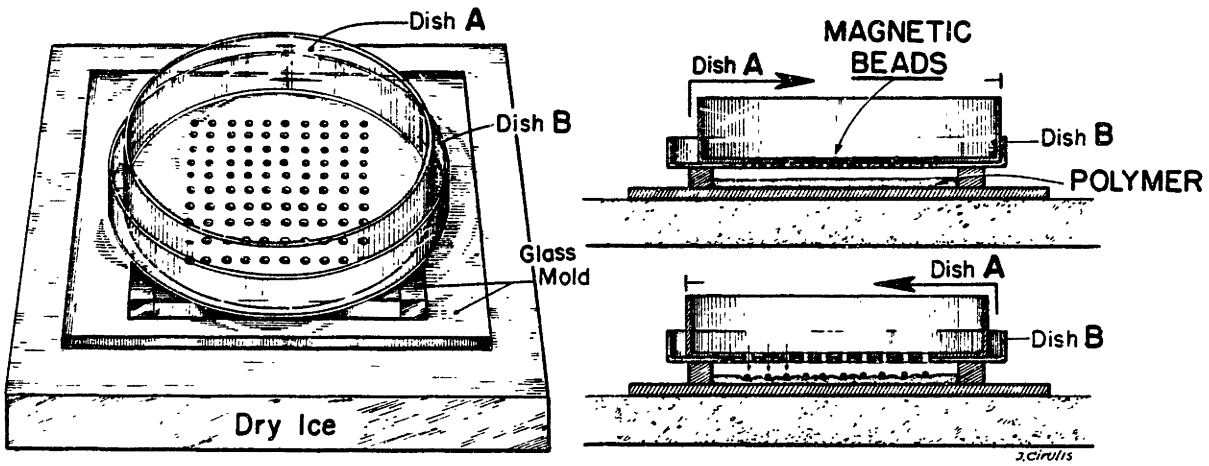

Figure 1.c: Device constructed to place magnetic spheres in an orderly array within the EVAc-BSA matrices. When the two plates were offset the spheres rested in the holes of the top plate against the bottom plate. If the offset was corrected and the holes aligned the spheres fell onto the first layer of the cast matrix below.

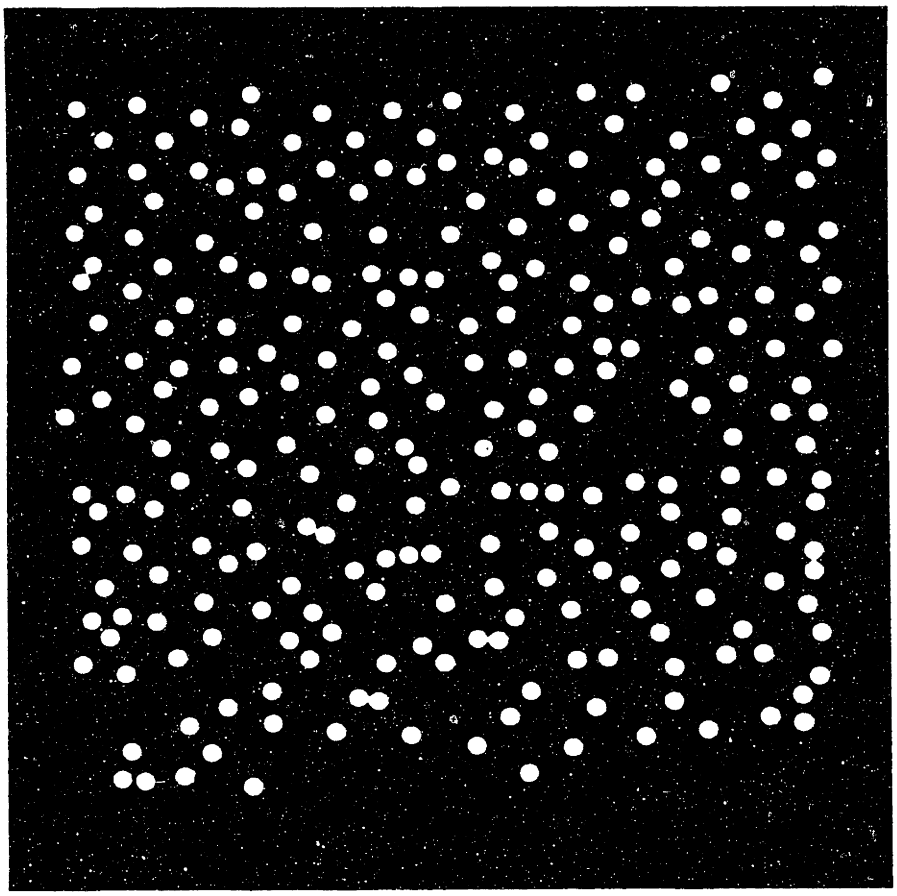

Figure 2.a: Radiograph of the EVAc-BSA matrices embedded with magnetic spheres using, petri dish device [2]. There is great disarray of the spheres

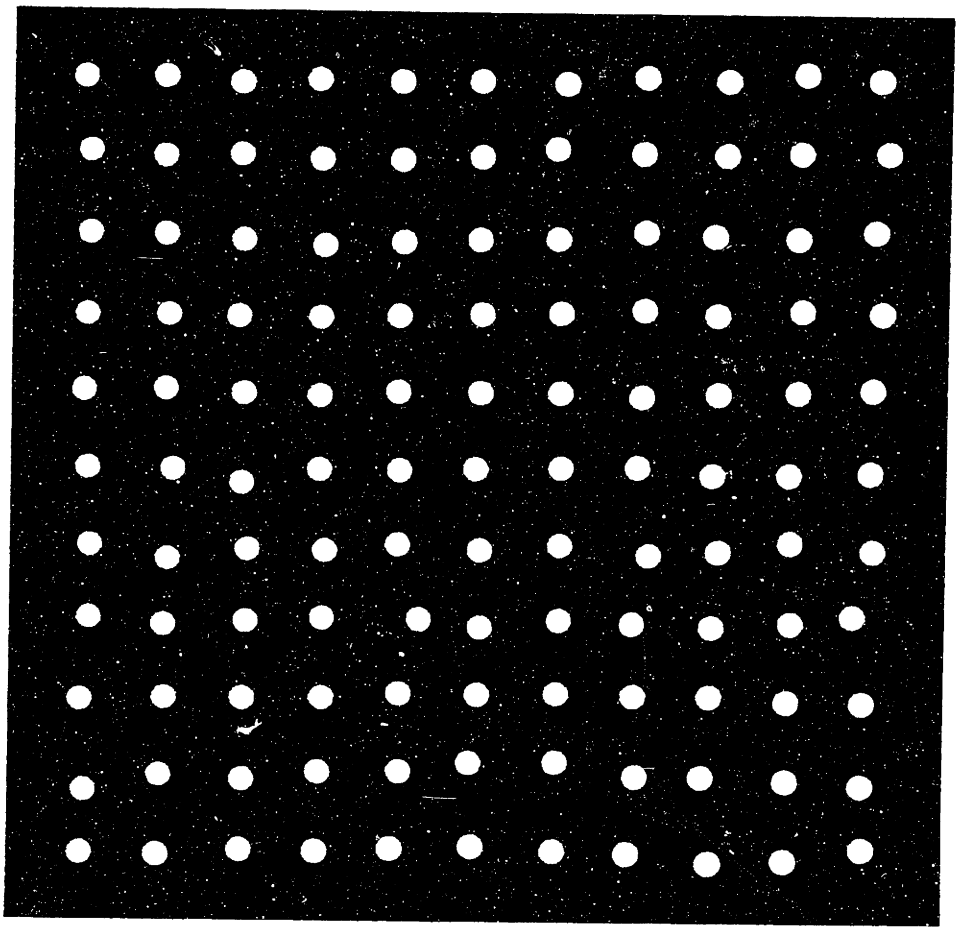

Figure 2.b: Radiograph of EVAc-BSA matrix embedded with 1.4 mm magnetic spheres by the modified plexiglass device (section III.2.1).

dry ice and then transferred to house vacuum at 600 mtorr in a -20°C freezer for 48 hours. Final samples, 1.0 x 1.0 x 0.2 cm squares, were cut from the larger unit such that they contained nine magnetic spheres or one cylinder each. The beads raised the surface of the slabs but were always covered by polymer material and never totally exposed. The sample height, length, width and extent of surface protrusion were measured with a micrometer (Fisher Scientific).

Fabrication of ethylene-vinyl acetate copolymer matrices embedded with small magnets was modified from the above technique. The powdered BSA was added to a 10% EVAc solution and the protein-polymer mixture (33% BSA by weight) vortexed for 15 seconds. The mixture rested for an additional 15 seconds to let air bubbles escape that might have been produced at the time of vortexing. The mixture was then poured into a glass tube, 1 cm high and 1 cm in diameter, that had been precooled on dry ice for 10 minutes. A samarium cobalt magnet was dropped into the center of the tube with a plastic forceps, 25 seconds after the mixture was poured. This delay allowed the bottom half of the matrix to harden and left the magnet to rest in the middle of the matrix. The tube remained on the dry ice for another ten minutes and was then transferred to a -20°C freezer. The matrix was removed from the tube after six hours, left in the freezer for another 42 hours and was then transferred to house vacuum (600 mtorr) for two days.

In the first study of modulated release, the polymer matrices were allowed to float freely in the vials above the magnets. Thus, with each pulse of the magnetic field the samples were observed to strike the glass

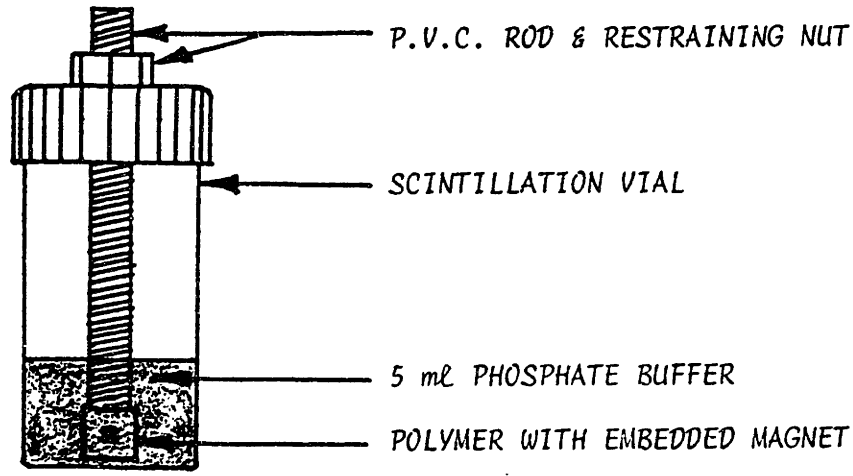

Figure 3: Depiction of the restraint of an EVAc-BSA matrix against a polyvinyl chloride rod. The rod was passed through the cap of a scintillation vial at a variable height above the magnet. This allowed for control over the strength of the magnetic field applied to the matrix.

bottom of the vials. In the current studies, a drop of ethylene-vinyl acetate was used to mount each sample to the end of a polyvinylchloride rod (World Plastics, Waltham, Massachusetts) which was inserted through the cap of a 20 ml glass scintillation vial (figure 3). The depth of the rod within the vial was adjustable but was usually set so that the bottom of the polymer slab face was one cm from the bottom of the vial. This assurred that all of the matrices were subjected to the same strength magnetic field and eliminated some of the possible artifacts that might have been produced by banging of the matrices against the vial. Ten ml. of 0.1 M phosphate buffer, pH 7.4, was added as release media. The solution was made with double glass distilled water.

II.2.2 Generation of an Oscillating Magnetic Field

The device used to generate the oscillating magnetic field in the initial report of modulated release is depicted in figure 4. It was adapted from a commercial speed-controlled rocker. "Crucore-18" permanent bar magnets, 5.0 x 5.0 x 2.5 cm,(Permag Northeast) were placed on one end and a balance on the other. Vials were positioned on a tray suspended above the rocker. The rocker brought the magnets up to the tray and then away from it at 0.3 Hz. The field varied from null, 0.5 G, to 1000 G. Unfortunately, the motion of the rocker was nonlinear, the rocker prone to instability and the tray on which the vials were placed subject to perturbation, as it was suspended by wires from a beam above [2].

In the current studies the above system was replaced with two more stable and versatile devices that permitted examination of a range of

frequencies or field strengths. The first rotated permanent magnets beneath the scintillation vials in which the samples were suspended. This device is depicted in figure 5, and consists of two 1.0 cm inch thick plexiglass plates approximately 3 cm apart. The top plate was stationary and had 24 holes, 3 cm in diameter, drilled into it. The vials rested in these holes and were secured in place with brass set screws. Two 5.0 x 5.0 x 2.5 cm "Crucore-18" permanent magnets (Permag Northeast) were mounted to the bottom plate. This material is a complex alloy of the rare earth metal Samarium Cobalt which possesses a high residual induction and coercive force and a maximum energy product of 18.0 x 10^6 GaussOersteds. The pole vectors of these magnets were oriented through the top and bottom faces. The bottom plexiglass plate was attached to a 70 hp, 8 lb. torque motor and rotated beneath the vial mounted samples. The force of the magnetic field generated by these magnets on the magnet embedded within EVAc matrices is inversely proportional to the square of the distance between the two. Thus, the amplitude of the force could be varied by adjusting the height of the vials above the rotating plate. Plate rotation, and therefore the frequency of the oscillating field, was measured with a Stewart Warner hand held tachometer (model 757-AA) and was regulated by controlling the motor voltage with a Variac electronic regulator.

A second system utilized a plate demagnetizer (model no. AXM 7167, O.S.Walker Co., Inc. Worcester, Mass.) generated a 60 Hz magnetic field. The input voltage was controlled by a Variac electronic regulator allowing for variation of the amplitude of the field from 0 to 900 Gauss (peak-to-peak). The relationship between field amplitude and the voltage

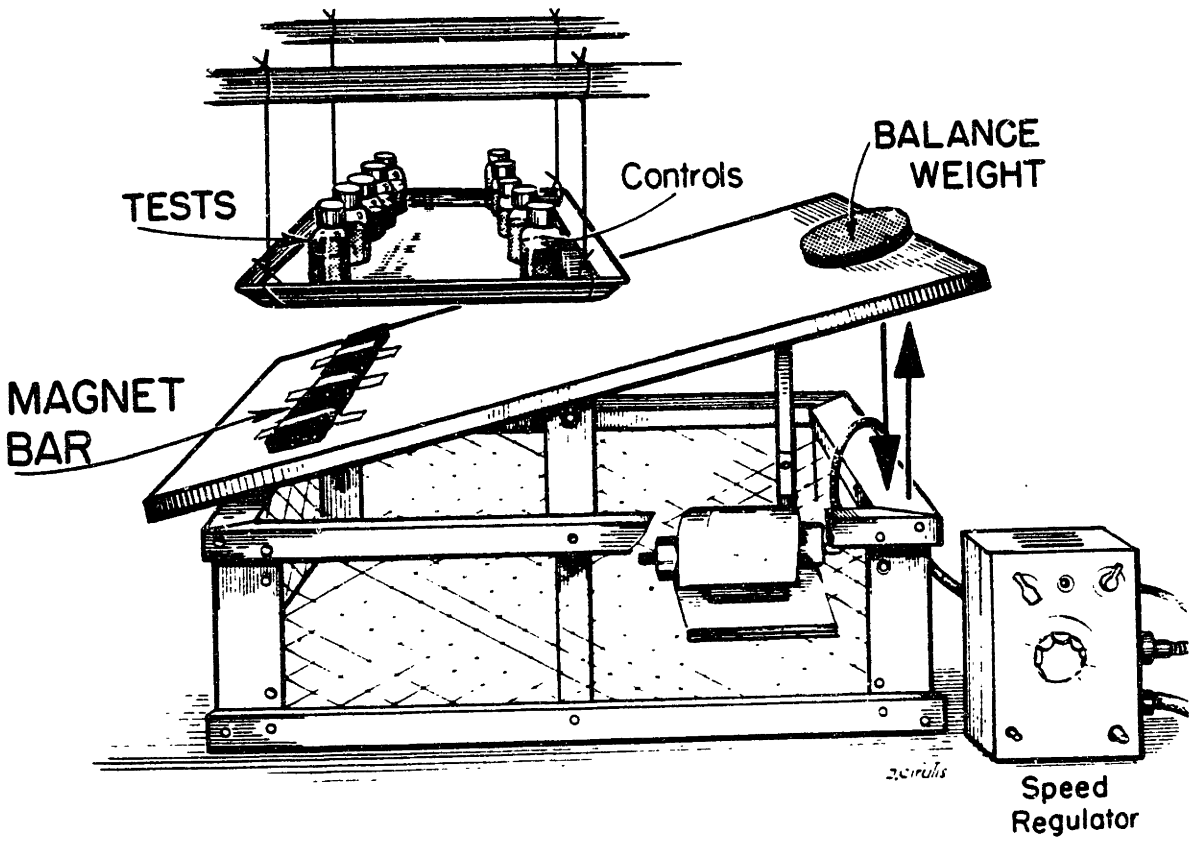

Figure 4: Magnetic field generating device used in the first reported studies of modulated release. A series of bar magnets were mounted to one end of an adapted commercial lab rocker and a weight added to the other side for balance. The motion of the rocker was still nonlinear and unstable. Nonrestrained samples were placed in vials which were placed on a tray suspended baove the rocker by wires [2].

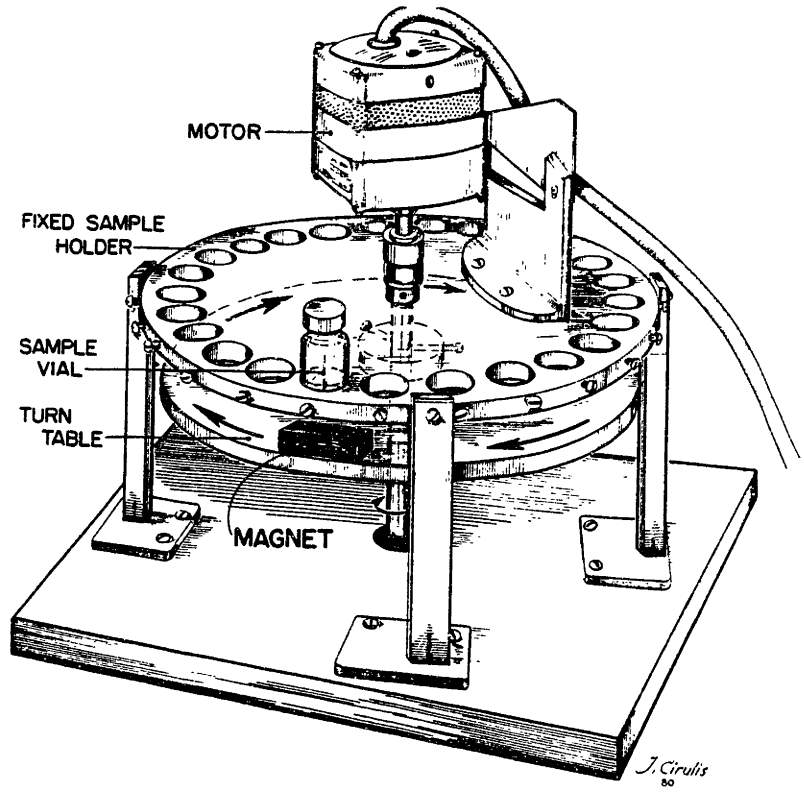

Figure 5: The first of two oscillating magnetic field generating devices used in this thesis. Permanent magents were secured to a rotating plate. The speed of the plate was controlled by an electronic regulator (not shown). This allowed for examination of modulated release over a frequency range from 0 to 11 Hz. Vials were secured in holes drilled into a second plate. This plate was stationary and suspended above the magents.

is provided in figure 6-a; the field dropped 5G/volt. The magnet field measured at a point above the face of the electromagnet fell 50 G every cm as depicted in figure 6-b.

Magnetic fields were measured with a self-calibrating Hall-effect Gaussometer (model 610, Fw Bell Inc.) with a transverse probe (model no. HTB-1-0608). This instrument has 11 ranges- one to 100,000 Gauss full scale, and is accurate to $\pm$ 0.5% full scale with a flat frequency response from DC to 2000 Hz.

II.2.3 Release Kinetics and Statistical Analysis

In each experiment the matrices were placed in ten ml of 0.1 M phosphate buffer for the first 48 hours before a magnetic field was applied so that BSA that might have adhered to their surfaces could diffuse away (section IV.2.2.i). Once the experiment commenced, BSA release was determined for the two hour periods preceeding, during and following exposure to a magnetic field by absorbance measurement of the release media at 220 nanometers [6]. The buffer was replaced at the end of each two hour period. Rates of release were calculated by dividing the amount of protein released by the elapsed time since the previous exchange. The extent of modulation was expressed as the ratio of the rate of BSA release during a given period of field exposure, compared to the average of the release rates achieved for the periods immediately preceeding and following this field application. This value was first computed for each sample and then averaged for all matrices to provide a single ratio of release rates.

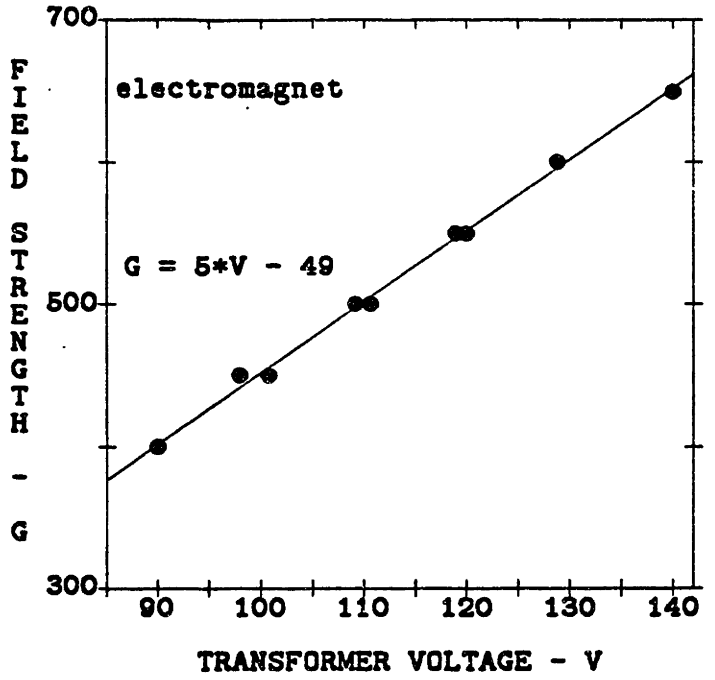

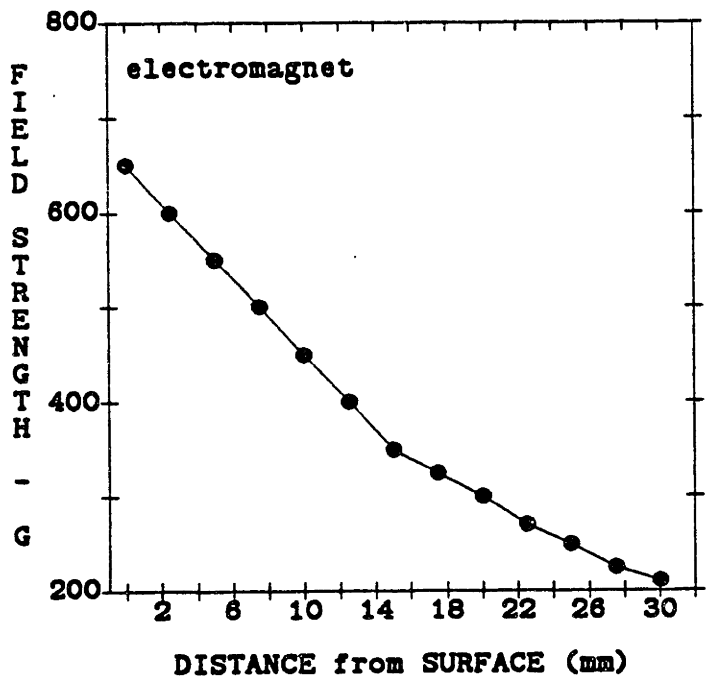

Figure 6: The change in the magnetic field from the electromagnet, with

a. variation of the magnet's input voltage, and

b. distance from the surface of the magnet,

Statistical analysis was performed with the aid of the RS/1 analysis routines available on a VAX-11/45 Digital Equipment Corporation computer system [7]. Data is reported as the average plus or minus the standard error about the mean. Linear regressions were determined with least squares analysis and coefficient of correlation, R^2, reported for each fit. Paired data comparisons were performed with Student's T-test and a significance level noted in each case.

II.2.4 REPRODUCIBILITY

The reproducibility of the system was tested by examining the same set of matrices exposed to the same field conditions for 20 days. As in all the experiments the matrices were prerelased for 48 hours. The rate of BSA release and extent of modulation was determined for five matrices containing one cylindrical 1100 G permanent magnet. The matrices were exposed to an 1800 G magnetic field from the mechanical turntable device rotating at 11 Hz, for 2 hours each day, for a total of 20 days.

II.2.5 CONTROLS

To assure that changes in the absorbance of the release media at 220 nm were due to BSA alone, the following materials were placed alone and then together in ten ml. of release solution which was replaced every three days for six months: slabs of EVA copolymer(EVAc), methylene chloride, the polyvinylchloride rods, and the embedded magnets.

In order to determine whether just the presence of the magnetic spheres within the polymer matrix would alter normal release profiles, matrices were prepared as above but only the right hand 66 of the 131 holes of the arraying device were loaded with the spheres. The slab matrix that was fabricated with this technique was cut into 1.0 x 1.0 cm samples; six contained spheres and six identical samples contained no embedded objects. BSA release was followed daily for one month in the absence of any applied magnetic field.

The necessity for both an applied alternating field and embedded magnets for modulation to occur was investigated in the following two sets of experiments. Three BSA-EVAc polymer slabs without any implanted magnets, and three possessing nine 1.4 mm nonmagnetic stainless steel beads (type 302 S, Ultraspherics Inc, Marie Michigan) were subjected to a magnetic field oscillating at 0.866, 1.0, 5.0, 6.67, 9.5 and 11.0 Hz. Simultaneously, three samples embedded with 1.4 mm magnetic spheres and five samples with 1.4 mm cylindrical magnets were examined at rest, free from a magnetic stimulus.

The effect of short term changes on the release of BSA from the EVAc matrices was tested in two fashions. Five copolymer matrices were moved from room tempertaure to 37^{o}C and then back to room temperature every two hours and the rate of BSA release measured before each change. Second, matrices were placed in the flow-through system described in section III.2.1 and release examined in the presence of a 650 G, 60 Hz magnetic field. The matrices resided in a swinex filter (Millipore) and the filter and a thermistor (Omega Engineering Inc., model 747, Stamford Ct) were

mounted to the electromagnet surface. The temperature at the electromagnet surface and the instantaneous continuous recording of absorbance from a matrix subjected to any potential changes in temperature were recorded simultaneously in this fashion.

II.3 RESULTS

II.3.1 Reproducibility

The rate of BSA release was measured for five matrices containing one cylindrical magnet each (figure 7.a). The clear bars in that figure represent the release rate for the two hours preceeding and following exposure to an oscillating magnetic field. The middle crosshatched bar of each group represents the two hour period of exposure to a magnetic field oscillating at 11 Hz. The release rates attained during the field applied times compared to the average of the rates during the adjacent field absent times was defined as the extent of modulation and is presented in figure 7.b. Over the course of the entire experiment this ratio was 9.35 $\pm$ 0.37 . The standard error about the mean ratio of release rates in all subsequent experiments presented in this paper was also less than 10%.

II.3.2 Controls

In the absence of a magnetic field, the six polymer matrices embedded with magnetic spheres and the six without magnets exhibited cumulative release of protein which followed the square root of the cumulative time

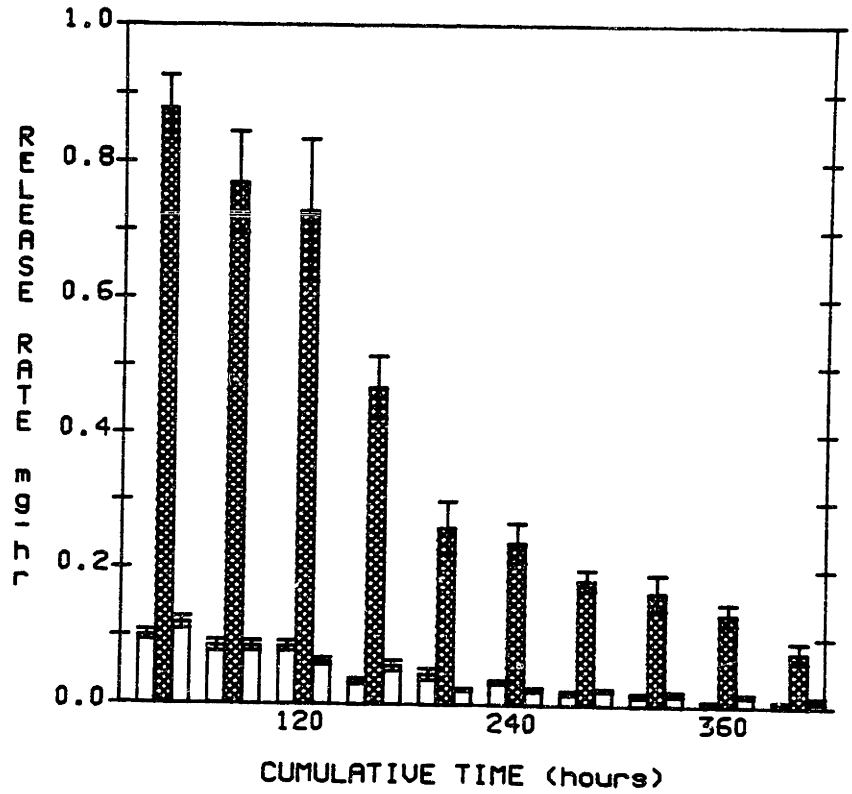

Figure 7.a: Bargraph plot of the rate of BSA release in mg/hour averaged over all samples studied in a given period of time for five ethylene-vinyl acetate copolymer matrices, each embedded with one cylindrical samarium cobalt magnet. The middle bar of each set of three bars represents a 2 hour period when an 1800 Gauss magnetic field oscillating at 11 Hz was applied to the samples, and the bars on either side represent the two hours immediately preceding and following it.

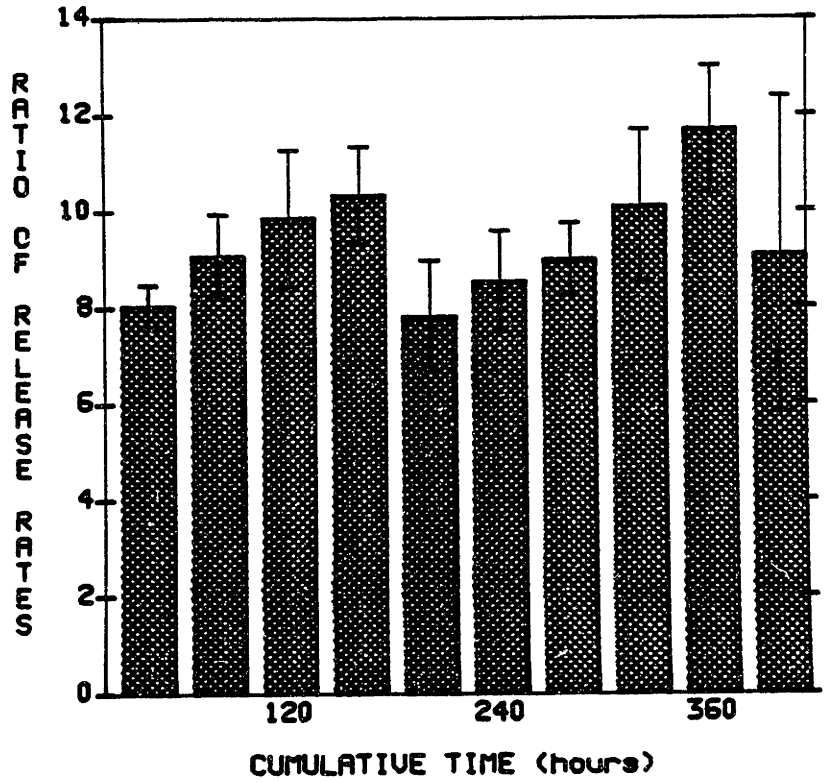

Figure 7.b: Comparison of the release rates during the field applied and field absent periods is the extent of modulation, and is depicted for the matrices from figure 7.a. The ratio for all the timepoints was 9.35 $\pm$ 0.37.

with slopes of 1.78 and 1.84 respectively (figure 8). Linear fits were achieved with multiple R-squares of 0.9979 and 0.9954, and the two sets of data were not significantly different ($p > 0.64$) .

When the three polymer matrices without magnets were exposed to an 11 Hz oscillating magnetic field the ratio of release rates achieved during sucessive periods of field exposure and field absence was 1.07 ± 0.12 . For those matrices embedded with nonmagnetized spheres an average ratio of 0.95 ± 0.067 was obtained, and if no magnetic field was applied, the ratio of sucessive periods of release was 1.01 ± 0.037 . In all of the control cases no augmentation of release was observed, and none of the materials that came into contact with the release media, aside from the BSA, changed the absorbance of the solution.

There was no change in the rate of release from five EVAc-BSA matrices when the temperature was raised from 25 to 37°C and then returned to 25°C every two hours. Figure 9.a shows that the temperature at the surface of the electromagnet rose 8°C in the hour during which it was examined. Over that same hour, and for 7 hours after that, the release of BSA from a matrix atop this device did not change during this time (figure 9.b).

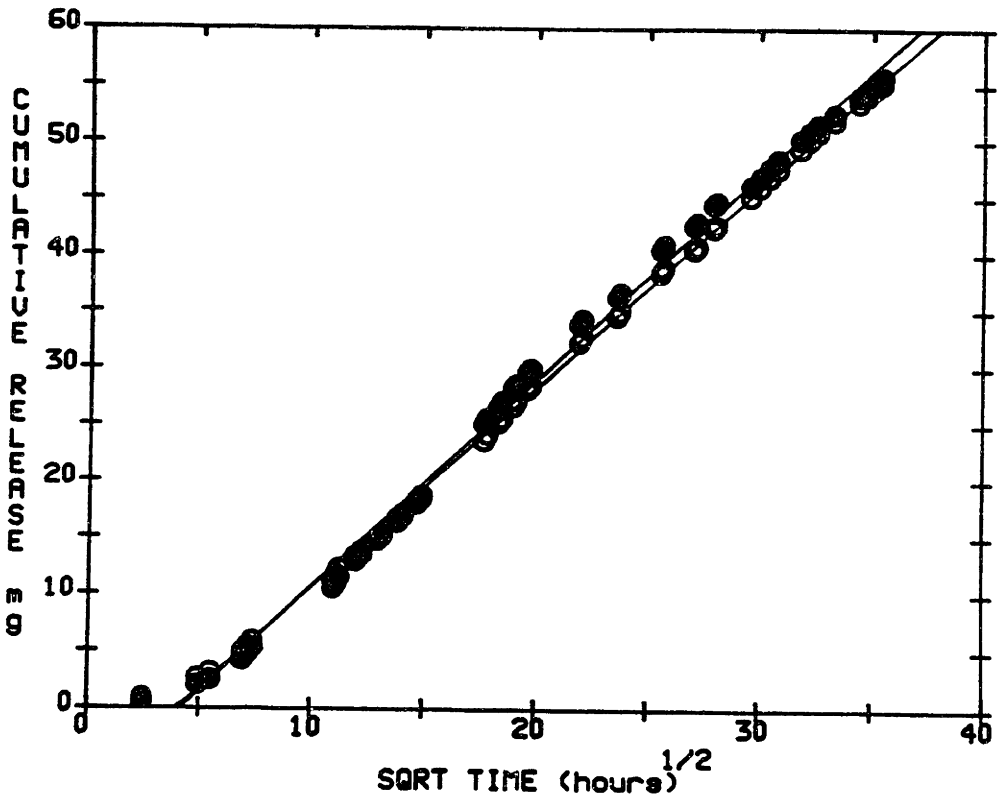

Figure 8: The cumulative amount of protein released (mg) plotted versus the square root of the cumulative time (hours) for six EVAc-BSA matrices (open circles) embedded with 1.4 mm magnetic spheres and six matrices (closed circles) without these spheres. No magnetic field was applied.

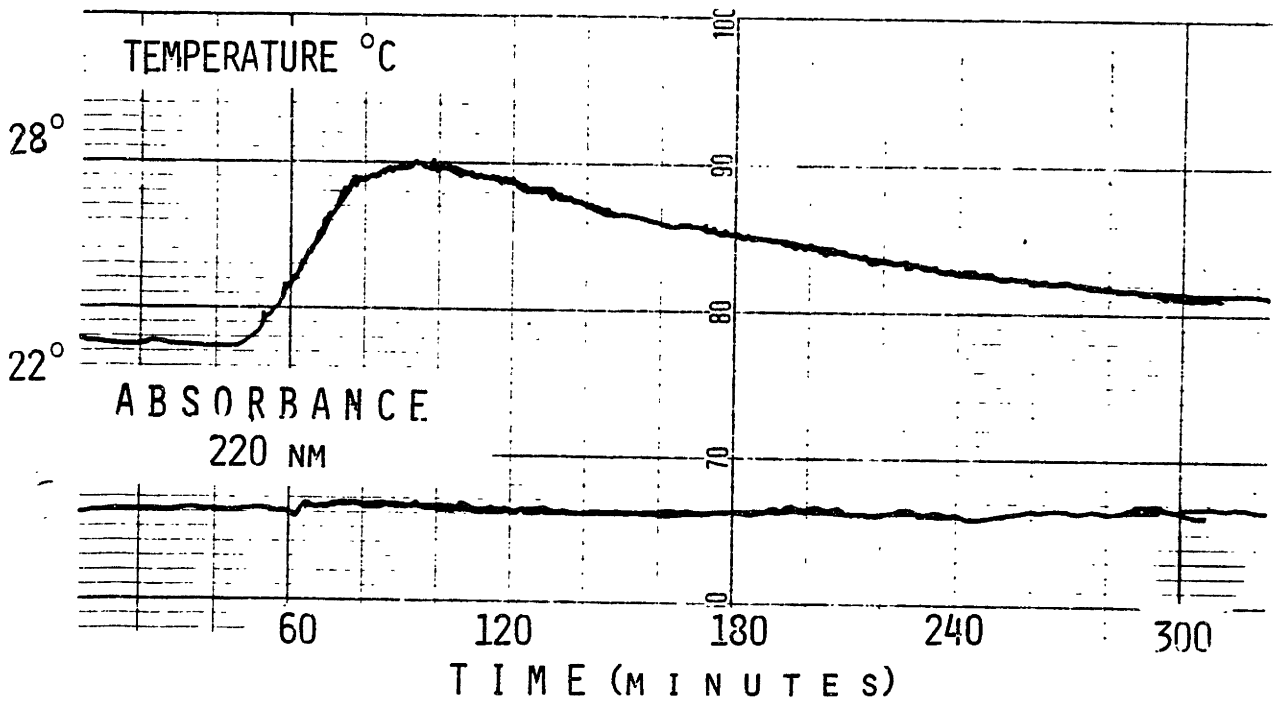

Figure 9.a: The change in electromagnet surface temperature with time. A net rise of 8°C per hour was observed.

b: In contrast, the rate of BSA release from an EVAc matrix mounted to the same electromagnet did not change during this time or for 7 hours afterwards.

II.4 DISCUSSION

The first report of modulated release from EVAc-BSA matrices exhibited standard errors about the mean that were on the order of the mean [2]. The reproducibility problems were contributed in part by the complexity of the fabrication technique, the means by which the oscillating magnetic field was applied to the matrices and the way in which the matrices were placed in the experimental configuration.

The technique for making 'magnetic ' EVAc-BSA matrices was adapted from the low temperature casting method [1]. The low temperature limited drug movement before hardening, and led to a homogeneous dispersion of drug with in the matrix. Kinetics of sustained release fell within 10% of the mean, and could be adjusted 50 fold by systematically varying the initial size and concentration of the BSA. When magnets were introduced into the matrix the complexity of the procedure increased significantly. Four different steps were required. Precise positioning of the spheres, and timing of two separate castings were needed. The petri dish based arraying device led to an imperfect arraying of the spheres. Furthermore, the very use of the spheres necessitated irreproducibility. The repeated ability to drop the spheres in the same configuration with each casting was important in reducing the sample to sample variability. Yet, because the spheres were geometrically isotropic it was impossible to align the pole vectors of all the spheres in one direction. Thus, the alignment of the magnetic beads differed from matrix to matrix and from sphere to

sphere within each matrix. When the beads were replaced with cylindrical magnets the reproducibility was increased, as well as the extent of modulation. Nonetheless, the four step procedure required two separate pourings of the drug-polymer solution and was both difficult and complex. Thus the final fabrication procedure described above was developed. Only one pouring was used in that technique and control over magnet placement and matrix shape could be achieved.

The device used to generate the oscillating magnetic field in the initial report of modulated release limited studies to a narrow range of frequencies and field strengths. Furthermore, the motion of the rocker was nonlinear, the rocker prone to instability and the tray on which the vials were placed subject to perturbation, as it was suspended by wires from a beam above. The devices that replace this system provided a stable and sturdy restraint for the vials or animals and allowed examination of the effects of the stimulus over a range of frequencies (turntable) and amplitudes (electromagnet).

In addition, in the earlier studies the matrices were allowed to float freely within the solution in the vials. Thus, as the magnet was raised towards the vials the samples were pulled down against the glass floor of the vial. Much of the magnetic force was spent on this motion and less on actually moving the spheres within the matrix. When the matrices were restrained against a PVC rod, as depicted in figure 3, this motion was eliminated.

Using all of these improvements, almost 10 fold augmentation of the release of a macromolecule, bovine serum albumin, from a polymer matrix was demonstrated at standard errors that were within 5 to 10% of the mean. Figure 7 shows that consistent augmentation of release occurred every time the magnetic field was applied even when the release rates decreased with time. The decline in the rate of BSA release was expected because flat slab matrices were used. In a flat slab the diffusion distance through the matrix interior to the external environment increases with time and the rate of release declines accordingly. Theoretically this baseline decay can be avoided if matrices are fabricated in the shape of hemispheres [8].

When no magnetic field was applied the cumulative release followed the square root of time in a linear fashion (figure 8) confirming previous work that demonstrated that diffusion was the predominant determinant of BSA release from the EVAc matrices [1]. The same kinetics were observed whether magnetic spheres were embedded in the matrix or not and whether two pourings or one were used. The mere presence of the magnets did not affect baseline release. Furthermore, the affect of the applied field on release from the matrices was not observed if either the field was not applied or the embeddded objects were absent or nonmagnetic. Previous reports have already shown that DC, non-alternating fields did not affect release [3,4].

Finally, release rates were not altered by changes in the temperature of the environment every 2 hours or by an $8^{o}C$ per hour increase in the temperature at the surface of the electromagnet. The temperature at the

surface of BSA release would not be the same as the temperature at the magnet's surface. The matrices are cooled by the buffer *in vitro* and insulated *in vivo* and, in both cases, raised above the electromagnet surface. In addition, calculation in section VIII.6 reveal that the magnet should induce few eddy currents and dissipate little heat under the fields and frequency of interest.

REFERENCES

[1] Rhine, W., D.S.T. Hsieh and R. Langer, Polymers for Sustained Macromolecule Release: Procedures to Fabricate Reproducible Delivery Systems and Control Release Kinetics, J. Pharm. Sci. 69(3)265-270 (1980)

[2] Hsieh, D., R. Langer and J. Folkman, Magnetic Modulation of Release of Macromolecules from Polymers, Proc. Natl. Acad. Sci. USA, 78:1863-1867 (1981)

[3] Langer, R., E. Edelman and D. Hsieh, Magnetically Controlled Polymeric Delivery Systems, Chapter 25, pp 585-596, in "Biocompatible Polymers, Metals, and Composites", M. Szycher ed., Technomic Pub. Co., Inc. (1983)

[4] Edelman, E., J. Kost, H. Bobeck, and R. Langer, Regualtion of Drug Rlease from Polymer Matrices using Oscillating Magnetic Fields, J. Biomed. Mat. Res., submitted (1984)

[5] Langer,R., Polymers for Release of Macromolecules, Methods of Enzymology, 73:48 (1981)

[6] Grutzer, W.B., Spectrophotometric Determination of Protein Concentration in the Short Wavelength Ultraviolet in "Handbook of Chemistry and Molecular Biology, Physical and Chemical Data", G.D. Fasman ed., Vol. II, p. 197, Cleveland: CRC Press (1976)

[7] RS/1 Users Guide,Bolt,Beranek and Neuman Inc., Cambridge MA (1984)

[8] Hsieh, D., W. Rhine and R. Langer, Zero-Order Controlled Release Polymer Matrices for Micro- and Macromolecules, J. Pharm. Sci., 72:17-22 (1983)

CHAPTER III: MODULATION DYNAMICS AND FIELD CONTROL

III.1 INTRODUCTION

Although the feasibility of magnetically modulated release was first demonstrated in 1980 [1], there has never been an adequate examination of the time course of modulated events. In the first studies release rates were observed to increase but the pattern of the increase was unclear. For example, it was not evident whether the response to the field was immediate or delayed, and whether the field displayed constantly increasing release rates or an effect that plateaued at a new baseline. Thus, the optimal form of the stimulus was unknown.

The experiments described in this chapter studied the dynamics of enhanced release. Once the relationship between the response and the stimulus had been determined, a second series of studies were performed to ascertain how variation in the strength of the stimulus would affect the extent of the response. In two separate sets of experiments, matrices were subjected to applied fields, whose frequency varied from 5 to 11 Hz, and whose amplitude ranged from 200 to 1800 G.

III.2 METHODS

III.2.1 Dynamics of Release Kinetics To examine the release kinetics of BSA from EVAc matrices continuously and in real-time a flow through spectrophotometer was implemented. Matrices were wedged inside a

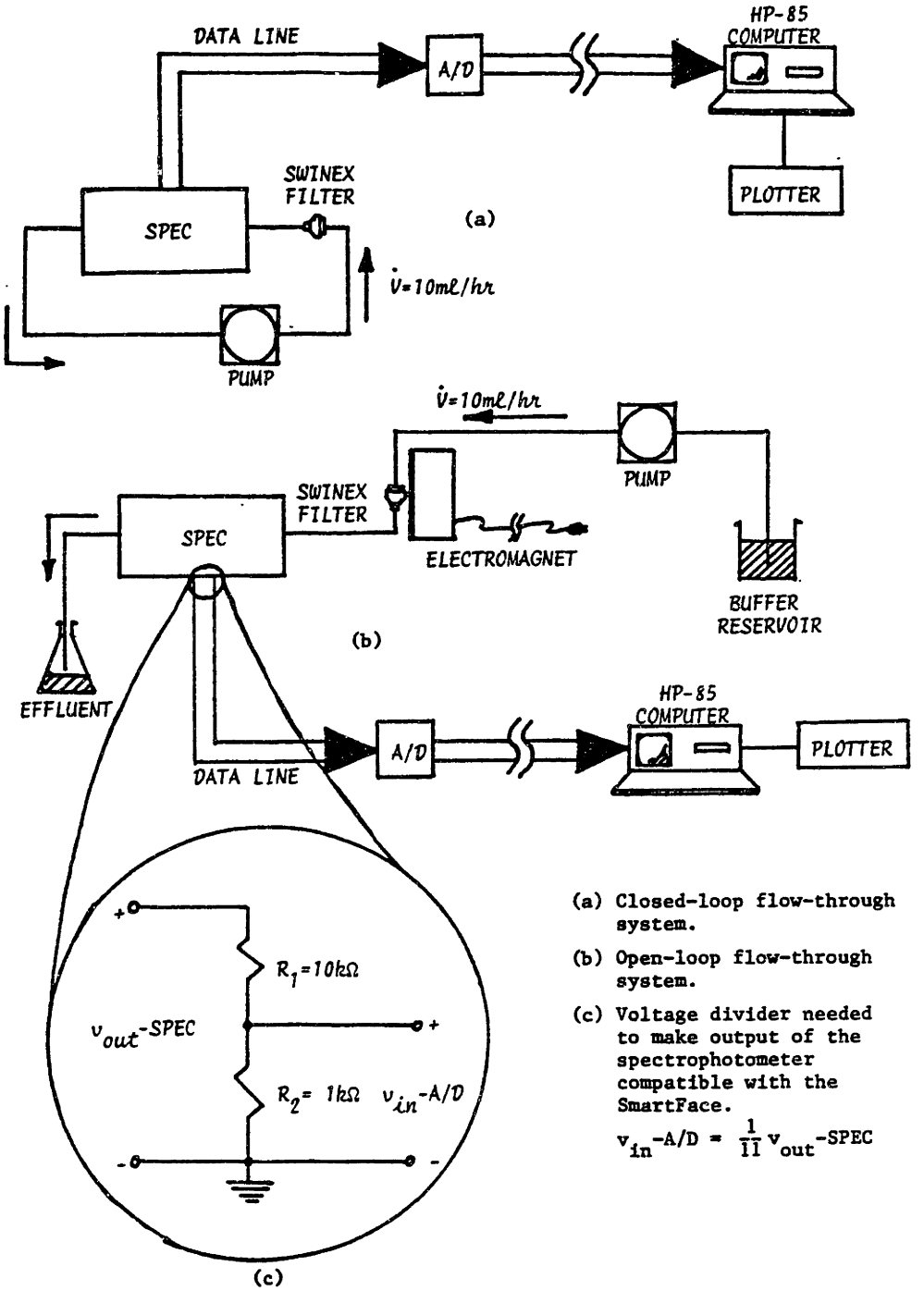

(a) Closed-loop flow-through system.

(b) Open-loop flow-through system.

(c) Voltage divider needed to make output of the spectrophotometer compatible with the SmartFace.

v_{in}-A/D = $\frac{1}{11}$ v_{out}-SPEC

Figure 1: Schematic of the flow-through spectophotometer configuration.

Millipore swinex filter and attached to the flow-through set up. The matrices could not move inside the filter, and did not alter the flow through the system. The full system is displayed in figure 1 and consists of an open loop circuit wherein 0.1 M phosphate buffer, pH 7.4, was pumped (LKB microperpex peristaltic pump) past the samples into an 65 ul flow cell (model no. 1047x26) of a spectrophotometer (model 250, Gilford, Oberlin, Ohio 44074). The absorbance was continuously recorded on a strip chart recorder (Kipp & Zonen, model BD 40) and transmitted to an HP-85 lab computer (Hewlett-Packard Co., Corvallis, Oregon 97330) for storage. Data was transmitted from the spectrophotometer every 6 seconds to the computer by a programmable interface (SmartFace, Analytical Computers, Elmhurst, Illinois 60126), converted to digital data by an HP-85 A/D converter and stored on cassette tape through an HP-85 serial interface(model no. HP 82939 A). The response time of the matrices to the application and withdrawal of an oscillating magnetic field was determined from the time needed to arrive at 63% of the peak and baseline once the field was turned on or off respectively. This value was chosen because it represents the percent of the peak response that should be attained after a time equal to the time constant of a system with an exponential time response.

The accuracy and time response of the system was tested with five solutions of BSA at concentrations ranging from 0.1 to 0.5 mg/ml. Phosphate buffer, 0.1 M pH 7.4, was pumped through the circuit to establish a zero baseline. One of the solutions replaced the plain buffer for 10 minutes, and the buffer replaced. This led to a transient rise in absorbance corresponding to the concentration of the BSA solution. The absorbance was recorded versus time, on the computer and strip chart

recorder, and the time needed to rise to the peak and fall back to baseline were determined using the 63% criteria. The flow profile was examined as the BSA solutions were pumped through the tubing alone, the tubing and a empty swinex filter, and finally the tubing and a filter housing a slab of EVAc containing no protein, to see if the addition of components to the circuit might alter the pattern of flow.

III.2.2 Refractory Time Matrices were placed in the flow-through system, prereleased in phosphate buffer for 48 hours and then exposed to repeated 4 minutes pulses of 500 G electromagnetic fields spaced 20 minutes apart. A repeatable series of absorbance spikes was achieved and the time between field pulses was then shortened to determine whether the matrix ever became refractory to modulation. The same strength fields were applied for 4 minutes at intervals from 0.5 to 20 minutes apart.

III.2.3 Field Strength The effect of varying the strength of the magnetic field generated by the electromagnet was studied by adjusting the input volatge to the electromagnet. Fields were applied to matrices over a range of 200 to 900 G in a random order and the dynamics were observed. An overall baseline release was first determined. The peak release achieved with field application above the baseline release was compared to the overall baseline and served as an index of the modulation.

III.2.4 Magnetic Field Frequency The importance of field frequency on regulating BSA release was examined using the mechanical field generating device. The flow through system was not utilized. A 1800 G alternating field was varied from five to 11 Hz for two hours each day for three

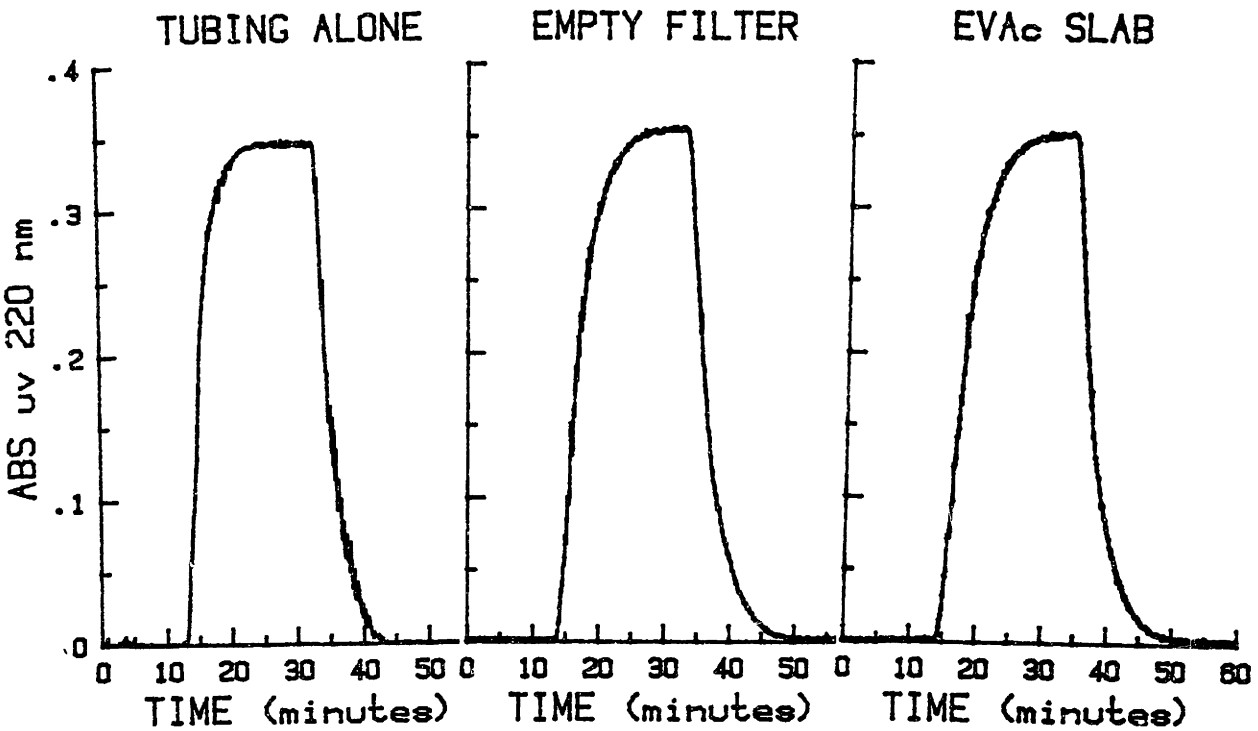

Figure 2: Flow profile for a BSA solution. Flow started into the circuit at 10 minutes and replaced with buffer at 30 minutes

.a tubing alone

.b tubing and an empty swinex filter

.c tubing and a swinex filter containing a slab of EVAc of dimensions of the matrices to be studied.

There was a delay from the time of injection until the rise in absorbance, and an exponential rise to peak and decay to baseline. The delay and rise times were all on the order of 4 minutes. The delay was due to the tubing that interceded between the site of injection and the spectrophotometer, and the exponential rise and decay were due to a small amount of mixing that occurred in the filter and tubing. There was, nonetheless, no significant difference in the three profiles.

weeks. Eighteen polymer slabs, each with nine magnetic beads, were studied in all; two groups of five samples at the extreme frequencies 5.0 and 11.0 Hz and two groups of four at 6.67 and 9.5 Hz. The samples were suspended on the ends of polyvinyl chloride rods which ran through the top of the caps of scintillation vials. The vials were filled with 10 ml of phosphate buffer and the solution changed two hours before field exposure, immediately after field exposure and two hours after field exposure. The ratio of the rate of BSA release during field exposure compared to the average of BSA release during the nonexposed times was used as the index of modulation.

III.3 RESULTS

III.3.1 Flow Through Dynamics Figure 2a-c shows that, despite some slight differences, the flow profile through the circuit was not altered by the addition of the tubing, filter or a slab of EVAc the dimension of the matrices to be tested. Figure 3 is a recording of the absorbance change for five different solutions of BSA and figure 4b is a standard curve that was determined by taking the heights of these peaks and plotting them against their concentrations. Figure 4a is provided as contrast. It is the standard curve that was generated when the solutions' absorbance was determined using standard cuvettes. The extinction coefficents in the two cases were 2.1 and 2.01 respectively and the two sets of data matched ($p>0.05$).

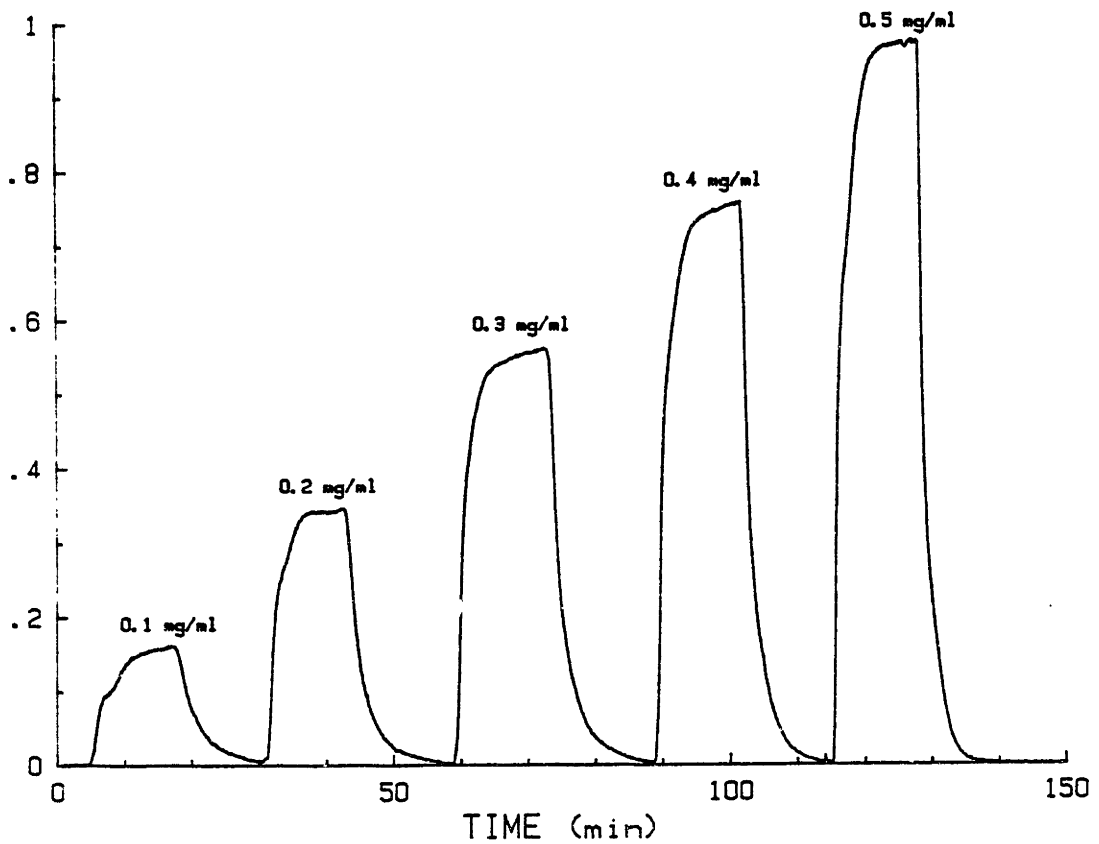

Figure 3: Absorbance at 220 nm achieved for injections of five different BSA concentrations, from 0.1 to 0.5 mg/ml, into the filter of the flow-through system. In all cases the absorption returned to baseline, indicating that none of the BSA adhered to the tubing or filter or was left in the flow cell. In addition, all peaks showed similar profiles.

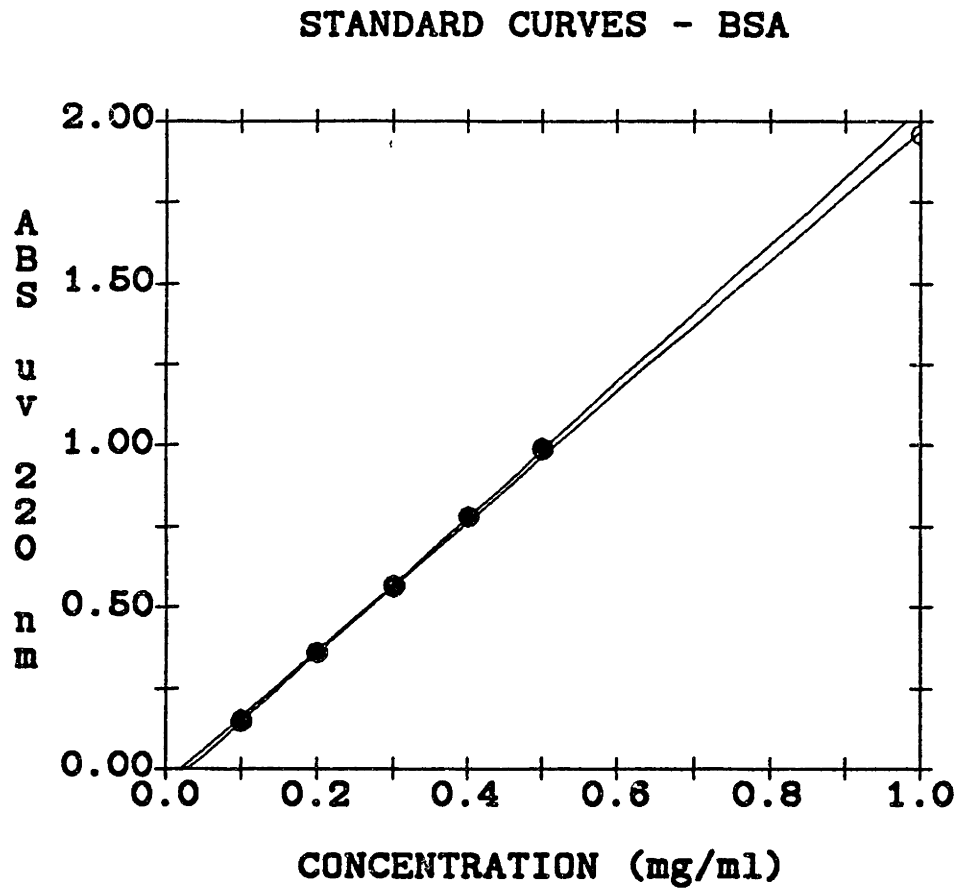

Figure 4(a) Standard curve generated from examination of the absorbance of six solutions using standard cuvettes (open circles).

(b) Standard curve generated from peaks attained in figure 3 using the flow through system (closed circles). The two curves were statistically indistinguishable ($p>0.05$).

III.3.2 Release Dynamics A representative sample of the strip chart recording output from the flow-through configuration is displayed in figure 5. The matrix was exposed to a 390 Gauss field for 10 minutes. The rise in the absorbance occurred 4 minutes after the magnetic field was applied, plateaued at this elevated level, and then returned to baseline 4 minutes after the field was withdrawn. The increased release remained at an elevated level for the duration of field exposure. The time constant of rise and decay, as computed from the time from baseline to 63% of peak and the time needed to fall 63% of the peak, were both 4 minutes respectively.

III.3.3 Refractory Time Figure 6-a and 6-b show the effect on modulation of the duration of the interval between repeated pulses. In the first figure there is ample time between pulses, and complete, identical response were observed. As less and less time was used between pulses of the magnetic field, reproducible peaks were still observed but the intervening return to baseline was obliterated. All of the peaks displayed responses that were within the time response of the system.

III.3.4 Magnetic Field Strength When the strength of the magnetic field was altered by adjusting the input voltage to the electromagnet, the amount of modulation changed accordingly. Figure 7 shows that, despite some minor changes due to mixing of the dissolved BSA in the filter and tubing, the shape of the peaks remained relatively the same over the range of different field strengths. The relationship between the extent of modulation and the strength of the applied magnetic fields ranging from

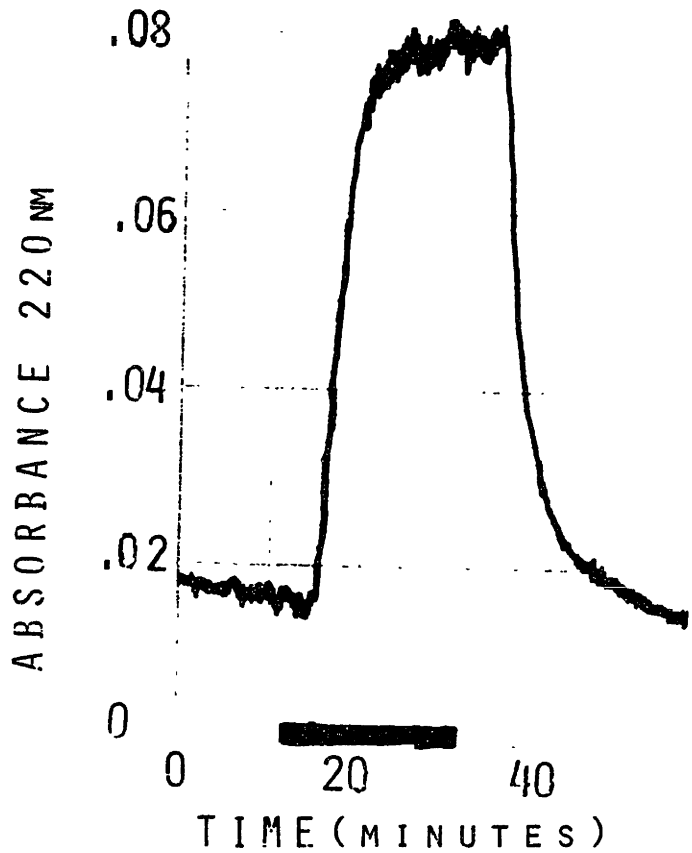

Figure 5: Increase in the absorbance from an EVAc-BSA matrix embedded with a cylindrical magnet and exposed to an oscillating magnetic field of 390 Gauss for 20 minutes. The extent of modulation was 7.4 . The dark bar at the bottom of the graph represents the time during which the field was applied.

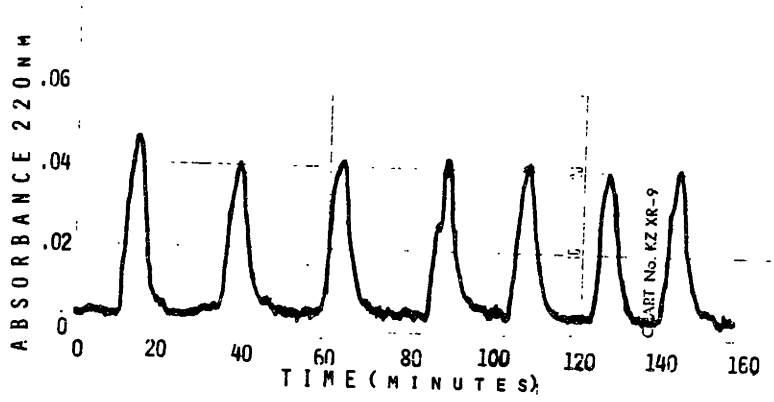

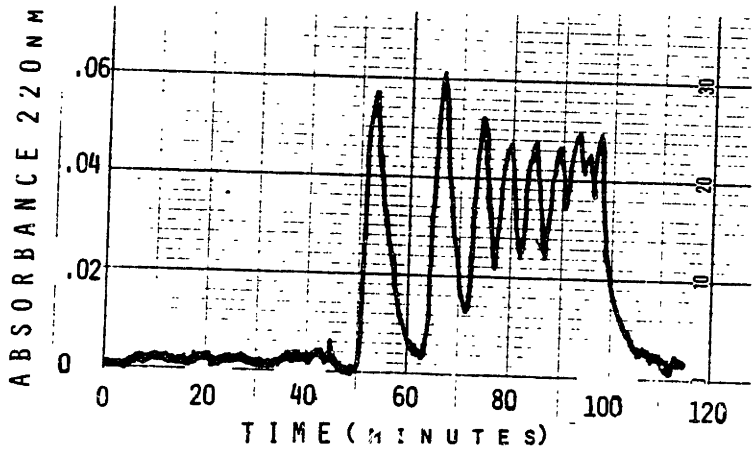

Figure 6: Depiction of the matrix response to pulses of a 60 Hz, 500 G electromagnetic field applied for 4 minutes. The interval between pulses was decreased from (a) 20 to 10 minutes and (b) from 7.5 to 0.5 minutes. The peak response was identical, highlighting the reproducibility of the system. Once the peak was attained it did not fall but the return to basline was obliterated because of mixing in the filter and tubing.

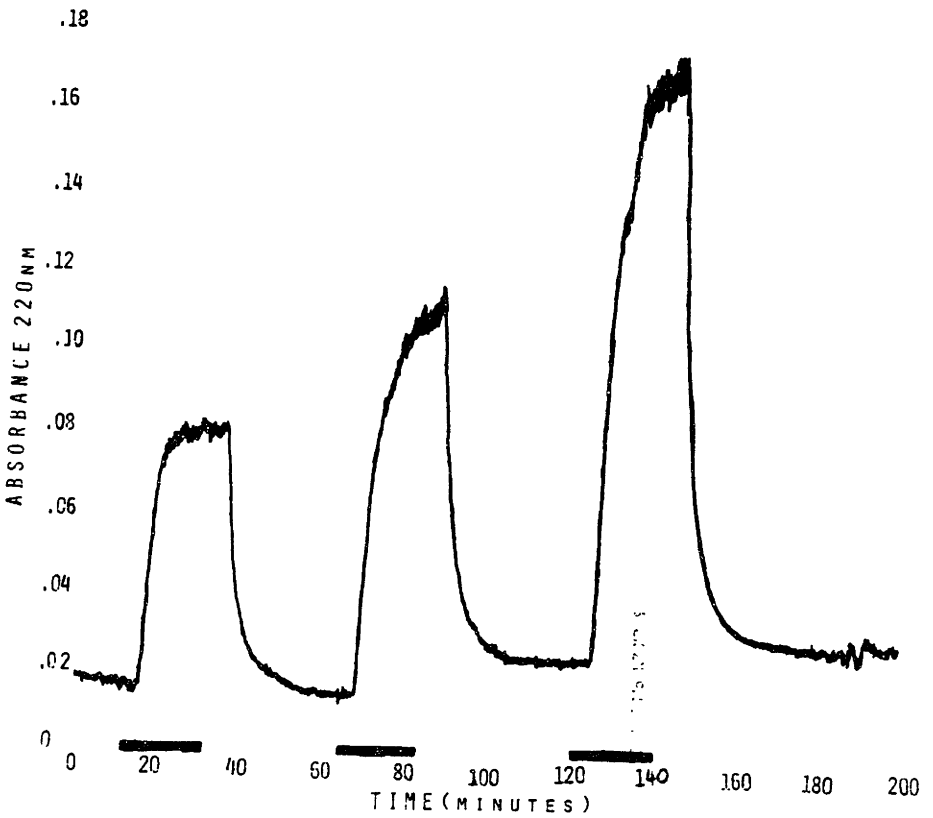

Figure 7: Dynamic responses of a polymer matrix, examined in the flow-through set-up, to to 20 minute pulses of 390, 550 and 650 G. The extent of modulation was 7.4, 10.5 and 16.0 respectively. The dark bars at the plot bottom represent the duration of field exposure.

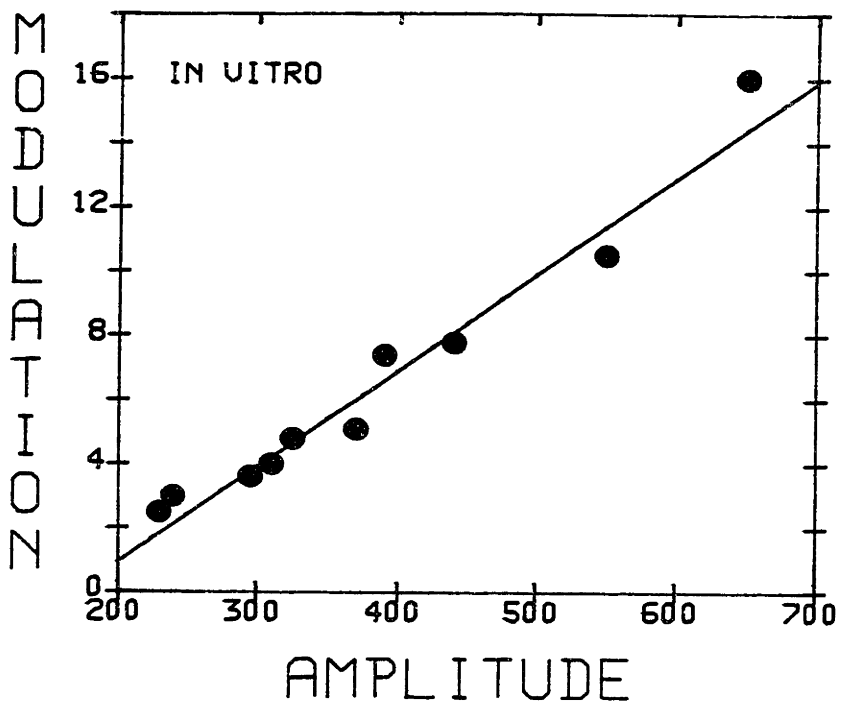

Figure 8: Extent of modulation plotted against the strength of the applied magnetic field. The matrices were placed in the flow-through setup and subjected to fields of different strengths. The field strength was varied by adjusting the input voltage to the electromagnet. A linear fit revealed a slope of 0.03 (R^2 = 0.962).

200 to 700 G is illustrated in figure 8. A linear regression fit to this data yielded a line with a slope of 0.03 (R^2 = 0.962).

III.3.5 Magnetic Field Frequency The mechanical turntable allowed for variation of field frequency from 5.0 to 11.0 Hz. In this range a difference in release rates was observed. Figure 9 shows that as the frequency increased the amount of modulation rose in a linear fashion (R^2 = 0.996) with a slope of 0.59.

III.4 DISCUSSION

The reproducible modulation of BSA release was demonstrated in the last chapter. In the experiments described above the ability to control the extent and form of modulation was described. In addition, the system was shown to respond, within a range of field strengths and amplitudes, rapidly, linearly and stabily. The dynamics of modulated release have to be interpreted in light of the characteristics of the flow through system. The tubing and filter dictated that the spectrophotometric detection of events occurring at the matrix were delayed. In addition, the volume of these components allowed for a minor amount of solute mixing to occur. Thus, the absorbance rose in an exponential fashion when boluses of BSA solution were injected into the system. The time constant of the rise was about 4 minutes and was identical to the amount of time needed to decay to baseline.

Figure 5 showed that the baseline release in the absence of any applied stimulus was constant. When an oscillating magnetic field was

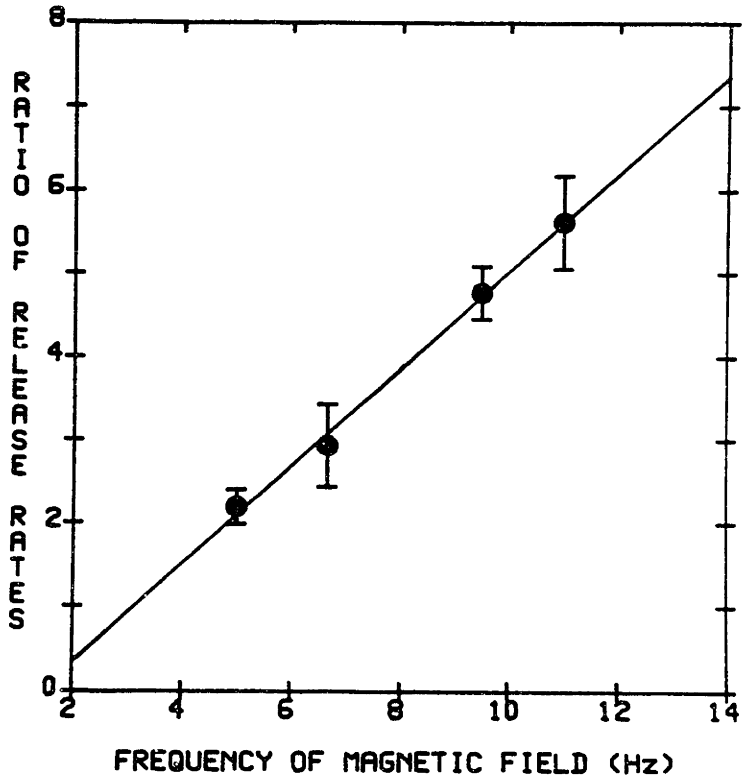

Figure 9: The variation in the extent of modulation achieved when the frequency of the magnetic field oscillation was altered from 5 to 11 Hz was linear with a slope of 0.59 (R^2=0.996). The magnetic field was generated from a mechanical device which rotated permanent bar magnets beneath samples suspended in phosphate buffer in scintilation vials. As the velocity of the plate bearing the magnets was varied the field frequency was changed accordingly.

applied to a matrix embedded with a high strength magnet an increase in BSA release was observed. The rise in absorbance after the field was applied, and the return to baseline after the field was withdrawn, occurred within the expected system time delay. The time constants of the exponential rise and decay were identical to the expected time constants of the system. Thus, within the sensitivity of our measurements, the matrix response to the magnetic field was instantaneous; rising immediately to peak after the field was applied, falling immediately back to baseline after the field was withdrawn.

As noted, the reproducibility of this system has already been discussed in chapter II, and figure 6 of this chapter graphically illustrates how consistent the results can be. In addition, there appears to be no significant refractory time. Matrices stimulated as early as 30 seconds after prior stimulation responded without attenuation. The return to baseline was obliterated because the time between pulses was decreased below the sensitivity of the system. At the flow rates and tubing lengths used events occuring faster than 4 minutes apart could not be adequately detected. Nonetheless, the elevated level of drug release was maintained for the duration of magnetic field exposure, and for repeated pulses independent of the rest time. Once the peak release rate was attained it was maintained at a stable level until the field was 'turned off' and did not decay with time.

The results obtained at the different frequencies and amplitudes indicate that these parameters can be used to control the amplitude of a response. The duration of the modulated release could be controlled by

alteration of the length of the stimulus. Therefore, an implanted matrix could be controlled externally. Large single pulses or prolonged intermediate elevated levels can be obtained by proper choice of these three parameters. The increase in modulation observed as the frequency and amplitude of the magnetic field were increased may represent the effect of more and stronger pulsations of the matrix. When the frequency was increased there were more interactions on the matrix by the magnet per unit of time. As the strength of the field was increased the force on the magnet and the power of each pulsation increased. The only question is whether it is logical to assume that the response to increasing both will rise in linear fashion continuously?

When a sinusoidal strain is applied to a linear, viscoelastic material, the resulting strain will be sinusoidal at the same frequency, but out of phase with the force. This is illustrated in figure 10 [2]. The phase angle is related to the time it takes for the material to respond to the stimulus. An ideal elastic material follows Hooke's law, and has a phase angle of zero. If the response, or relaxation, time is greater than the period of the stimulus sinusoid, the successive stimulus arrives before the material has had time to finish responding to the previous stimulus. This leads to an attenuation of the response. For sinusoidal staedy state systems, evaluation of this phenomena is embodied in terms of the phase angle, δ. This is the degree to which the response is out of phase with the stimulus. For a stimulus at a frequency ω, the response goes as $r = R \sin(\omega t + \delta)$. (R is a constant).

In the case where the material can be modelled by an ideal two or three element system, there is one time constant associated with the entire system. The phase angle can then be related to the frequency such that $\tan(\delta) = \omega\tau$, where τ is the viscoelastic relaxation time of the polymer material. If the degree to which the two signal are out of phase, $\tan(\delta)$, exceeds half of the period of the stimulus oscillation, $\omega\tau$, the response will be impinged upon, for there will not have been a response before the next wave of stimulus.

HARMONIC OSCILLATION-Maxwell Element Material

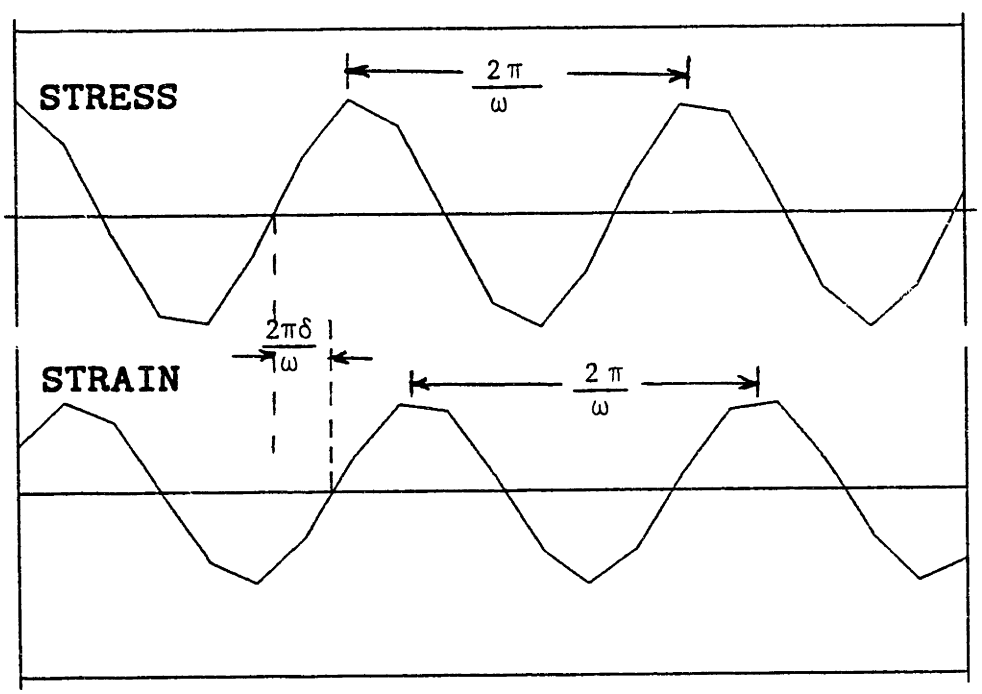

Figure 10: Stress and strain curves for a Maxwell element model of a polymer material. When an oscillating stress or strain is applied to a material, the resulting strain or stress will oscillate at the same frequency, but out of phase. This phase is the time it takes for the material to respond to the stimulus and has been identified as the loss angle, δ.

The phase angle can be measured for a given material using standard dynamic strength of materials testing procedures. A description of the tests and the results of the data analysis are presented in appendix A. The tangent of the phase angle fell within a narrow ranged from 0.2 to 0.3, as the frequency was varied from 1 to 60 Hz. Thus, the time response of the EVAc material was very fast, on the order of a msec, and it would be expected that the system could respond to modulation of increasing frequencies up to about 500 Hz. This crude analysis does not take into account the inertia of the magnet or other properties of the magnet-matrix system. In addition, it assumes that the material can be modelled as possessing one time constant. In truth, the EVAc matrix is probably a complex material with a hierarchy or superposition of time constants. If so, the stress will still lead the strain as depicted in figure 10, but the phase angle computation will be far more complex than what was presented above. More rigorous analysis and more detailed examination of the system at higher frequencies is warranted for the future.

REFERENCES

[1] Rhine, W., D. Hsieh, and R. Langer, Polymers for Sustained Macromolecule Release: Procedures to Fabricate Reproducible Delivery Systems and Control Release Kinetics. J. Pharm. Sci., 69:265-270 (1980)

[2] Nielsen, L.E., "Mechanical Properties of Polymers", Reinhold Pub. Co., NY (1947)

CHAPTER IV: MATRIX-MAGNET PROPERTIES

IV.1 INTRODUCTION

The previous chapters demonstrated the modulated release of BSA from an EVAc matrix and showed how control of the parameters that governed the the applied magnetic field could be used to control the response of the matrix. In this chapter the properties of the matrix and the embedded magnet will be studied to determine the extent to which they control the matrices' response.

A number of studies of EVAc based delivery systems have indicated that the kinetics of the sustained release of drugs could be accounted for by the geometry and morphology of the drug-polymer matrix [1-4]. Scanning and transmission electron micrographs of microtomed sections of the matrices at different points into the course of drug release established the existence of a network of interconnecting pockets [2,3]. A schematic of this morphology is presented in figure 1. The dimensions of the pockets were on the order of the size of the macromolecule powders and it was concluded that they were formed at the time of matrix fabrication. Since the drug or macromolecules were insoluble in the solvent used to dissolve the polymer, the drug remained intact in the solution. When the drug-polymer solution was cast the drug displaced the polymer material and when the matrix hardened a tortuous network of drug pockets connected by smaller channels was formed. The connecting channels were 1 to 10 microns

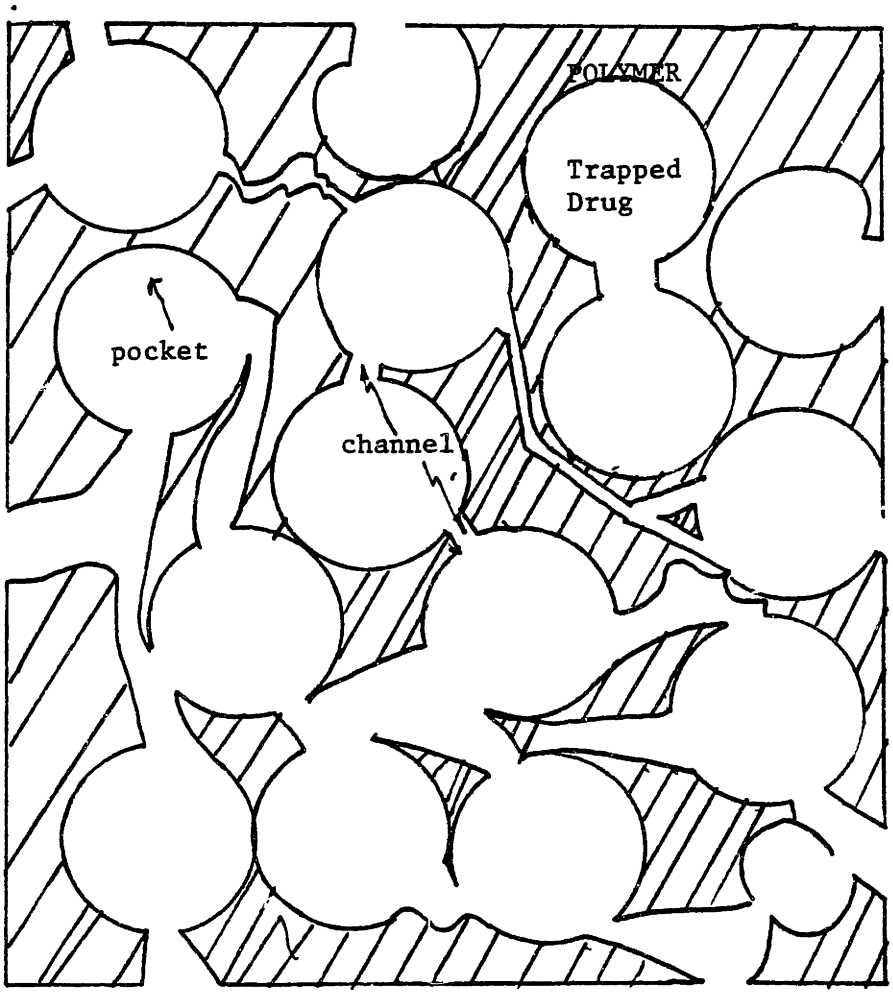

Figure 1: Schematic of the internal morphology of an EVAc-BSA matrix. The BSA created pockets were surrounded by walls of EVAc. The size of the pockets were on the order of the particle size of the dry powdered protein. The pockets were connected to each other by smaller channels to form a tortuous network within the matrix. The tortuosity of the matrix and the existence of the small interconnecting channels can account for the sustained release of protein. At low drug loadings and particle sizes some of the pockets are isolated and never communicate with the surface. The drug that resides within them is forever trapped within the matrix.

in diameter [2]. The drug resided in the pockets and was dissolved by water entering the pockets through these channels. The solubilized drug diffused through the matrix, from pocket to pocket, by way of the interconnecting channels until the surface was reached and the drug was released into the surrounding media. Some pockets never communicated with the external environment and the drug that resided within them was forever trapped inside the matrix. This especially occurred at the lower drug loadings and particle sizes. The form of this network and the relationship between the pockets and the connecting channels were used to formulate a statistical model to predict release rates from these matrices [4].

It was already shown that the form and extent of the matrix' response to an applied magnetic field could be determined by the duration, amplitude and frequency of the field. This chapter describes investigations into the influence of the properties of the matrices and the embedded magnet upon modulation when the field parameters were held constant. The modulated release from matrices of different sizes and shapes and the use of embedded objects of different geometries and magnetic strengths was examined.

At various times during release the polymer matrices were examined to search for changes in the matrix morphology that could explain the observed release kinetics. The amount of drug that was trapped in the matrix was quantified. A scanning electron microscope was used to search for surface effects, light microscopy of microtome sections of the matrices was used to visualize the matrix interstices and video recordings

of magnified images of the matrices when exposed to oscillating magnetic fields were utilized to observe the system 'in operation'.

In this chapter the methods and results for each of the four subtopics are presented together. The first subtopic deals with the effect on modulation of the embedded magnets, the second, the effect of the matrices on release regulation, and the third and the fourth, the influence of the combined magnet-matrix unit. The third section refers to a possible macroscopic model that incorporates all data presented so far, and the fourth is a discussion of the morphological examination of the matrix unit. A unified discussion of all of these sections follows at the end of the chapter.

IV.2 METHODS and RESULTS

All the matrices used in this chapter, like all the matrices studied in this thesis, were dispersed with BSA seived to a particle size range of 150-180 microns, at a 33% loading, and examined at room temperature.

IV.2.1 MAGNETS

The modulated release from matrices embedded with three different magnetic objects was studied in the following experiments. The extent of modulation that was achieved when the position and orientation of the objects were varied was investigated, as well as, the difference observed when the different objects were embedded in the matrices. The three objects were displayed in figure II.1.b. They included, 11 mg, 1.4 mm

diameter, stainless steel spheres (80% iron, 17% chromium) which were slightly magnetic, and cylindrical or torroidal samarium cobalt magnets coated with nickel and magnetized to 1100 Gauss. Both magnets were 1.35-1.45 mm long. The cylinders weighed 15 mg and had a diameter of 1.5 mm. The torroids weighed 60 mg and had an inner diameter of 1.5 mm and an outer diameter of 3.0 mm.

IV.2.1.i Embedded Magnet Position:

Magnetic Spheres The magnetic spheres embedded in matrices protruded from the surface of the polymer slabs, though they were at all times covered by polymer material. The extent of this protrusion was measured by subtracting the average width of the polymer sample at nine places along the edge of a slab from the average width taken at points over the nine spheres in a sample. The extent of protrusion was then contrasted to the average ratio of release rates achieved for given slabs. The magnetic fields applied to these matrices were generated from the mechanical turntable device and were approximately 1800 G at 0.87 Hz.

The effect on release rate of the position of the magnetic spheres within the polymer slab is illustrated in figure 2. The average ratio of release rates for the ten samples is plotted against the degree to which the spheres extended from the flat surface of the sample slab face. While little, if any, modulation was observed at depths less than 0.75 mm from the slab face, there was a precipitous rise in the effect thereafter.

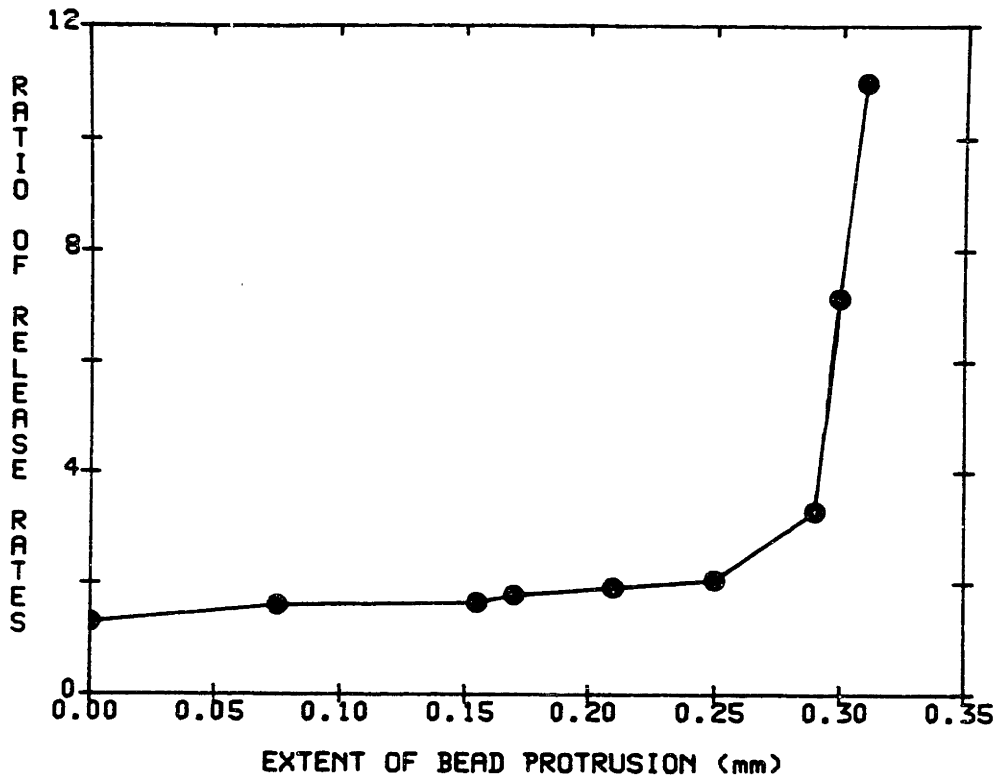

Figure 2: The extent of modulation plotted versus the extent of protrusion of the magnetic spheres (mm) from the surface of the polymer matrices. The matrices were slab shaped and fixed to polyvinyl chloride rods mounted in scintillation vials. The 1800 G, 0.87 Hz magnetic field was generated from the rotating permanent magnets.

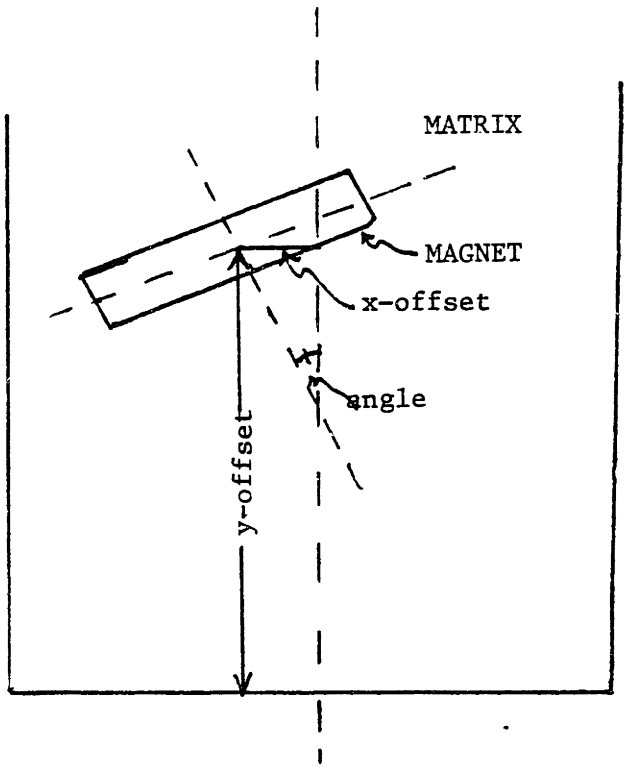

Figure 3: The position and orientation of the $SmCo_5$ magnets were determined from radiographs of the matrices taken in three orthogonal directions. A line was drawn through the true vertical of the matrix and was used as the axis of the matrix. The horizontal and vertical axes of the magnets were defined from lines drawn along the true vertical and horizontal of the magnet. The intersection of these lines was the center of the magnet and the lateral displacement of the magnet center from the matrix axis was used as the x-offset of the magnet. The y-offset was the distance between the magnet center and the matrix bottom. The orientation of the magnet within the matrix was computed from the angle that the vertical axis of the magnet deviated from the vertical axis of the matrix. A perfectly aligned magnet had an angle of 0, the cosine of which is 1. Magnets completely misaligned yielded an angle whose cosine was 0.

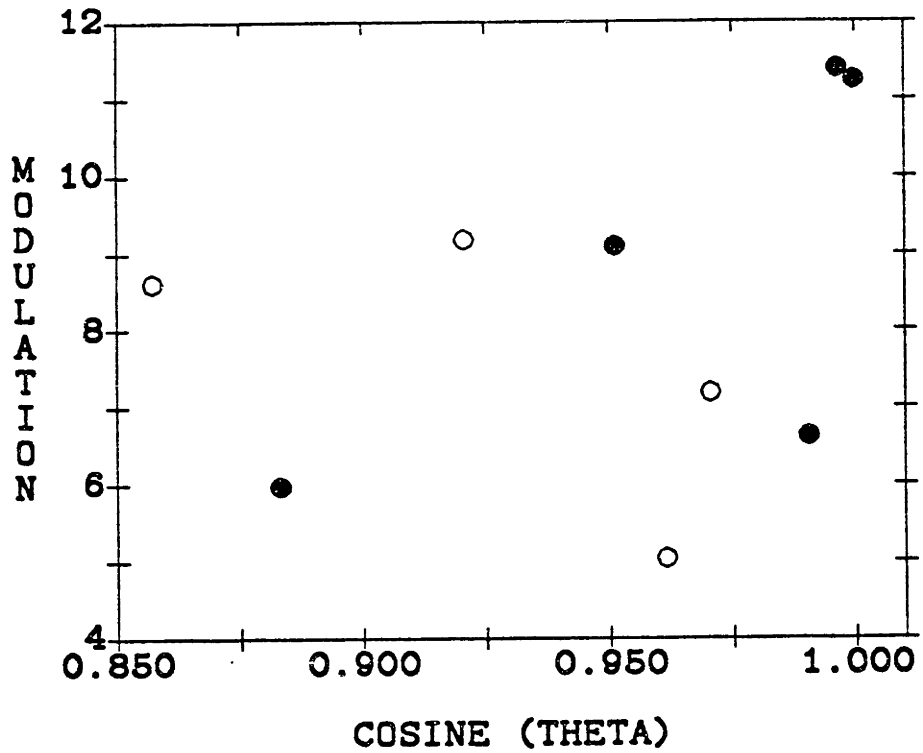

Figure 4: The extent of modulation plotted against the cosine of the angle of orientation of the embedded magnet with respect to the applied field. There is no statistically significant identity between the two parameters. A 650 G, 60 Hz field was generated by the electromagnet and applied as 20 minute pulses to four matrices with cylinder magnets (open circles) and four matrices embedded with torroidal magnets (closed circles). This data represents the average of 40 field exposures over the course of 2 weeks.

$SmCo_5$ Magnets The geometric anisotropy of the magnetic spheres made it impossible to determine the alignment of their pole vectors with respect to the field. The samarium cobalt magnets on the other hand, had a very definite shape and the orientation of the magnet in the field could be determined. In the following experiment the degree of alignment of the magnet with respect to the field, and the lateral and longitudinal position of the magnet in the matrices were established. This data was then used to see if it could explain the difference in the extent of modulation achieved from different matrices.

Torroidal and cylindrical magnets were embedded in cylindrical matrices (radius = 3 mm, height = 6 mm). The matrices were fabricated by the second of the techniques discussed in section II.2.2 . This involved pouring the BSA-EVAc mixture into a tubular glass mold that rested on dry ice and had been precooled for 10 minutes. The magnets were held with a plastic forceps over the tube filled with the hardening mixture and dropped into the mixture after various times had elapsed. The different times between pouring and dropping left the magnet at different positions in the matrix after complete hardening. Radiographs of the matrices were taken in three orthogonal directions using a standard clinical x-ray machine. A 44 kvolt pulse of 120 mA was exposed to the matrices for $1/30^{th}$ of a second. The position and orientation of the $SmCo_5$ magnets were determined, as depicted in figure 3, from these radiographs. A line was drawn through the true vertical of the matrix and was used as the axis of the matrix. The horizontal and vertical axes of the magnets were defined from lines drawn along the true vertical and true horizontal of the magnet. The intersection of these lines was the center of the magnet

and the lateral displacement of the magnet center from the matrix axis was used as the x-offset of the magnet. The y-offset was the distance between the magnet center and the matrix bottom. The orientation of the magnet within the matrix was computed from the angle that the vertical axis of the magnet deviated from the vertical axis of the matrix. The cosine of this angle was 1 for a perfectly aligned magnet, and 0 for magnets completely misaligned. The orientation angle cosine was compared to the extent of modulation from matrices exposed to 500 G, 60 Hz oscillating magnetic fields for 20 minutes. A total of 40 field exposures were applied over the course of 2 weeks.

The relationship between the magnet alignment and the extent of modulation is displayed in figure 4. No obvious correlation existed between the modulation and the orientation of the magnet alone. The extent of modulation and the orientation and position of the magnets are presented in appendix G.

IV.2.1.ii Embedded Magnet Shape The extent of modulation from matrices fabricated in the cylindrically shaped molds (section II.2.1) and embedded with either cylindrical or torroidal $SmCo_5$ magnets was examined. Six matrices were made with a single torroid, and six with a single cylinder, and both sets of matrices subjected to a 60 Hz oscillating magnetic field from the electromagnet, at a strength of 500 G, under the same conditions described in the last section.

The data from these two experiments is summarized in Table I. It shows that, there was a significant difference between the use of the

different shaped magnets, cylindrical or torroidal ($p<0.05$).

TABLE I: EXTENT OF MODULATED BSA RELEASE FROM EVAc MATRICES WITH TORROIDAL AND CYLINDRICAL $SmCo_5$ MAGNETS

$SmCo_5$ magnets 500 G, 60 Hz	EXTENT OF MODULATION
CYLINDRICAL (n=6)	7.54 ± 1.19
TORROIDAL (n=6)	11.31 ± 1.89

IV.2.2 MATRICES

The sustained release of proteins and other macromolecules from EVAc matrices immediatley after being placed in solution was different than the steady state release achieved later in the course of experiments [1]. During the first 1 to 2 days BSA was detected at much higher concentrations than were observed later. Furthermore, the rate of release was independent of temperature implying that diffusion was not the factor determining or limiting release. This pattern was attributed to the dissolution of surface protein that did not have to travel through the tortuous network of channels and pockets within the matrix before being released from the matrix. In addition, other studies showed that the form of release was strongly influenced by the size and shape of the matrices [5]. In the experiments that follow the pattern of modulation from matrices early in release were examined and the extent of modulation for different size and shape matrices was investigated.

IV.2.2.i Effect Onset The maximum amount of modulation was not observed immediately after release was intiated. Three sets of polymer matrices were studied to establish the determining factors in achieving the maximum effect. Electromagnetic, 60 Hz fields of 650 G were applied to the cylindrical matrices containing one torroidal magnet each, for 20 minutes out of every hour, for 12 hours a day. All the matrices were mounted to the end of a polyvinyl chloride rod with a drop of ethylene-vinyl acetate. The rod was passed through the top of a scintillation vial cap so that the bottom of the matrices rested just above the bottom of the vial. Ten ml of 0.1 M phosphate buffer was placed in the vial and replaced with fresh buffer every 20 minutes. The absorbance at 220 nm was measured from the replaced solution and a rate of BSA release determined. One set of matrices was placed in the scintillation vials with 10 ml of the buffer and immediately exposed to the fields. There were five matrices in this group and the group was called "non-released, non-triggered". A second set was placed in the vials with the buffer but not exposed to the fields until 24, 48, or 72 hours after release. This was termed the 'pre-released' group. A third set was exposed to the 650 G fields every 20 minutes on the hour but buffer was not added until 24, 48 or 72 hours after the intiation of field application. This meant that the matrices were exposed in the absence of any release media to 12, 24, 36 field exposures, respectively, before they protein could be released. Thus, this group was classified as 'dry pre-triggered'. The extent of modulation was determined for all of these cases and compared.

The criteria for peak or maximum modulation was that the peak response to four successive pulses of the same field, be within 10% of each other. The number of field applications necessary to achieve this peak after release was intiated, is detailed in table II for the three different cases. It shows that each group required 4 field exposures after protein release had been intiated by submersion of the matrix in phosphate buffer. This number was the same whether or not the matrices had been exposed to magnetic fields prior to release or not. Further, if polymer matrices were placed in buffered solution and immediately exposed to an oscillating magnetic field, 48 hours of release was needed before the peak effect was observed. The group of matrices that was exposed to the magnetic fields 'dry', ie. they were not placed in buffered solution until the third day, also required an additional 48 hours of release before peak modulated release was observed. In contrast, those matrices that were released in buffered solution for 48 hours or more before any magnetic field was applied, achieved a peak effect after about 4 applications of magnetic fields, and no additional release was needed.

IV.2.2.ii Amount of Trapped Drug Mass balance studies on EVAc-BSA polymer matrices not exposed to magnetic fields have revealed that a certain percentage of the embedded protein is trapped within the matrix and never released [1]. The amount of protein that remained in matrices after BSA was no longer released in detectable amounts was determined for 18 matrices embedded with 9 magnetic spheres each. Release of less than 15 ug per day was deemed undetectable release, for it was below the sensitivity of our assay. Ten of the matrices were exposed to an 1800 G, 11 Hz magnetic field generated by the magnet rotating device, for two

TABLE II:

TIME AND NUMBER OF FIELD EXPOSURES NEEDED TO ACHIEVE PEAK MODULATION FOR PRERELEASED, PRETRIGGERED AND NONTRIGGERED, NONRELEASED MATRICES

		PEAK ATTAINED AFTER ADDITIONAL RELEASE (hours)	FIELD EXPOSURES (#)
NON-RELEASED NON-TRIGGERED	(n=5)	48	4 ± 2
PRE-RELEASED (n=3)	24 hours	24	4 ± 0
	48 hours	0	5
	72 hours	0	4
PRE-TRIGGERED (n=3)	12 triggers	48	3 ± 1
	24 triggers	48	4
	36 triggers	48	4

hours a day, five days a week and 8 matrices were examined at rest. The intial amount of BSA in the exposed group was 84.2 $\pm$ 0.22 mg and 84.74 $\pm$ 0.43 mg in the non exposed matrices, and as in all the the experiments, 33% loading of BSA seived to a 150-180 micron range was used. The amount of trapped drug was calculated by subtracting the net amount released at the time of negligible release, from the total amount embedded in the matrix at the time of fabrication, and then dividing this value by the intial quantity of drug.

$$\text{percent trapped} = \frac{\text{intial amount - amount released}}{\text{intial amount}}$$

The percent of total BSA trapped in matrices after release could no longer be detected with the absorbance assay is displayed in table III. Over 30% of the original protein remained in matrices that were not exposed while only 5% was left in the exposed group.

TABLE III: PERCENT OF EMBEDDED BSA REMAINING IN EVAc MATRICES EXPOSED AND NOT EXPOSED TO OSCILLATING MAGNETIC FIELDS

nine magnetic spheres in flat slab matrices	percent remaining BSA
NOT EXPOSED CONTROLS (n=8)	31.2% $\pm$ 3.5
EXPOSED (1800 G, 11 Hz) (n=10)	5.5% $\pm$ 5.1

IV.2.2.iii Matrix Geometry The role of the form and shape of the polymer matrix in achieving modulated release was examined. Different shape molds were used to cast three different shaped matrices.

Glass molds, 5.0 cm x 5.0 cm x 2.5 cm, were used to cast long BSA-EVAc slab matrices. Smaller units 1.0 cm x 1.0 cm x 0.2 cm were excised from the larger slab. Torroidal samarium cobalt magnets were embedded within these slabs as described in sections II.2.1 and IV.2.1 . Cylindrical matrices were made from molds either 1.0 cm high and 1.0 cm wide or 1.5 cm high and 1.5 cm wide. The matrices shrunk after the solvent evaporated and the final approximate volumes of matrices made in these molds was 0.226 cm^3 and 0.95 cm^3, respectively. All the matrices were embedded with one magnet each.

A 500 G magnetic field was generated from the electromagnet. This 60 Hz field was applied to the matrices for 20 minutes. In a 14 day period a total of 40 exposures were applied. The extent of modulation was determined for the different shaped matrices and is displayed in table IV. Matrices with a net volume of 0.226 mm^3 did better than the larger cylindrical matrices and the smaller flat slabs.

TABLE IV: EXTENT OF MODULATED BSA RELEASE FROM EVAc MATRICES OF DIFFERENT SIZES AND SHAPES

1 torroidal $SmCo_5$ magnet	500 G, 60 Hz
FLAT SLAB MATRIX n=3 ($0.089\ cm^3$)	2.5 ± 0.16
CYLINDRICAL MATRIX n=6 ($0.226\ cm^3$)	11.31 ± 1.89
CYLINDRICAL MATRIX n=3 ($0.95\ cm^3$)	5.21 ± 0.30

IV.2.3 MAGNETS and MATRICES

IV.2.3.i Volume of Influence The influence of the volume of the matrix on modulated release was examined in the following experiment. Cylindrical matrices were embedded with magnets at various distances from the bottom face of the matrix. This was accomplished by varying the amount of time between the pouring the polymer-BSA solution into the glass mold and the dropping of the magnet into the matrix. Radiographs of the matrices were taken in three orthogonal projections and the position of the magnet within the matrix was determined. Matrices were subjected to 20 minute pulses of 500 G, 60 Hz magnetic field for a total of 40 field exposures in 2 weeks, release of BSA monitored, and indices of modulation established as described above.

The volume of matrix that was encompassed by an imaginary sphere with a radius of 1.5 mm plus the radius of the embedded magnet (0.7 mm for the cylinders and 1.5 mm for the torroids), was numerically determined using a VAX-11 computer (Digital Equipment Corp., Maynard, MA, the program listing is in appendix F). The origin of the sphere was the center of the magnet. The 1.5 mm value was used because video recorded magnified images revealed that only matrix material within 1.5 mm of the embedded magnets were observed to move under deformation by the magnets (section IV.2.4.iv). The computer program generated a random array of points in and about the cylindrical matrix. If the points fell within the intersection of the sphere and the matrix the points were added to a running tally. The total number of points in the tally represented the integrated intersecting

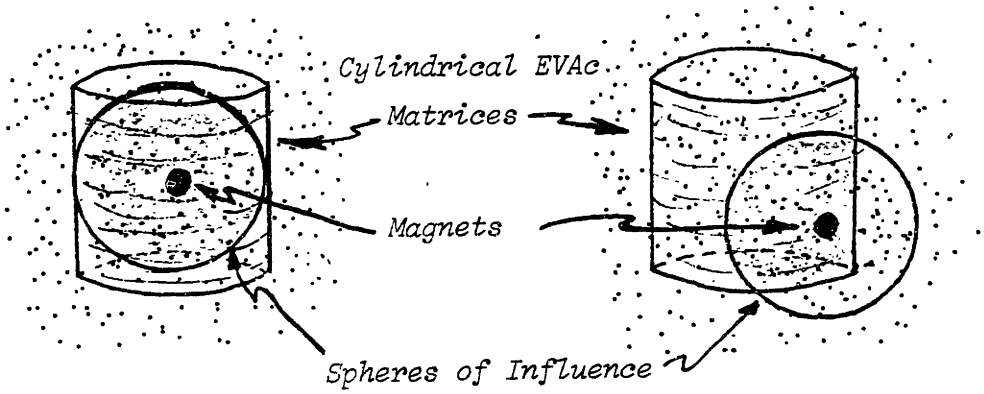

Figure 5: The volume of influence or activation was determined from the intersection of an imaginary sphere, of radius 1.5 mm plus the magnet radius, within the cylindrical matrix. The center of the sphere was the center of the magnet within the matrix. Panel (a) shows the ideal case, where the radii of the sphere and the cylinder exactly coincide. In contrast, panel (b) shows the typical situation where the magnet was slightly off-center.

volume. A characterization of this method is presented in figure 5. The value that was obtained was then multiplied by the cosine of the angle of the magnet orientation with respect to the vertical. This was done to account for the attenuation in displacement due to misalignment, since the force exerted by the magnetic field is equal to the strength of the magnetic field times the cosine of this angle (section IV.3). The aligned volume was then compared to the extent of modulation achieved for matrices made with torroidal or cylindrical magnets. In the case where the sphere and matrix perfectly overlapped and the magnet was perfectly aligned with the field, ideal volumes could be computed for the two magnets. The ideal volume in the matrices with the cylinders was 11.79 cm^3 and, for the matrices with the torroids, was 13.66 cm^3.

The relationship between the aligned volume and the extent of modulation for the two populations of matrices is presented in figures 6 and 7. Within the middle range of volumes a linear relationship was obtained for both sets of data. Matrices embedded with the cylindrical magnets had a slope of 4.61×10^{-2} ($R^2 = 0.9405$) and those with torroidal magnets a slope of 3.61×10^{-2} ($R^2 = 0.9799$). One of the data points fell more than 3 standard deviations from the expected value. Examination of the embedded magnet revealed its hole had been drilled eccentrically (figure 8). None of the points exceeded the modulation expected for the ideal volumes.

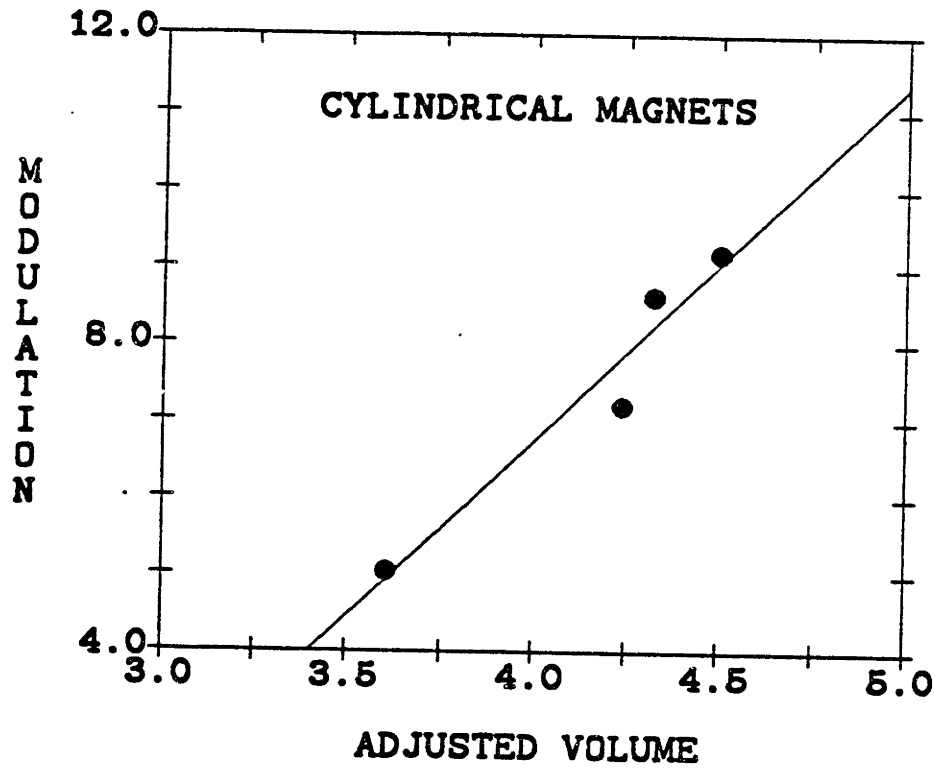

Figure 6: The extent of modulation plotted against the calculated volume of influence (mm^3 x 10^2) for EVAc-BSA matrices embedded with cylindrical magnets. A linear fit revealed a slope of 4.61 (R^2 = 0.941) . The matrices were exposed to 20 minute pulses of 650 G electromagnetic fields oscillating at 60 Hz. This data represents the average of 40 field exposures over the course of 2 weeks.

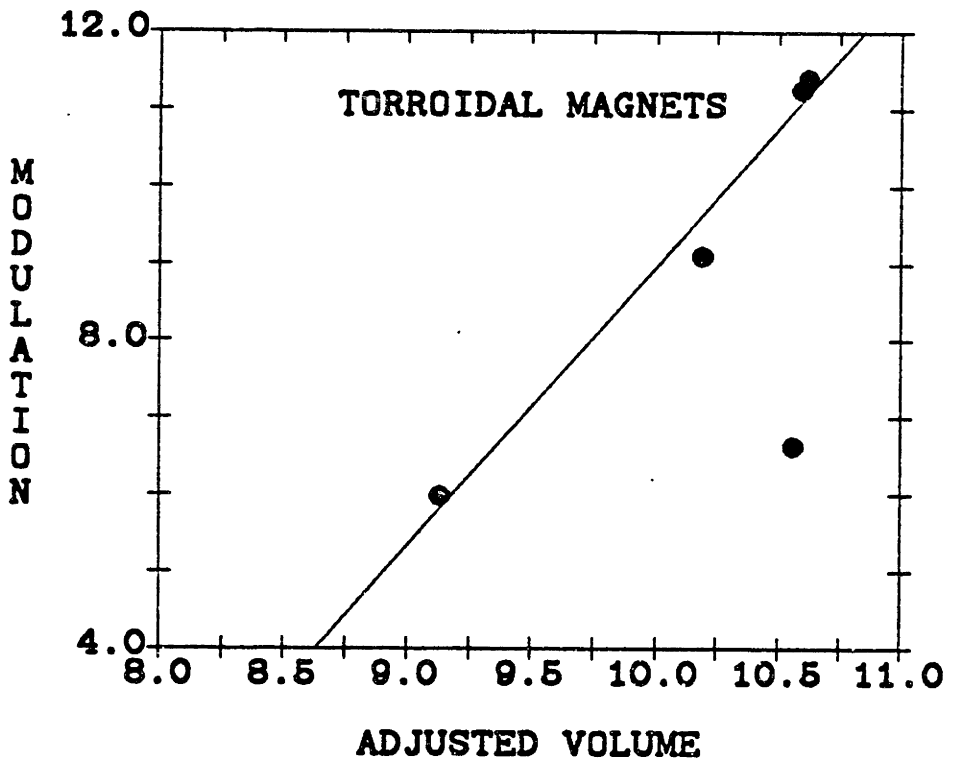

Figure 7: The extent of modulation plotted against the calculated volume of influence (mm^3 x 10^2) for EVAc-BSA matrices embedded with torroidal magnets. A linear fit revealed a slope of 3.61 (R^2 = 0.9799) . The matrices were exposed to 20 minute pulses of 650 G electromagnetic fields oscillating at 60 Hz. This data represents the average of 40 field exposures over the course of 2 weeks.

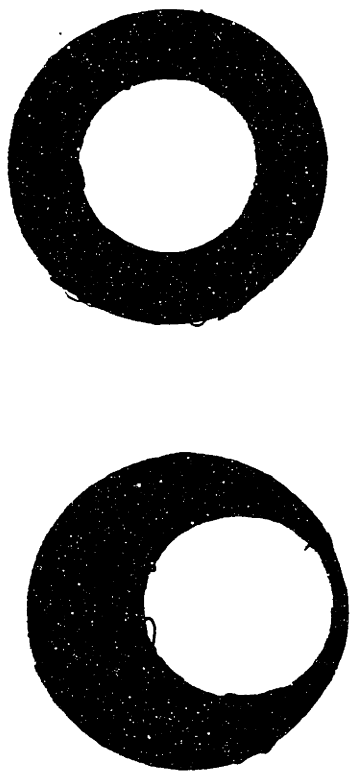

Figure 8: The eccentrically shaped torroidal magnet that led to significantly aberrant release is contrasted to a more 'normally' shaped magnet.

IV.2.4 MATRIX MORPHOLOGY

Matrices were examined at progressively higher magnifications to visualize the pattern of drug release and potential changes in matrix morphology with exposure to magnetic fields.

IV.2.4.i Radiograph Light Box The pattern of BSA remaining in matrices at various times into the release could be observed when the flat slab matrices, 1.0 x 1.0 x 0.2 cm^3, were placed against the high contrast background of a radiograph light box. These matrices were embedded with the magnetic spheres and exposed to 1800 G magnetic fields from permanent magnets rotated at 9.5 Hz. Light was transmitted through the virtually translucent copolymer material and refracted by any residual protein. After release had slowed to almost indetectable amounts, matrices never exposed to magnetic fields revealed a random array of isolated pockets of residual drug, while, in matrices embedded with magnetic spheres only those areas far from the spheres showed this arrangement. Few, if any, pockets of BSA were visible adjacent to the magnetic spheres. As the distance from the sphere increased so did the density of the residual pockets. Interestingly, the areas of matrix cleared of trapped BSA by two adjacent spheres did not overlap. In the areas of matrix between neighboring spheres pochets of trapped BSA were visible; similar to the control case.

IV.2.4.ii Microtome Sections The interstices of the cylindrical matrices used in the experiments in section IV.2.3.i were studied from cut sections three months after release had been intiated. Release from these matries had ceased to be detectable. Control matrices that had never been released were also examined. Matrices were embedded in Tissue-Tek II O.C.T. compound embedding media (cat # 4583, Lab-Tek products Division, Miles Inc. Naperville, Illinois) and 10 micron sections cut and mounted to pre-cleaned glass microscope slides (cat # 3050, Clay-Adams, Becton Dickson Labware, Oxnard, CA). The mounting and microtome techniques were modified from those described by Bawa [2] and Kunica [6]. A Minotome Cryostat microtome was used (International Equipment, Div. of Damon, Needham, MA) to cut either cross or broad sections of the matrices. The slide mounted sections were studied under a light microscope (ICM 405, Zeiss, Oberlochen, West Germany) at magnifications varying from 20 to 160 fold. Photographs of the magnified images were taken with an ocular mounted camera using Kodak plus-X pan black and white film (PX 135/ISO 125, Eastman Kodak Co., Rochester NY). The area of the section that was occupied by the pockets of protein was compared to the total section area and this value was used as the section's porosity. The BSA pocket area was calculated by overlaying the photographs with graph paper and counting the number of graph line intersections which covered the pockets. An average pocket area was determined by dividing the total area occupied by the pockets by the number of pockets in each section. Values were determined from sections of four matrices embedded with magnets and exposed to the oscillating magnetic fields, two matrices embedded with magnets but never exposed to magentic fields and for two matrices never embedded with magnets. In addition, areas close to the surface, termed

the periphery, were contrasted to areas close to the magnet, termed the center. The surface areas were more than 2 mm from the magnet,and the center was as close as could be approached to the magnet. The field exposed samples were subjected to the 650 G, 60 Hz oscillating magnetic fields generated by the electromagnet. Fields were applied every 20 minutes on the hour, 12 hours a day for two weeks. To assure that all BSA that could be released would leave the matrix, the matrices were then released in phosphate buffer for an additional month before microtome sectioning.

The average porosity for areas of matrices adjacent to the embedded magnet or the matrix surface are presented for sample exposed and not exposed to magnetic fields in table V. It shows that the porosity of all areas of the matrix in the control groups and of the peripheral areas in the experimental group was close to the 33% loading of the BSA in the matrix. In contrast the area ajacent to the magnet had enlarged pores in the experimental case and a net porosity of over 42%.

TABLE V: POROSITY AND PORE SIZE OF EVAc-BSA (33% LOADING)
IN AREAS ADJACENT TO THE MAGNET OR CLOSE TO THE MATRIX SURFACE
FOR SAMPLES BEFORE AND AFTER EXPOSURE TO 60 Hz, 500 G MAGNETIC FIELD

POROSITY:	$SmCo_5$ magnets	500 G, 60 Hz
	PERIPHERAL	CENTRAL
NOT EXPOSED (n=2)	.34	.317
EXPOSED (n=4)	.305	.424
NO MAGNET (n=2)	.3	.27

IV.2.4.iii Scanning Electron Microscopy Eight EVAc-BSA matrices were fabricated such that 2 mm magnetic spheres protruded from the matrix surface and were not covered by copolymer material [7]. This permitted examination of the matrix surface and the area of the matrix immediately adjacent to the embedded magnetic spheres with a scanning electron microscope (SEM) (International Scientific Instruments, Inc. model ISI DS-130). Four of the matrices were exposed to 1800 G, 9.5 Hz oscillating magnetic fields for two hours each day for two weeks and four released at rest. After release the matrices were freeze dried under vacuum and sputter coated with gold pallidium to enhance contrast.

Scanning electron microscopy of the post release surfaces of both field exposed and nonexposed samples revealed irregularities, such as grooves and pores, especially in those areas between or adjacent to the magnetic spheres. However, those matrices that had been exposed to an alternating magnetic field developed a gap, approximately 100 microns wide, between the magnetic sphere and polymer material surrounding it (figure 9). This was found around all spheres in matrices subjected to an oscillating magnetic field but in none of those that resided in samples that were never exposed to such radiation.

IV.2.4.iv Magnets 'in action' The surface of matrices embedded with the high strength magnets was observed under the light microscope (160 fold magnification) when oscillating magnetic fields were applied alongside. The images were recorded on video cassettes (Scotch-3M UCA-20S) by a portable video recorder (Panasonic, model NV-9400) for slow speed playback and examination.

At this magnification motion of the polymer material was observed each time the magnetic field was applied and withdrawn. The 1800 G alternating field elicted about 60 micrometers of surface translation from matrices embedded with cylindrical magnets. Outside of a 1.5 mm window from the embedded magnet, however, no perceptible movement of the surface could be detected. These were the maximum values obtained. Motion of lesser degree in a smaller window was observed for lower strength fields and different field alignments. The magnet displacement was independent of the field frequency.

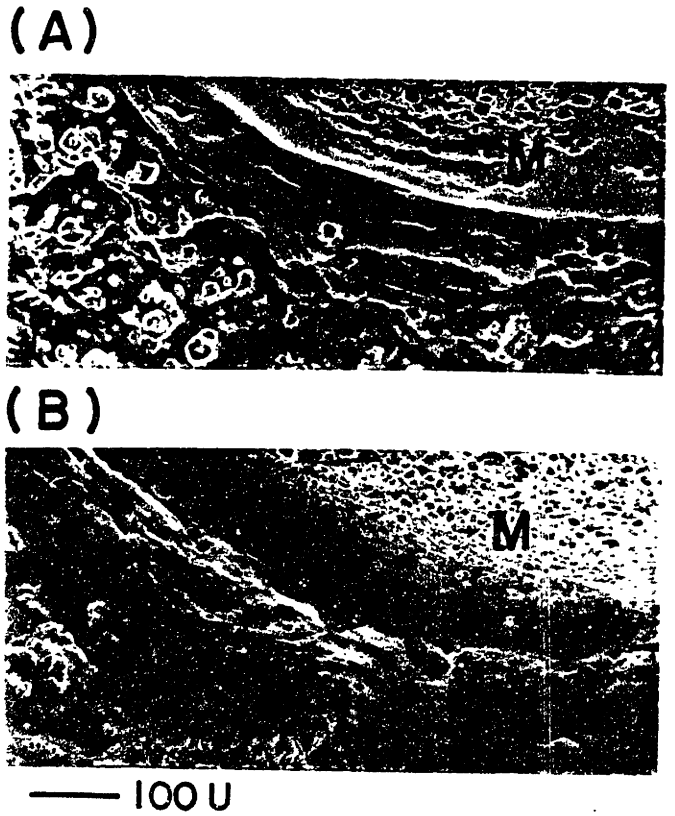

Figure 9: Scanning electronmicrographs of the surface of two different EVAc matrices embedded with 2 mm magnetic spheres, at 104x original magnification, (a) before and (b) after repeated exposure to an 1800 G magnetic field oscillating at 9.5 Hz. The field was generated from rotating permanent magnets and was applied in a three week period, for two hours a day for a total of 16 exposures. In both panels the magnetic sphere is labelled with a capital M, and a capital P is used to identify the polymer matrix. In the matrix that was never exposed to a magnetic field the polymer material immediately surrounding the sphere is adjacent to and overlapping with the sphere. In contrast, a gap, approximately 100 microns wide, developed between the sphere and adjacent polymer material in the field exposed matrix.

IV.3 DISCUSSION

The results of the previous chapter showed that the extent and form of modulated release could be controlled by variation of the duration, amplitude and frequency of the applied magnetic field. The experiments described in this chapter can be summarized as follows:

(1) Peak modulated release was achieved during the first 2 days of release. A period of prerelease wass required, as well as, a number of initial exposures to the field stimulus (table II).

(2) Modulation increased with increasing size and strength of the embedded magnets (table I).

(3) While, the amount of protrusion of the magnetic spheres above the plane of the matrix surface was related to the degree of modulation (figure 2), the orientation and position of the $SmCo_5$ magnets alone were not sufficient to account for differences in modulation (figure 4).

(4) Modulation from a cylindrically shaped matrix was a function of the size of the matrix and there appeared to be a critical size, above and below which the enhanced release was diminshed (table IV).

(5) The magnet could be seen in magnified video taped images, to move a maximum of 60 microns in response to an 1800 G field passed along side of the matrix. The motion was independent of field frequency and apparently alternatingly compressed and dilated ajacent matrix material. At a distance 1.5 mm from the magnet surface no movement of the matrix was detected.

(6) In nonmodulated matrices a certain portion of the incorporated drug was never released because it resided in pockets enveloped by the matrix ([1,4] and table III).

(7) Areas of the matrix about embedded magnetic spheres appeared to be virtually free of any entrapped drug at the end of release, while pockets of drug remained in the areas of the matrix where there were no spheres.

(8) Microtome sections of cylindrical matrices embedded with magnets and exposed to oscillating magnetic fields revealed that the matrix pockets adjacent to the magnet were broken open. Those areas close to the magnet had a greater porosity than other areas of the matrix farther away or from any section of matrices never exposed to the magnetic fields. In

addition, after release had ceased, pockets of BSA were found far from the magnet, while, the areas around the magnet were completely cleared of drug (table V).

(9) Mass balance studies of release from matrices containing BSA 30% by weight and embedded with spheres revealed a net excretion of 70% of the incorporated drug when no magnetic field was applied and a net excretion of 95% of incorporated drug after field exposure (table III).

The discussion that follows will try to incorporate all of the data and observations into a coherent model of modulated release. The mechanics of modulation will be interpreted and the dependence on volume explained.

It appears that modulated release was related to the movement of the embedded magnets or magnetic spheres within the copolymer matrix under the magnetic field stimulus. This motion caused changes in the matrix. The permanence and extent of this change decreased with distance from the magnets in all directions. Thus, the geometry of the matrix and the position and type of embedded object should have played a role in determining eventual modulation.

The data in table II indicated that the optimal amount of release was not seen immediately after release was started. A period of 'pre-release' and a number of intial exposures were required. This might imply that there existed a population of drug that was immune to modulation and had to be released before regulated release could occur. Even in sustained, nonmodulated release, the early pattern of drug release from matrices was different from what was observed once a steady state was attained. There was a burst of drug release during the first 2 days of release. This burst has been attributed to the release of drug from matrix pockets adjacent to the surface [1]. The lack of a tortuous matrix structure to hinder release led to accelerated release. The release of this drug has been shown to be independent of diffusion [1], since it was not affected by long term changes in environmental temperature. It may be that this was the same drug that was immune or resistant to modulation. The rate of release at the time of the burst might already be so accelerated that it could not be enhanced further, or the channels and pockets in which the drug resided might not have been affected by the displacement of the embedded magnets.

Photographs of matrices showed that before release the surfaces of the matrices were smooth. After release of the BSA a pocked surface was revealed. These surface irregularities, however, were not observably different whether the matrices were exposed to the magnetic fields or not. The size of the pockets and the porosity of the matrix in areas far from the magnet was equal to the values determined for the controls. Interestingly, both were quite close to what would be expected from the 33% loading of BSA in the matrix. The absence of change to the peripheral

pockets suggest that the immune population was the surface drug and until it can be released, modulation was blocked.

The porosity of the central regions, however, was almost 15% greater than the porosity of the periphery, because pockets deeper in the matrix were found to be enlarged (table IV). This not only implied that the surface pockets were under less pressure than their deeper counterparts, but also accounted for the increased amount of drug that was ultimately released from the exposed matrices. Mass balance studies revealed that over 30% of the BSA intially loaded in the matrices was trapped there at the end of detectable release. This value was also obtained for similar matrices in other investigations. Seigel [8] identified a range of trapped drug corresponding to the porosity and width of the matrix. The more porous and the thinner a matrix was, the more BSA was eliminated from the matrix. A model was developed based on percolation theory to predict the amount of BSA that might be released from a matrix of known dimensions and at a porosity of 30%, 70 % of the BSA (150-180 micron particle size) was eliminated from the matrix [9]. In matrices that were embedded with magnets and exposed to magnetic fields, only 5% of the original drug was trapped in the matrix. Thus, 83% (25%/30%) of the BSA that might have been trapped inside the matrix was freed by the interaction of the magnet on the matrix. The BSA that was never released presumably was in areas beyond the influence of the magnets.

The SEM photographs also provided a potential explaination for the delay in modulation. Embedded magnets were held in place by adjacent matrix material until a number of pulses of an oscillating magnetic field

were applied. Once this restraint was broken a gap was formed between the magnet and the material, and the magnet could move within this gap. The observed 60 micron motion corresponds to the size of the gap. The difference between the amount of displacement and the gap width reflects the fact that the gap was formed by spheres which were only partially restrained, while, the motion was seen in deeply embedded magnets. In addition, the displacement of material over the entire matrix should and did vary from a maximum of 60 microns adjacent to the magnet, to no movement in areas far from the magnet, and should decrease with diminishing magnetic fields.

Figure 2 showed that the closer the magnetic spheres were to the surface of the polymer matrix, the greater the extent of modulation. Though studies were not performed to verify this, this might be due to the increased freedom to move within the matrix, as there is less matrix material retraining the more protruding spheres. The high strength magnets were embedded deeper within the matrices and did not raise the surface at all. In addition to the restraint on magnet movement by the surrounding matrix, magnets not perfectly aligned with the field and far from the field source will experience an attenuated magnetic force.

The force that is exerted by a magnetic field of strength $\bar{B}$ and gradient $\nabla\bar{B}$, on a magnet of magnetic moment $\bar{m}$, can be written as the vector dot product of $\bar{m}$ and $\nabla\bar{B}$. It has already been demonstrated that the field from the elecromagnet decreases linearly with distance from the electromagnet (section II.2.2). This is particularly true in the near field, the region in space adjacent to the surface of the electromagnet.

In regions far from the magnet surface the field drops off as the square of distance. The experiments were conducted within the near field, and therefore, the magnetic field at any point in space in this region can be expressed as $\bar{B} = i_z(B_s - B_o z)$. This means that the field is equal to some value, B_s, at the surface of the electromagnet, and decreases in strength with increasing distance, z, from the magnet. The slope of the field decay is B_o (figure II.7 shows this relationship to be B = 650 G - 20mm). Thus, the field gradient is $\nabla B = -i_z B_o$. Only the z component of the field remains because the field is unifrom in the other directions. The force equation can be expanded as follows,

$$\bar{F} = \bar{m} \cdot \nabla\bar{B} = (\bar{m} \cdot \nabla)\bar{B}$$

$$= (i_z m_z \cdot i_z \frac{\partial}{\partial z}) B_z$$

$$= (i_z m_z \cdot i_z \frac{\partial}{\partial Z}) (B_s - B_o z) = - m_z B_o$$

The component of the magnetic moment of the magnet in the direction of the field's vector, m_z, is strongest when the magnet aligned with the field. Hence, the moment can be written as the product of a net magntization, m, and the cosine of θ, the angle between the net direction of the field and the magnet's pole vector. Such that $m_z = m_o \cos \theta$, and the final form of the force generated by a magnetic field on a magnet is $F = - m_o B_o \cos \theta$.

If modulation is determined by this force, then the extent of modulation should follow cos θ in a linear fashion. This was not observed, instead, as illustrated in figure 4 there was no correlation when modulation was compared to the orientation of the magnet with respect to the field alone.

When the volume of matrix acted on by the magnet was taken into account, along with the position of the magnet in the matrix, a linear relationship was obtained (figures 6 and 7). The dependence on volume was supported by the following observations.

The light box studies showed that trapped drug was freed in greater amounts the closer the pockets were to the magnet. The amount of clearing, however, decreased with increasing distance from the magnet and the effect was no longer visible in areas equidistant from two adjacent spheres. This implies that at the spacing used, the magnets could not exert ample force to act together on portions of the matrix. If the magnets were placed in greater proximity they might have acted synergistically. Yet, the magnetic repulsion between two magnets may not allow for them to be placed close enough together. The position they maintain in the matrix is the position in which the forces they apply on each other are balanced or nil. Additional evidence for the volume model was that modulation observed for cylindrical matrices was not only greater than that observed for flat slabs but also greater than what was obtained for larger cylinders (table IV). It is possible that the slabs did not allow for optimal use of the matrix and that while the magnet might have been freer to move, less BSA-matrix was available to be acted on. The

sphere of influence model implied that a maximum amount of modulation should be achieved when the sphere and the cylindrical matrix perfectly overlapped. This was never exceeded in practice (figures 6 and 7). At the same time, in the experiments displayed in table IV, increasing the volume without limit did not increase the extent of modulation. The large matrices showed modulation that was less than those of intermediate volume. The additional matrix might have restrained the movement of the magnet, or forced release to be limited by the channels and pockets beyond the influence of the magnet. Unaffected areas should act like nonexposed matrices, where release is a diffusion mediated process.

When stronger magnets were embedded in the matrices, the magnetic moments increased and the force on the object increased accordingly. One should expect the modulation from matrices with magnets to be greater than from matrices embedded with magnetic spheres. The difference observed with the different magnets may be due to a number of effects. Though the moments of the two samarium cobalt magnets used in these experiments were similar, their mass was not. Thus, once inertia was overcome, the heavier torroids exerted more torque on surrounding matrix than the lighter cylinders. The geometry of the two might also have played a role. The torroids were not only surrounded by matrix material, they also had material inside the ring. There was more interaction between the material and the magnet and possibly more effect, as well. The eccentric torroidal magnet exhibited modulation that was lower than predicted from the volume model. Its abnormal shape negated the advantages expected from torroids. Finally, as the volume of the matrix acted on by the magnet was an important parameter, the torroids should have a greater sphere of influence since they have a larger radius.

REFERENCES

[1] Rhine, W., D. Hsieh, and R. Langer, Polymers for Sustained Macromolecule Release: Procedures to Fabricate Reproducible Delivery Systems and Control Release Kinetics. J. Pharm. Sci., 69:265-270 (1980)

[2] Bawa, R.S., "Controlled Release of Macromolecules from Ethylene-Vinyl Acetate Copolymer Matrices: Microstructure and Kinetic Analysis", M.S. Thesis, Department of Nutrition and Food Science, M.I.T., Cambridge, MA, (1981)

[3] Miller, E.S, N.A. Peppas and D.N. Winslow, Morphological Changes of Ethylene/Vinyl Acetate-Based Controlled Delivery Systems During Release of Water-Soluble Solutes, J. Membrane Sci., 14:72-92 (1983)

[4] Siegel, R.A., "Macromolecular Drug Release from Porous Implants: Sources of Matrix Tortuosity", Ph.D. Thesis, Department of Electrical Engineering and Computer Science, M.I.T., Cambridge, MA, (1984)

[5] Hsieh, D., W. Rhine and R. Langer, Zero-Order Controlled Release Polymer Matrices for Micro- and Macromolecules, J. Pharm. Sci., 72:17-22 (1983)

[6] Kunica, E., "Release Kinetics from Various Ethylene-Vinyl Acetate Copolymers", M.S. Thesis, Department of Nutrition and Food Science, M.I.T., Cambridge, MA, (1984)

[7] Edelman, E.R., J. Kost, B. Bobeck, and R. Langer, Regulation of Drug Release from Polymer Matrices using Oscillating Magnetic Fields, J. Biomed. Mat. Res., submitted, (1984)

[8] Siegel, R.A., "Macromolecular Drug Release from Porous Implants: Sources of Matrix Tortuosity", Ph.D. Thesis, Department of Electrical Engineering and Computer Science, pps. 90-133, M.I.T., Cambridge, MA, (1984)

[9] ibid., p. 126

CHAPTER V: MATRIX DEFORMATION STUDIES

V.1 INTRODUCTION

The movement of the magnet within the matrix was observed to alternatingly compress the adjacent matrix material. The following experiments were performed to determine whether oscillating mechanical compression of an EVAc matrix containing BSA would also lead to regulated release of this macromolecule. In addition to verifying some of the data obtained with magnetic modulation the results seemed to verify the observations that the volume of the matrix acted on by the magnet was an important determinant of modulation.

V.2 METHODS

The Dynastat dynamic testing device used to determine the modulii of elasticity of the polymer materials offered the ability to deform the matrix at frequencies between 0.01 and 100 Hz over a wide range of displacements. The apparatus is described in detail in appendix A and elsewhere [1]. A special restraining cell was constructed from plexiglass. As depicted in figure 1 it was shaped as a cup with a raised pedastal in the center. The cup was 3 cm wide and 2.5 cm high and the pedastal, 1.25 cm high and 1.5 cm in diameter. Matrices were fabricated as described in section II-2.1 with BSA seived to 150-180 micron particle size, 30% loading. No magnets were used. The bottom and top faces were cut flat on a microtome so that the surfaces were even and regular. The matrices were placed atop the pedastal,

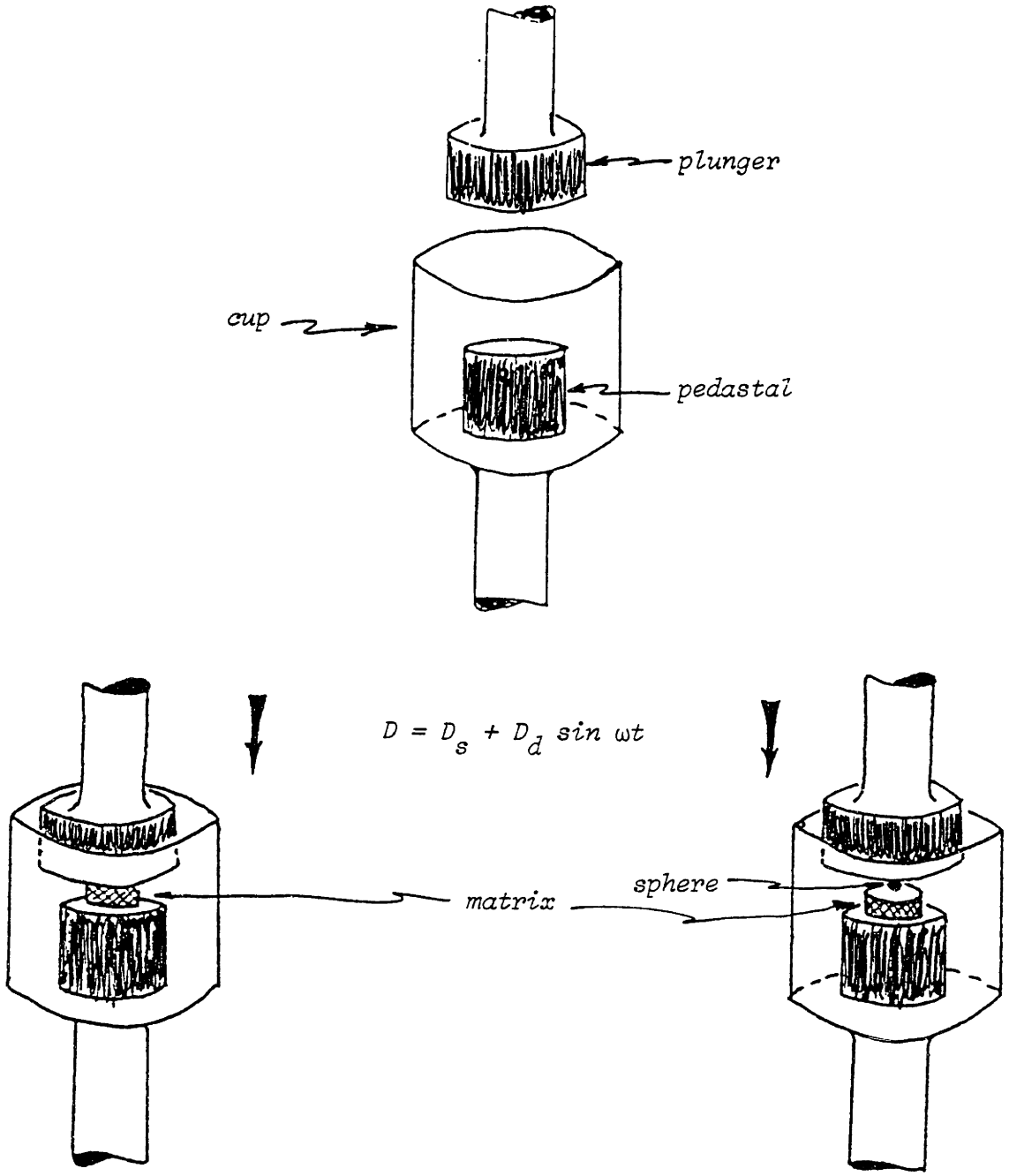

Figure 1: Schematic of the cell used to house the polymer matrices during the deformation studies, for (a) plane deformations and (b) point deformations. The net displacement, D, of the matrix was the sum of a static displacement, D_s, and a dynamic displacement, D_d, sinusoidally oscillating at 1.

8 ml of 0.1 M phosphate buffer, pH 7.4, inserted in the cup and the samples compressed by a Dynastat controlled plunger. The plunger face was 2 cm in diameter and covered the entire matrix. In separate experiments one of the 1.4 mm diameter magnetic spheres was placed between the plunger and the matrix to furthur simulate conditions in the experiments with embedded magnets (figure 1.b). The plunger experiments were referred to as "plane" displacement or deformation studies and the experiments with intervening spheres, as "point" displacement. In both cases a static displacement was applied to keep the matrix in position and a dynamic displacement applied to test for potential modulation of BSA release.

Release was followed either dynamically or periodically. A flow through spectrophotometer was employed in the open loop configuration to continuously monitor BSA release from the matrix with time. When this was not used, the solution in the cup was removed every 5 minutes and replaced with fresh buffer. The absorbance of the solution at 220 nm was used to determine the amount of BSA released in that period of time. Before matrix release studies were initiated solutions of known concentrations of BSA where injected into the cup to determine the time response of the flow through configuration. The time to onset of absorbance change, time to peak absorbance and time to clearance of the protein were all monitored. Matrices of different diameters and widths were then studied under displacements of different strengths over a range of frequencies. The extent of modulation was determined by dividing the absorbance attained after the deformation was applied, to the baseline absorbance achieved in the absence of any deformation.

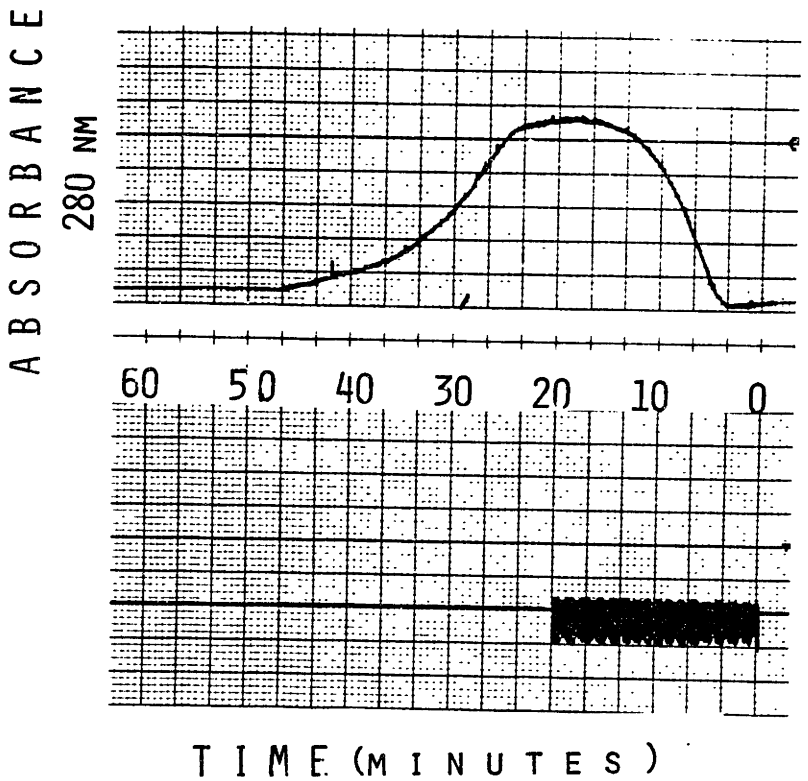

Figure 2: Dynamic release profile from an EVAc-BSA matrix subjected to a 10 minute pulse of a 60 Hz plane deformation of 50 microns. The abcissa represents time in minutes (3 mm/min) and the ordinate, absorbance at 280 nm (0.05 v FS). The load that developed on the matrix is diplayed in the bottom in panel (10 v FS, 1 kg/volt) .

V.3 RESULTS

V.3.1 Dynamics Solutions of known concentrations of BSA injected into the cup appeared as a rise in absorbance after 2 minutes. The time constant of the system was approximately 6 minutes and was identical for rise and decay. This was due to the mixing of the BSA in the solution within the cup and the tubing. Figure 2.a shows that the baseline release of BSA was almost negligible. When the polymer matrix was compressed 50 microns at 60 Hz for 10 minutes, release of BSA increased after 2 minutes. Six minutes after the rise began, it peaked and plateaued. Release returned identically to baseline. The decay began 2 minutes after the deformation was withdrawn with a time constant of approximately 6.5 minutes which was similar to the rise.

V.3.2 Point versus Plane Deformation When a magnetic stainless steel sphere was placed between the plexiglass plunger and the EVAc-BSA matrix modulated release of BSA was also observed. The matrix was indented by the sphere when the static displacement was applied. The plunger however, never touched the matrix surface.

While, the dynamics of modulated release to a point displacement was identical to that seen with the plunger, there was a marked difference between the two types of deformation when the amplitude and frequency of displacement was varied. In all cases there was a greater amount of modulated release when the plunger was used (figure 3 and 4).

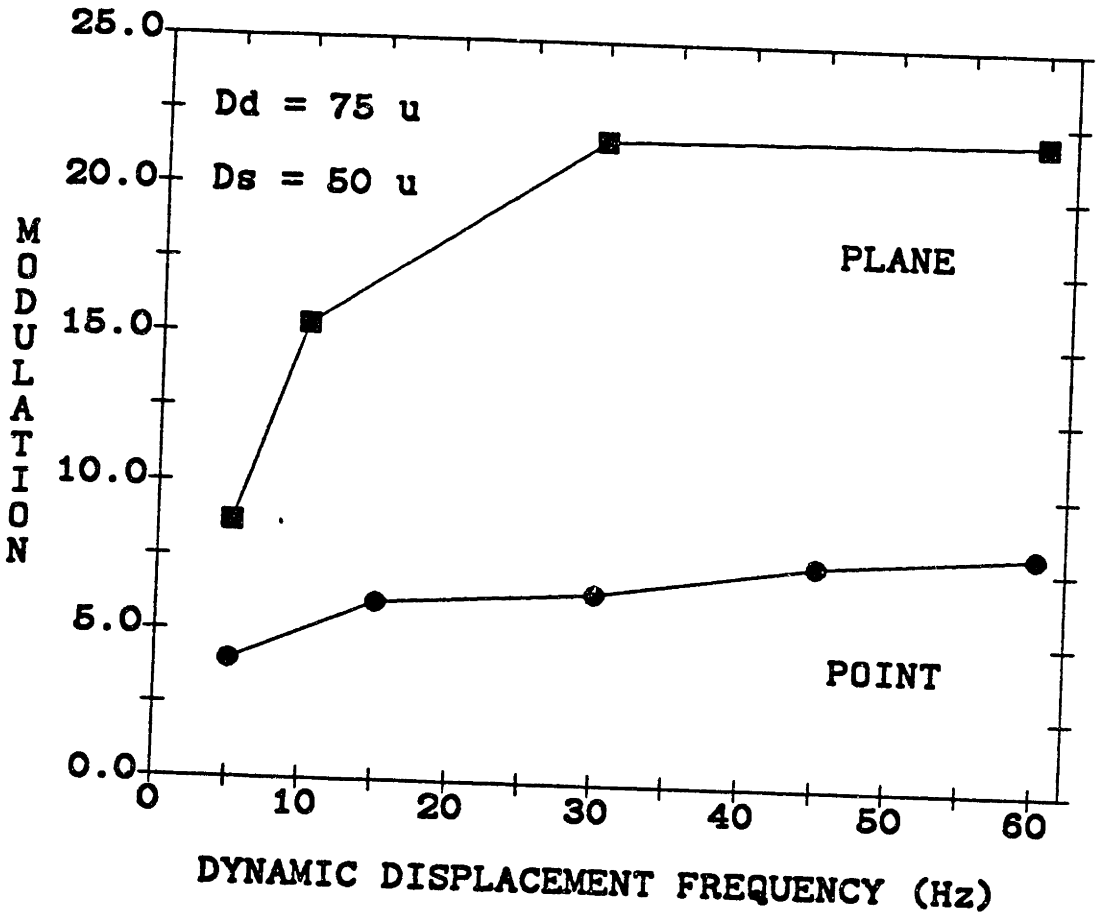

Figure 3: Extent of modulation achieved from EVAc-BSA matrices subjected to dynamic deformation of 75 microns over a range of frequencies.

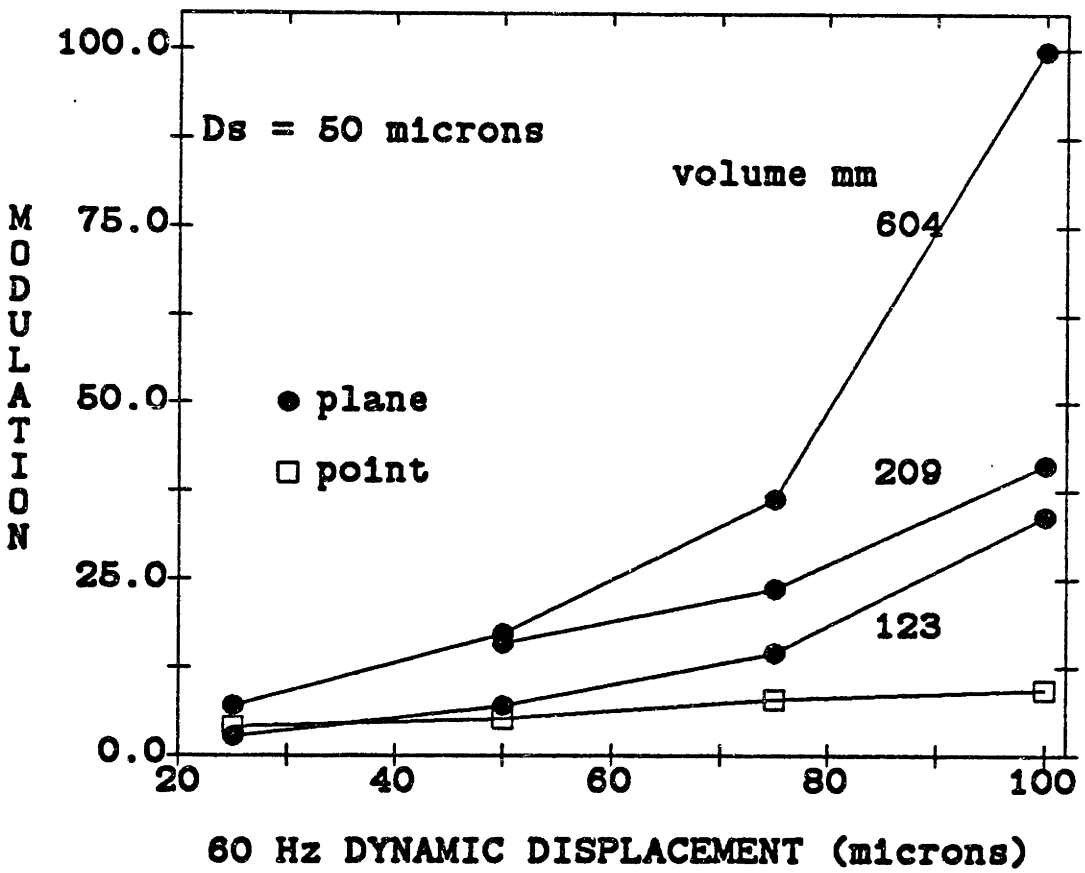

Figure 4: Extent of modulation achieved from EVAc-BSA matrices subjected to 60 Hz dynamic deformations over a range of amplitudes. The different curves, for planar displacements, represent studies with matrices of different volumes (mm^3). The point displacements for these same matrices all fell within a narrow range.

V.3.3 Frequency of Deformation The extent of modulation achieved at different frequencies of deformation is displayed in figure 3 for both point and plane displacements. The reponse is linear for the point deformation with a slope of 0.06 (R^2 = 0.898), and linear for plane displacements until 30 Hz, at which point the rise levels off.

V.3.4 Amplitude of Displacement The extent of modulation varied with the degree of dynamic displacement and was a strong function of the volume of the matrix. There was a different response to the two different forms of displacement. Matrices subjected to plane displacement showed increasing modulation with volume. The extent of modulated release of BSA matrices that were subjected to point displacements was maximum at an intermediate volume. For volumes of the matrix above or below this value, modulation was slightly lower. The curves in figure 4 show that the amount of BSA increased above baseline when the amplitude of a 60 Hz dynamic displacement was varied. While there was a different response to planar displacement for matrices of different volumes, the values for point displacement all fell within a narrow range.

V.4 DISCUSSION

The alternating compression of the EVAc-BSA matrix by the magnets is remarkably similar to mechanical deformation of a membrane. In the experiments reported above a dynamic strength of materials testing device was used to apply displacements of the order observed for the magnet in the matrix, to determine whether such displacements could induce modulation of BSA release. BSA release was increased from less than 0.05

mg to 0.275 mg with a dynamic displacement of 50 microns, as displayed in figure 2. In addition, the time course of events was similar to the dynamics of magnetically modulated release. Taking into account the characteristics of the flow through system, the reponse of the matrix to mechanical deformation was always instantaneous, and once a peak was attained, it remained stable for the duration of the deformation.

Equally as interesting, was the reponse of the matrices to different types of displacements. Deformations of the matrix applied across the entire face of the sample caused release to increase without limit for increasing amplitude, and to plateau with increasing frequency. Deformations applied to a point in the middle of the matrix showed different results. The amount of BSA released increased slightly with increasing amplitude and frequency of deformation, but the response was attenuated at large and small matrix volumes. This same type of phenomenon was observed in the matrices embedded with magnets (table IV-IV). At some intermediate volume modulation was maximum, at higher and lower values modulation dropped off.

The difference between the use of the plunger and the use of the a sphere is that while the plunger produces a force over the entire planar face of the matrix, the sphere only establishes a point force. Thus, the deformatory force on the matrix will decay only in the direction of the force and not in the other two orthogonal directions. This is not the case for a point deformation. When such a force is applied the deformations u and w, in the two orthogonal directions, r and z, will decay with distance from the point of application. This decay can be

specified in terms of the strength of the applied deformation, P, the modulus of elasticity of the matrix material, E. The derivation is provided in appendix C and the equations are of the form

$$\frac{u}{\frac{3P}{4\pi E}} = \frac{r^2 z + z^3}{(r^2 + z^2)^{5/2}}$$

and

$$\frac{w}{\frac{P}{4\pi E}} = \frac{r^3 - rz + 2/r}{(r^2 + z^2)^{3/2}}$$

In these normalized forms the distances can be chosen as in any arbitrary set of units, as long as the dimensions of u, w, P and E match. Thus, the displacement of matrix material at a distance one normalized unit length away from the point of deformation in the r and z direction will be only 25% of the full deformation, and at 10 units the force of the deformation will have been attenuated 100 fold. If too small a volume is used it is possible that there is insufficient amount of matrix and drug to be acted on. Therefore, there seems to be an optimal volume above which modulation is ineffective and below which is not used to its fullest potential.

Interestingly, the amount of modulation that was achieved was in the range of values observed from the polymer matrices dispersed with the same loading and particle size of BSA, embedded with magnets and subjected to oscillating magnetic fields. At the same time, the extent of modulation did

not exceed the extent of modulation computed for the 'ideal' volumes in chapter IV. The ideal case was the situation in which the amount of matrix material available for drug release coincided with the amount of material under the influence of the embedded magnet.

The deformation experiments described above were difficult to perform because the face of the matrices had to be perfectly flat for the application of the load to be even. Some of this problem was overcome by the use of a point deformation. In general, the results of these studies imply that the action of the magnet on the matrix is strikingly similar to the mechanical deformation of the matrix. The dynamics of the modulation and the response to changes in the frequency and amplitude of the stimulus were also the same. Finally, these experiments verified the validity of a volume of influence model.

REFERENCES

[1] Sternstein, S.S., Transient and Dynamic Characterization of Viscoelastic Solids, chapter 7 in "Polymer Characterization", Am. Chem. Soc. pps. 123-147 (1983)

CHAPTER VI: MICROSCOPIC MODEL

VI.1 INTRODUCTION

The experiments and discussion in the last chapters attempted to supply a general mechanistic view of the magnetically modulated system. A macromolecular model was developed that implied that the action of the magnet on the matrix was limited to a specific sphere of influence (section IV.3). The effect of the magnet within this sphere was deemed to be the pulsatile deformation of the surrounding matrix. Mechanical pulsatile deformation of the EVAc-BSA matrix led to modulated release in accordance with this model (chapter V). In the discussion that follows a theory is proposed to explain modulation on a microscopic scale.

The use of pulsatile flow to enhance mass transfer has been reported in the chemical engineering literarure, for liquid-liquid extraction columns [1-3], solid-fluid transfer in packed towers[4], and increasing sublimation to room air [5]. Harris and Goren developed a model to account for the increased mass transfer rates from pulsatile flow through a tube connecting two solute reservoirs [6]. The mass transfer rate between the reservoirs was obtained by solving the diffusion equation at points far from the ends of the tube, using the velocity profile set up by a piston at one end of the tube. Transfer rates were increased several orders of magnitude over that due to molecular diffusion alone. The data they obtained fit a theory based on Taylor diffusion [7,8].

The increase in mass transfer rates was found to be a function of three dimensionless groups: an oscillating Reynolds number, $r_c^2/$ (where is the frequency of pulsation, r_c is the radius of the tube and is the fluid kinematic viscosity), an amplitude factor, D_p/r_p, (where D_p is the displacement of the piston) and the Schmidt number Sc= /D (where D is the diffusivity of the diffusing species in the fluid filling the cylinder).

McCarthy and Soong [9] first suggested using this theory to understand magnetically enhanced release of macromlecules from EVAc matrices. The matrix network is analagous to the two reservoir system. In several reports the morphology of the matrix was determined to consist of a network of drug pockets connected by a series of smaller channels [10,11]. The size of the pockets were on the order of the particle size of the macromolecule, in the 100-200 micron range, and the radius of the channels was found to be about 1-5 microns (see figure IV.1). The magnet was oscillated within the matrix by the applied field creating an sinusoidal pressure source (section IV.2.4.iv). In the analysis that follows a polydispersion of channels, and sphere displacement over a wide range, were incorporated into the model. The polydispersion of channels was included to account for the different sizes of channels observed under electronmicroscopy of EVAc matrices. The decreasing amplitudes were used to account for the attenuation of deformation with increasing distance from the point of force application. The sensitivity of the model to its various independent parameters was examined as well.

VI.2 THEORY

If the oscillation of the magnet, x, is considered in terms of the strength of the pulse, D_p, and the frequency of oscillation, ω, then

$$x = \frac{1}{2} D_p \sin \omega t \tag{1}$$

An instantaneous volumetric flow rate, q, can be determined for flow through any cross section of the channel that connects two drug pockets or a tube that connects the two reservoirs. This will be the product of the channel cross sectional area and the first derivative of x, such that

$$q = \frac{1}{2} P\, \omega\pi\, r_c^2 \cos \delta t = \frac{1}{4} P\, \omega\pi\, r_c^2 \,(e^{j\omega t} + e^{-j\omega t}) \tag{2}$$

where r_c is the radius of the tube or channel.

Sufficiently far from the ends of the tube the only component of velocity is the axial component, w, and it also varies sinusoidally. The form of the solution for the velocity has been shown [12,13] to be

$$w = \frac{\omega D_p \{1-J0(\alpha r/rc)/J0(\alpha)\}}{\{4-8J1(\alpha)/\alpha J0(\alpha)\}} e^{j\omega t} + \frac{\omega D_p \{1-J0(\alpha' r/rc)/J0(\alpha')\}}{\{4-8J1(\alpha')/\alpha J0(\alpha')\}} e^{-j\omega t} \tag{3}$$

where $\alpha = (-j\omega r_c^2/\upsilon)^{1/2}$, $\alpha' = (j\omega r_c^2/\upsilon)^{1/2}$ and J_n is the Bessel function of the first kind of order n.

The transfer of solute in parts of the tube far from from the ends will be governed by the unsteady diffusion equation

$$\frac{\partial c}{\partial t} + w \frac{\partial c}{\partial z} = D \left(\frac{\partial^2 c}{\partial r^2} + \frac{1}{r} \frac{\partial c}{\partial r} + \frac{\partial^2 c}{\partial z^2} \right) \tag{4}$$

For boundary conditions that indicate no mass flux through the pore wall and fixed time averaged concentrations at the pore ends, as determined by the concentration in the reservoir and the external fluid, equations (3) and (4) have been solved [6] to yield, $\bar{Q}$, the time averaged total rate of mass transfer.

$$\frac{\frac{\bar{Q}}{Q_{diff}} - 1}{\frac{D_p^2}{r_c^2}} = \frac{Sc^2 \ \text{REAL}\left[\frac{4J_o(\beta)}{\beta J_1(\beta)} - \frac{4J_o(\alpha)}{\alpha J_1(\alpha)}\right]}{[Sc^2-1]\left[\frac{4J_o(\alpha)}{\alpha J_1(\alpha)} - \frac{8}{\alpha^2}\right]\left[\frac{4J_o(\alpha')}{\alpha' J_1(\alpha')} - \frac{8}{\alpha'^2}\right]} \qquad (5)$$

where $\beta = (-j\omega r_c^2/D)^{1/2}$, and can be considered as an oscillating Peclet number.

McCarthy has shown that 6 of the 8 terms of the equation cancel [9] and the equation can be considered to be

$$\frac{\frac{Q}{Q_{diff}} - 1}{(D_p/r_c)^2} = \text{REAL}\ \frac{4\ J_o(\beta)}{\beta\ J_1(\beta)} + 1 \qquad (6)$$

This last equation compares enhanced flow to diffusive flow. The ratio of these two, the numerator of the left hand side of the equation, provides an extent of modulated release or enhanced flow. The overall effect is, therefore, dependent on the radius of the connecting flow-limiting channels, the diffusivity of the solute, and the amplitude and frequency of the pulsatile displacing force. The model is depicted in modular form in figure 1. The system is depicted as a black-box whose transfer function is overened by equation 6. The transfer function is dependent on the four independent parameters, and the output is enhanced flow.

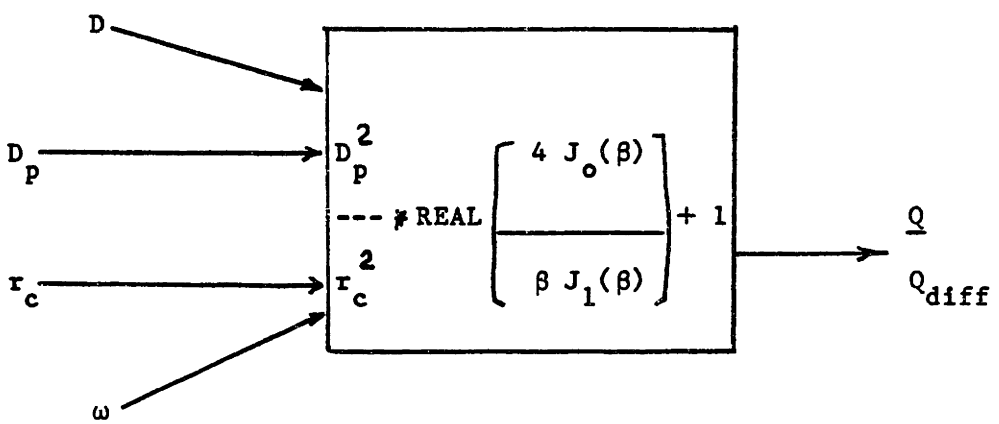

Figure 1: Depiction of microscopic model in modular form. The equation that governs enhanced flow is depicted as a 'black box' with four independent input parameters: the radii of the flow-limiting connecting channels within the matrices, r_p, the diffusivity of the solute, D, and the amplitude, D_p, and frequency, ω, of the pulsatile pressure source.

VI.3 METHODS

A computer program was written to solve these equations using standard expansions for the J bessel function. The sensitivity of the model to changes in individual parameters was examined in the following analysis. The different predictions obtained when one parameter was varied and the remainder held constant were evaluated. Literature values and data from experiments described in previous chapters were used to obtain reasonable estimates for the parameters. A number of studies have shown that the radii of the connecting channels within the EVAc matrices span a range from 1-5 microns [10,11]. The magnified images of the matrix during magnetic field exposure, and the data from chapter IV, showed that the magnetic spheres displaced adjacent polymer material about 30 microns. In addition, this displacement decreased with increasing distance from the magnet. Thus, an average ratio of enhanced to diffusive flow was determined over these ranges of channel radii and sphere displacements, at a given frequency of sphere displacement. Frequencies from 0 to 100 Hz were examined, and the maximum channel radius was varied from 1 to 17 microns. Higher ranges could not be studied because of the computational limitations of the computer program and system. The ratios computed for the four frequencies examined in the frequency variation experiments (section III.3.5) were compared to the experimental results using Student's T-test. A listing of the computer program is provided in appendix F.

VI.4 RESULTS

The extent of modulated release or enhanced flow is plotted versus the connecting channel radius in figure 2. Four different frequencies were examined, corresponding to the frequencies studied in section III.3.5 . The curves peak for dispersions whose maximum radii were between 5 and 7 microns, and increase with increasing frequency of oscillation. This increase is also manifested in figure 3, where the frequency range is extended to 60 Hz, for the three channel radii about the peak response range. At the higher frequencies enhanced flow is greater for the smaller range channels, reversing the trend that occurred at the low frequencies.

The values obtained for a dispersion of pores from 1 to 5 microns, and a displacement ranging from 1 to 31 microns, and the extent of modulation observed from polymer matrices embedded with magnetic spheres and exposed to 2 hour pulses of 1800 G, oscillating magnetic fields are displayed in table I. Statistical analysis showed the predicted values to be indistinquishable from the experimental results ($p>0.05$) .

TABLE I: PREDICTED AND OBSERVED MODULATION

FREQUENCY (Hz)	OBSERVED (1800 G, 2 hours)	PREDICTED
5.	2.19	2.65
6.7	2.93	3.49
9.5	4.77	4.91
11.	5.62	5.62

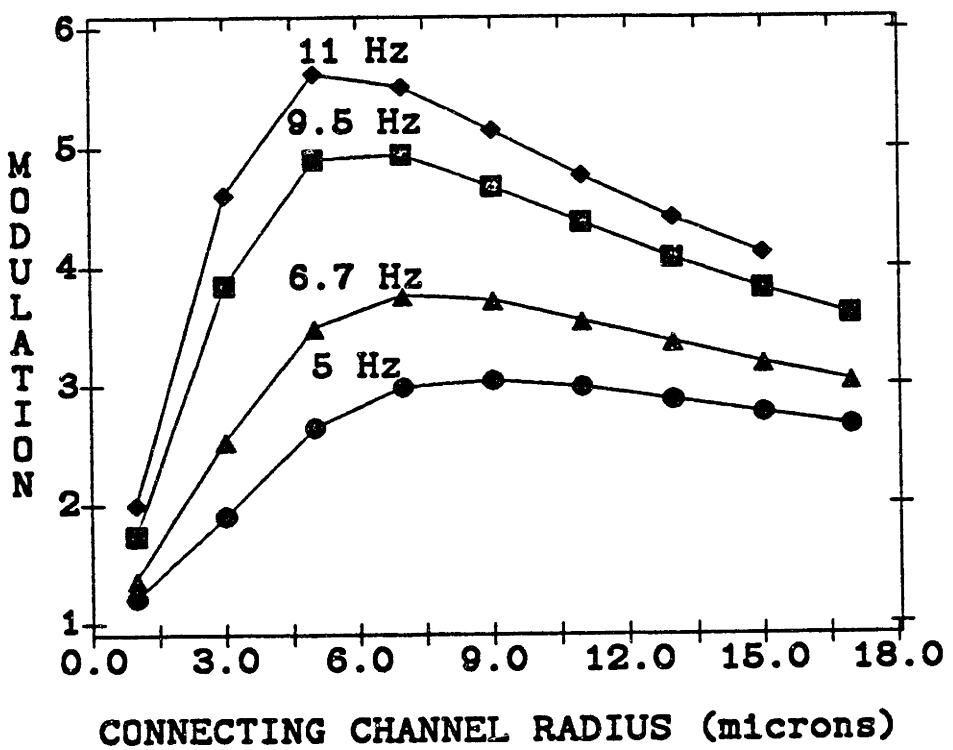

Figure 2: Extent of modulation predicted, for frequencies from 5 to 11 Hz, as the dispersion of connecting channels is increased to include maimum radii of 1 to 17 microns.

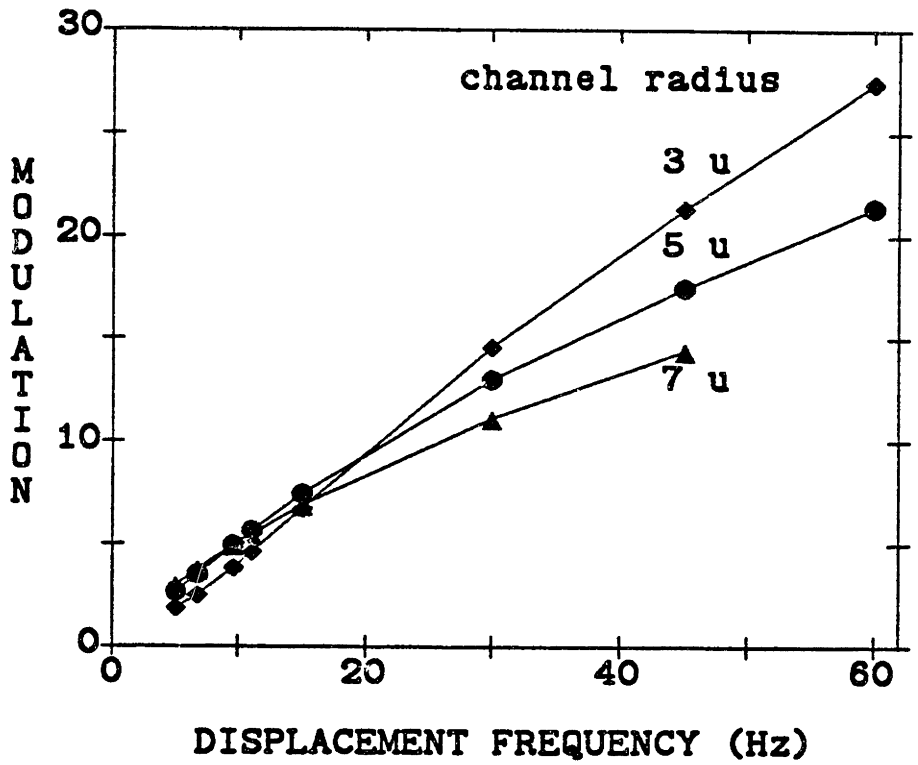

Figure 3: Modulation predicted for three dispersions of connecting channels, over a range of pulsatile flow frequencies from 0 to 60 Hz.

VI.5 DISCUSSION

A possible model of the events surrounding the modulated release of BSA from EVAc polymer matrices can be derived by incorporating the results and discussions presented in this and past chapters.

In the steady state, before any perturbing stimulus was applied, protein release was mediated by diffusion from the polymer matrices [1]. Release was sustained over a long period of time because of the existence of a tortuous porous network of protein pockets connected by smaller channels [10]. The schematized view of this structure presented in figure IV.1 showed the relationship between the pockets and the channels. A recently developed model explained the sustained phenomena by examining the statistics of a random walk of macromolecules through such a network [14]. Protein molecules had to travel from pocket to pockets via the channels to ultimately arrive at the external environment. If the channels were wide, and not much smaller than the pockets, this was easy. However, as the radii of the channels decreased, the chance of a given molecule finding a channel opening diminshed. This increased the time molecules resided in any one pocket, and the matrix in general, looking for a way out. When the magnetic field was applied a new steady state release was attained which was no longer diffusion-limited. Other, faster processes dominated and dictated release. It is likely that the matrix deformation caused the increased release (see chapter V). The microscopic model described in this chapter details how such enhanced release might have occurred. The model utilizes Taylor diffusion to explain net mass

transfer from pulsatile flow. This type of diffusion implies that as a high concentration BSA solution was pushed through the channels of the matrix by the oscillations of the magnet, the laminar concentration profile was broadened [7]. This led to a dispersion of the profile, and when the solution was pulled back during the negative phase of the oscillation some of the BSA did not return with it. This allowed for net mass transfer. If this effect had not occurred, whatever was pushed out would have been pulled back in. It is also possible that the surface channels acted as unidirectional flow valves only allowing flow out of the matrix.

Analysis of the microscopic model indicated that the connecting channels could, not only account for the sustained release of macromolecules, but enhanced release as well. Figure 2 showed that very small channels, and much larger ones should exhibit a minimal effect. Channels, whose radii were in the middle range would be expected to show a peak response. This peak range coincided with the range of dimensions of channels observed in electronmicroscopic studies [10,11], and the peak in modulation corresponded to the values obtained at these frequencies in reality. At lower values Taylor diffusion might be inhibited. The channels may be too small to allow for adequate flattening of the moving solute profile. Enhanced flow increased as the size of the channels was increased. At some point diffusion will also begin to increase and the relative difference between enhanced and diffusive flow will lessen.

The increase in modulated release with increasing frequency (figures 2 and 3) is expected intuitively, and from equation 6. As the frequency

increases the solute profile should be flattened out to a greater extent. Solute is pushed forward by the pulsatile flow, and its concentration profile is deformed. Standard diffusion allows for the profile to maintain its original shape, but only if there is adequate time for these processes to take place. At higher frequencies successive pulses impinge on the reforming diffusive processes and the profile can not be reshaped fast enough. This should lead to a greater degree of enhanced release.

The response, as predicted by equation 6, varies linearlly with the square of an amplitude factor. One should not try to compare this relationship to the data obtained from EVAc matrices exposed to different strength magnetic fields. In those studies the matrix response was linear with the field. The two cases differ because the relationship between the field strength and matrix displacement by the embedded magnet is as yet unknown. If the matrix was a simple elastic material, the displacement would follow the force linearlly. This is Hooke's law. The EVAc matrix material not only possesses visous properties, but as displyed in appendix A, is nonlinear with a range of viscoelastic time constants.

The sphere of influence model developed in chapter IV accounted for the influence of the properties and geometry of the matrices and the embedded magnets. The observed decrease in the effect of the magnet on the matrix with increasing distance from the magnet was used to establish a sphere of matrix material within which the magnet operated. If there was substantial matrix material outside of this sphere the response was attenuated, and if there was insufficient matrix material within the sphere the effect was sub-optimal. When these two views of the system,

the micro- and macroscopic, are combined a rough idea of the mechanism of modulated release can be formulated. Extensions of the models and generation of additional data might allow for a more rigorous means of predicting magnetically enhanced release. Approaches towards this goal are described in chapter IX.

REFERENCES

[1] Karr, A., Performance of a Reciprocating-Plate Extraction Column, A.I.Ch.E.J., 5:446 (1963)

[2] Smoot, L.D. and A.L. Babb, Maa Transfer Studies in a Pulsed Extraction Column, Ind. Eng. Chem. Fund., 1:93 (1962)

[3] Miyauchi, T. and H. Oya, Longitudinal Dispersion in Pulsed Perforated Plate Columns, A.I.Ch.E. J., 11:395 (1965)

[4] Krasuk, J.H. and J.M. Smith, Mass Transfer in Packed Pulsed Columns, A.I.Ch.E. J., 10:759 (1964)

[5] Lemlich, R. amd M.R. Levy, The effect of Vibration on Natural Convective Mass Transfer, A.I.Ch.E. J., 7:240 (1961)

[6] Harris, H.G. and S.L. Goren, Axial Diffusion in a Cylinder with Pulsed Flow, Chem. Eng. Sci., 22:1571-1576, (1967)

[7] Taylor,H.M. and E.F. Leonard, Axial Dispersion During Pulsating Pipe Flow, A.I.Ch.E. J.,11(4)686-689 (1965)

[8] Taylor, G.I., Dispersion of Salts Injected into Large Pipes or the Blood Vessels of Animals, Applied Mechanics Reviews, 6(6)265-267 (1953)

[9] McCarthy, M. and D. Soong, personal communication, Department of Chemical Engineering, University of California at Berkeley, Berkeley, CA.

[10] Bawa, R.S., "Controlled Release of Macromolecules from Ethylene-Vinyl Acetate Copolymer Matrices: Microstructure and Kinetic Analysis", M.S. Thesis, Department of Nutrition and Food Science, M.I.T., Cambridge, MA, (1981)

[11] Miller, E.S, N.A. Peppas and D.N. Winslow, Morphological Changes of Ethylene/Vinyl Acetate-Based Controlled Delivery Systems During Release of Water-Soluble Solutes, J. Membrane Sci., 14:72-92 (1983)

[12] Schlichting,H., "Boundary Layer Theory", 4th ed., p. 229, McGraw Hill (1960)

[13] Richardson, E.G., "Technical Aspects of Sound", vol. 1, p. 19, Elsevier (1953)

[14] Siegel, R.A., "Macromolecular Drug Release from Porous Implants: Sources of Matrix Tortuosity", Ph.D. Thesis, Department of Electrical Engineering and Computer Science, M.I.T., Cambridge, MA, (1984)

CHAPTER VII: MODULATED BSA RELEASE IN VIVO

VII.1 INTRODUCTION

The preceding chapters have shown that the modulatory response can be controlled *in vitro* by regulation of the duration and amplitude of the magnetic field stimulus. In this chapter, experiments were done to determine whether the same type of external control of modulation that was demonstrated *in vitro* could be achieved *in vivo*.

The continuous monitoring of BSA release from polymer matrices *in vitro* was accomplished through use of a flow-through spectrophotometer. This is not applicable *in vivo* because of the abundance of blood borne proteins that absorb in the ultraviolet and visible range, and because of the rapid degradation of the albumin in the body. Therefore, in order to quantify the modulation of BSA release from implantable polymer matrices, [^{3}H]inulin was used. Inulin is a polysacharride (MW 5200-5500) which is not metabolized *in vivo* nor reabsorbed by renal tubules. Once absorbed into the bloodstream it is completely excreted into the urine [1]. Thus, it can be used to monitor the release of macromolecules from implanted matrices by collecting the urine from rats housed in metabolic cages. *In vivo* inulin release rates were found to precisely match release *in vitro* [2]. This is shown in figure 1, where the amount of [^{3}H]inulin that appeared in the urine of rats per hour matches the amount of [^{3}H]inulin that was released from identical matrices *in vitro* in the same period of

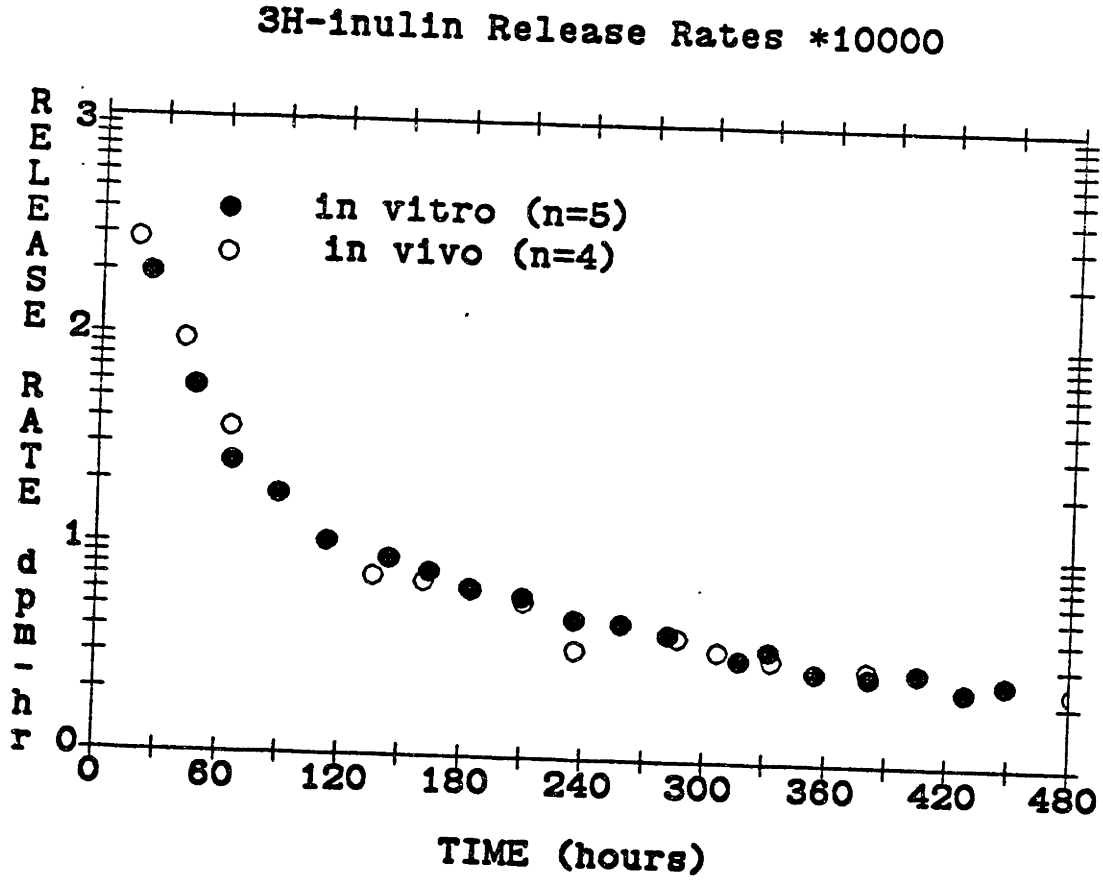

Figure 1: In vivo - in vitro comparison of release rates from EVAc matrices containing [^{3}H]inulin [2].

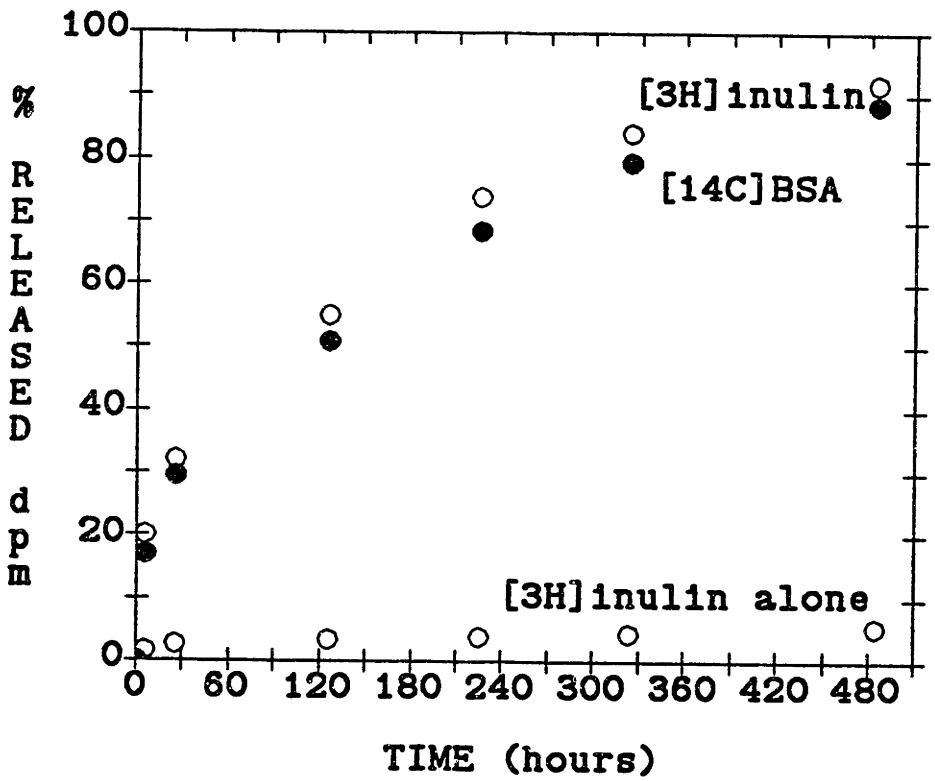

Figure 2: In vitro release rates of [^{3}H]inulin (open circles) and [^{14}C]BSA (closed circle) from EVAc matrices. In the top curves a matrix 39% BSA, 1% inulin by weight is shown to release over 90% of the incorpoarated substances at equivalent release rates. When BSA was absent only 5% of the incorporated inulin was released from the matrices (bottom curve) [3].

time. When placed in tracer quantities in polymer matrices with other labelled macromolecules in vitro release kinetics of the inulin followed the kinetics of the other macromolecules identically [3]. Figure 2 shows that the presence of BSA determined the release of inulin. When no albumin was present, only 5% of the incorporated inulin was released by the end of a 3 week experimental period. In contrast, when albumin was present as 39% of the matrix weight, 90% of the incorporated [^{3}H]inulin was released during the same period of time. Furthermore, the percent of incorporated [^{3}H]inulin that was released at each point in time was not significantly different from the percent of incorporated [^{14}C]BSA. The facilitated release of the inulin is a result of an increased matrix porosity when the much larger BSA is used. Larger pores are formed within the matrix and there is much less resistance to flow. The inulin is then, presumably, swept out along with the BSA. The same results were achieved with a varierty of macromolecules, including epidermal growth factor [4], B-lactoglobulin, and insulin [5]. Thus, the rate of release of any macromolecule from an implanted device can be quantified by using tracer quantities of [^{3}H]inulin.

In the experiments that follow inulin was used to follow the response of an implanted polymer matrix to a variety of magnetic field stimulii.

VII.2 MATERIALS and EQUIPMENT

VIII.2.1 Matrix Fabrication Matrices were fabricated as described in section II.2.1 but 0.36 mCuries of [^{3}H]inulin (500 ug) was added to 252 mg of BSA in 5 ml of distilled water. The solution was lyophilized to give a

powder with a specific activity of 3.18 x 10^6 dpm of [^{3}H]inulin/mg BSA. The powdered mixture of inulin and BSA was dispersed in methylene chloride to a 10% wt/vol solution and matrices fabricated in the glass tube molds, as described in section II.2.2 for the fabrication of identical matrices studied in vitro. Twenty-six seconds after the solution was poured into the tube a single torroidal samarium cobalt was dropped into the hardening matrix. The cylindrical matrices were mounted to an 8 cm diameter, 2 mm wide teflon disk with a drop of methylene chloride. Four 1 mm holes had been drilled in the disk so that suture could be tied to the disk and the disk secured in the implantation site. This unit was then placed under UV light for an hour of sterilization, and the prereleased in 5 ml of phosphate buffer for 48 hours to allow surface BSA to be dissolved.

VIII.2.2 Matrix Implantation and BSA Release Assay Male Sprauge Dawley rats, approximately 250-330 grams in weight, (Charles River Breeding Laoratories, Boston MA) were anesthetized by inhalation of methoxyflurane (Pitman Moore Tnc., Washinton Crossing NJ). Their abdominal and cervical fur were shaved with an electric animal hair clipper (Oster, model A2, Milwaukee WI), and the shaved area was cleansed with betadine solution. The betadine was wiped off with a sterile alcohol pad and a 2 cm long midline abdominal incision made with a #10 scalpel blade (Bard-Parker, Rutherford, NJ) through the abdominal musculature. The bladder was exposed, a #6 gut suture (Ethicon Inc., Somerville, CT) was looped around the top of the bladder, a nick was made in the bladder top and 10 cm of PE-50 polyethylene tubing slipped through the nick into the bladder. The loop of suture was pulled down the bladder and then pulled tight to secure the catheter in the bladder. After urine flow was verified, the abdominal

musculature was closed with a running #4 nylon suture, and the skin incision repaired with the remaining suture material.

A 1-2 cm lateral incision was then made with a #10 scalpel blade through the top layer of skin in the exposed area on the neck. A round edge scissors was inserted in the closed position subcutaneously, and opened wide to produce a pocket. The scissors were removed and the disk mounted polymer was placed inside the pocket and positioned so that the embedded magnet would be aligned with the field when it was applied. Suture (#3 nylon Ethicon Inc., Somerville, NJ) was passed through the four holes in the disk and the disk secured to underlying fascia. The remainder of the suture was used to close the incision. The rats were placed in a Bollman restraining cage and the electromagnet placed adjacent to the cage. The distance from the magnet was recorded and the magnetic field determined from this distance and the input voltage to the electromagnet (see section II.2.2). The bladder catheter emptied into scintillation vials which rested beneath the cage and urine was collected throughout the day. When the experiments were being conducted the vials were changed every fifteen minutes. After a vial change 50 ul of hydrogen peroxide was added to the vials to diminish color quenching along with 10 ml of hydroflur scintillation flour (National Diagnostic, Somerville, NJ). Finally, 50 ul of 0.1 N hydrochloric acid was inserted to minimize the chemiluminescence. Radioisotope counting was performed in a tracor-analytic model 6892 scintillation counter.

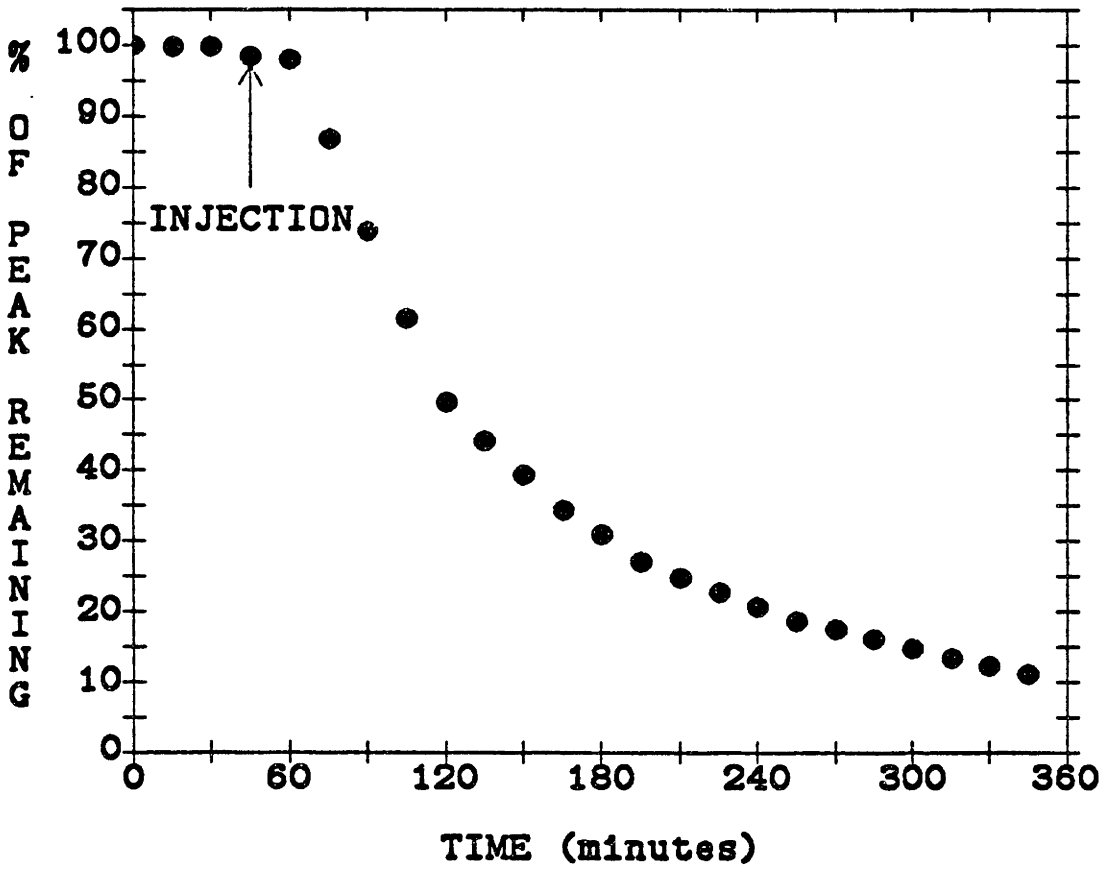

Figure 3.a: Amount of [^{3}H]inulin that appeared in the urine of a rat injected with a bolus of 164,000 dpm of triated inulin in 0.2 ml of distilled water, divided by the total amount injected.

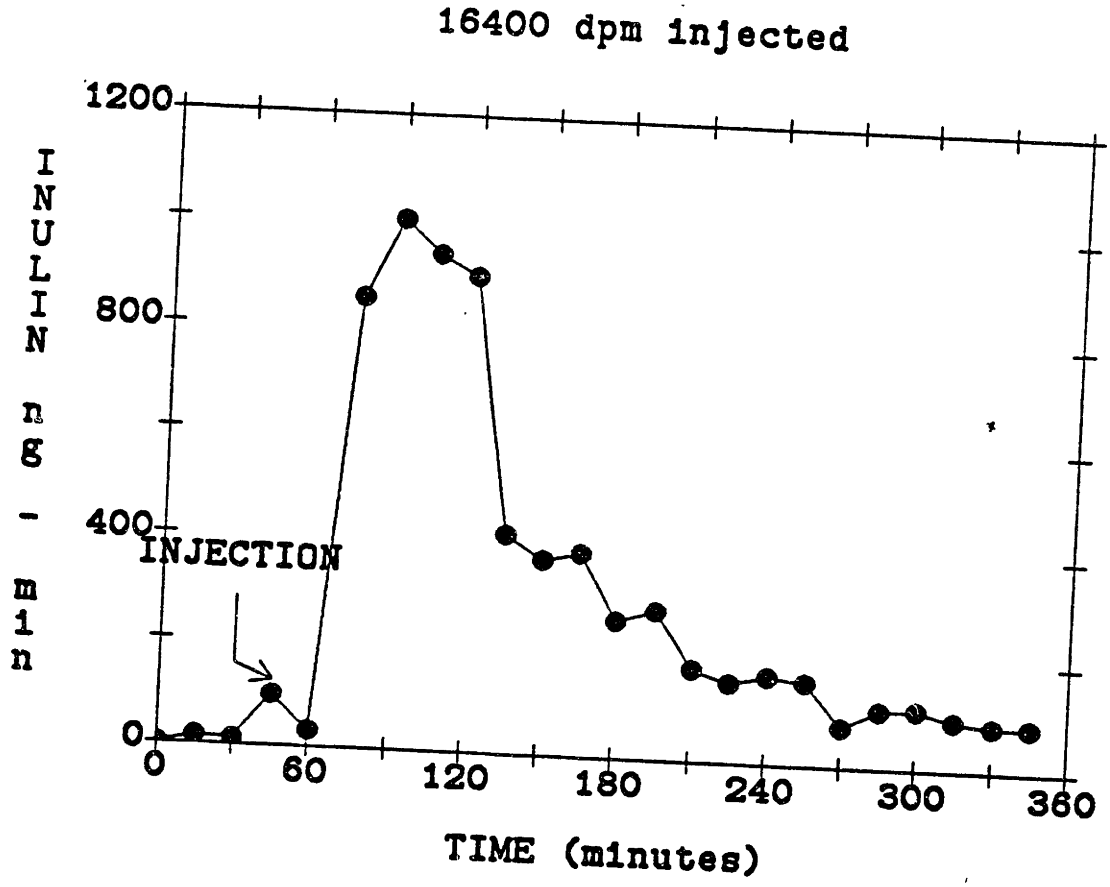

Figure 3.b: Urinary inulin release rate, ng/min, for the situation in 3.a .

VII.3 METHODS and RESULTS

VIII.3.1 Inulin-BSA Absorption A bolus injection of 164,000 dpms of [^{3}H]inulin diluted in 0.2 ml of distilled water was injected subcutaneously in the rat's neck area to model the addition of a pulse of BSA, and to determine the absorption and clearance times of the protein from a subcutaneous site. The amount of [^{3}H]inulin that appeared in the urine of a rat after injection with a bolus of tritiated inulin in solution divided by the amount of inulin intially injected is displayed in figure 3.a . This gives an indication of the amount of inulin absorbed and cleared from a subcutaneous site after a given period of time. When this is displayed as a release rate of inulin the pattern of inulin clearance and absorption can be discerned (figure 3.b). It shows that inulin can be detected in the urine within 15 minutes after injection and by 2 hours, only about 25% remains in the animal.

VIII.3.2 Duration of Response and Matrix Refractoriness The rate of BSA release from EVAc matrices examined *in vitro* was elevated for the duration of exposure to an oscillating magnetic field. Furthermore, matrices manifested no refractoriness. Protein release could be increased to identical values by a train of similar stimulii, independent of the rest interval between the pulses (section IV.3.3). To study the duration of the matrix response and refractoriness of the matrices *in vivo* the following studies were done. First, 60 Hz electromagnetic field pulses of 500 to 600 G, were applied for 10, 20, and 30 minutes. Longer field exposures were not studied. Then 20 minute pulses of 600 G electromagnetic fields were applied 40 minutes apart. Shorter rest

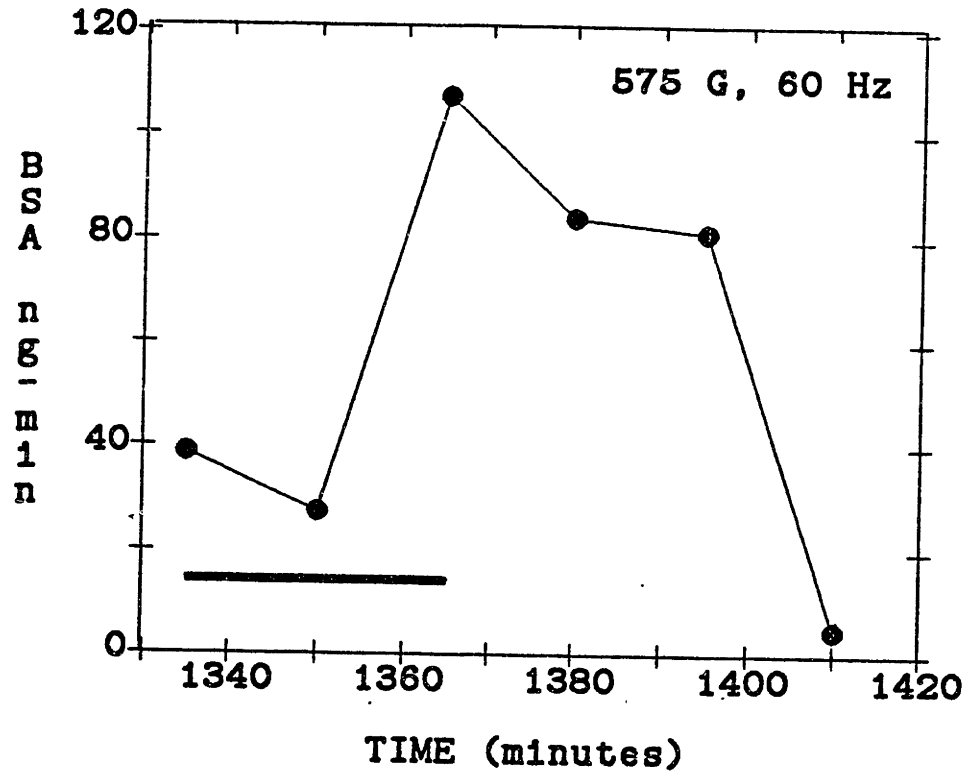

Figure 4: Representative sample of the increase in urinary [^{3}H]inulin excretion after a 575 G, 60 Hz oscillating magnetic field was applied for 30 minutes. The extent of modulation for this example was 6.75 . The delay in the increased release was expected, and is equal to the computed absorption time.

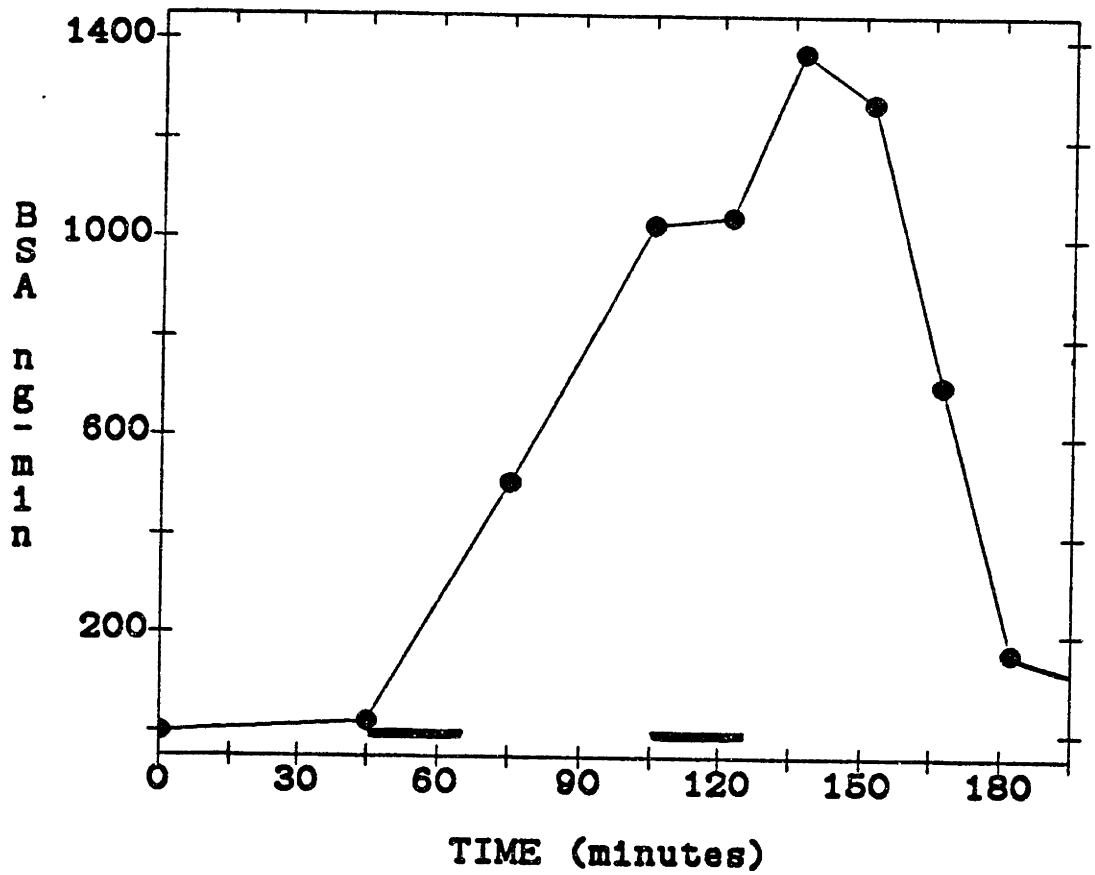

Figure 5: BSA release rate in ng/min from an implanted matrix after exposure to two 20 minute pulses of a 600 G, 60 Hz electromagnetic field, spaced 40 minutes apart.

intervals were not used because the response would have been blurred by the fifteen minute sample time.

Figure 4 shows that BSA release was increased for 30 minutes by a 30 minute pulse of a 575 G, 60 Hz field. There was no decrease in the rate until the field had been withdrawn, at which point the rates returned to baseline within the expected clearance and absorption delay. These delays also accounted for the time lapse between the application of the field and the onset of the release rate increse. If the interval between pulses was shortened to as close as 40 minutes, the rate of BSA release plateaued after elevation with the first field pulse, and then rose further when the second pulse was applied (figure 5).

VIII.3.3 Modulation vs. Field Amplitude In a separate set of three rats, matrices with magnets were implanted in the neck area and magnetic fields of different amplitudes were applied for 30 minutes every two hours. This was accomplished by adjusting the electromagnet input voltage after a baseline release rate was achieved. The amount of inulin that appeared in the urine was compared to the baseline release. An index of modulation was determined by dividing the increase in the amount of urinary inulin to the baseline release noted at the beginning of the experiment.

Figure 6 shows the different degrees of modulation achieved over a span of magnetic field strengths. A linear regression fit to this data yielded a line with a slope of 0.055 (R^2 = 0.956).

VIII.3.4 Animal Controls Rats without polymer matrices or with matrices without magnets were subjected to magnetic fields in the same manner as the rats with magnetic polymers. The rate of inulin clearance did not change for these controls.

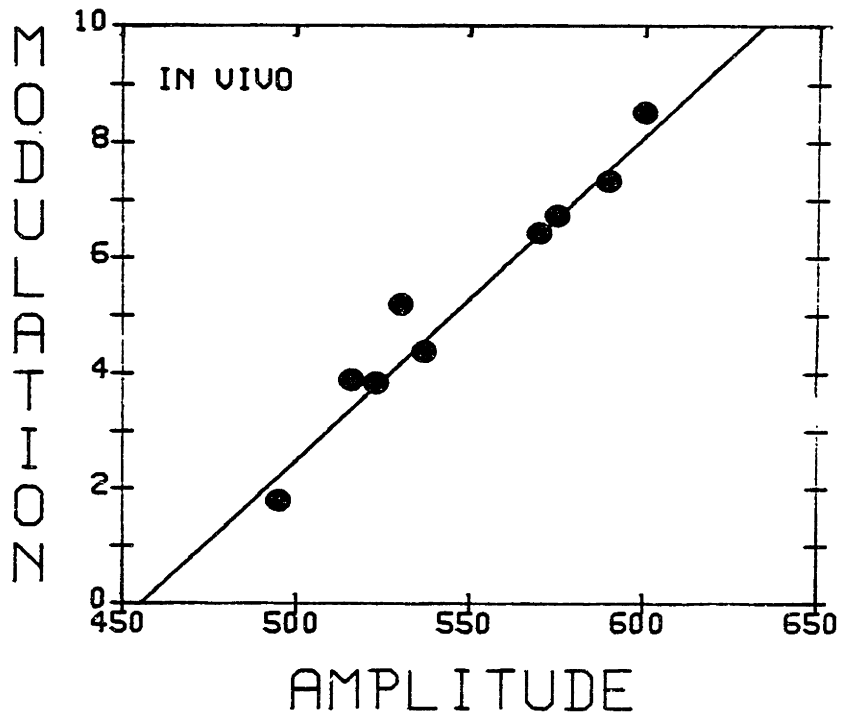

Figure 6: The extent of modulation achieved over a span of field strengths from 400 to 600 G. A linear fit revealed a slope of 0.055 (R^2=0.956).

VII.4 DISCUSSION

The assays used to quantitate and follow modulated BSA release *in vitro* can not be used *in vivo*. BSA is a macromolecular protein that is rapidly degraded, and an absorbance assay can not be used with animals. The use of [^{3}H]inulin allowed monitoring of release every 15 minutes. The absorption and excretion characteristics of a bolus injection of inulin in a rat were displayed in figure 3.a-b . When inulin release was increased from a magnetic BSA-[^{3}H]inulin polymer matrix a similar characteristic response was observed. Thus, as in the *in vitro* studies, within the sensitivity of our measurements, the release response to a magnetic field stimulus was instantaneous.

In addition, as in the *in vitro* studies, the form and extent of the response could be controlled by the stimulus. The elevated levels were maintained for the duration of field exposure (figure 4), and when the field was withdrawn release rates returned to baseline. This was examined over a span of exposures from 10 to 30 minutes, and longer time periods need to be studied. The matrix was not refractory to a series of pulses spaced as close as 40 minutes apart (figure 5). Shorter intervals might be examined, especially if a system is used with sample times shorter than 15 minutes. When the strength of the applied field was increased the extent of modulation rose as well. This rise was linear and similar to the *in vitro* response, but attenuated. The same strength magnetic fields applied to the matrices when they were implanted in rats evoked a lesser reponse than was observed from the matrices *in vitro*. The difference

might be caused by the way in which the matrices were restrained. In vitro the matrices were held rigidly in place. This diminished any extraneous effects that might occur if the matrix rubbed or banged against the sides of the tubing. Thus, a great deal of the force exerted by the applied field on the embedded magnet was transferred to the inside of the matrix. In contrast, the matrices implanted in vivo rested against the teflon disk which was mounted to adjacent soft tissues. It is possible that some of the magnetic force was spent in moving the entire matrix against these tissues. Thus, greater strength magnetic fields were needed to achieve the same effect in vivo.

The possibility that increasing the temperature at the surface of the electromagnet increased BSA release, absorption or rat urine flow was discounted as the cause of modulated release. Despite a maximum rise of $8^{\circ}C$ per hour at the surface of the magnet there was no detectable change in urinary inulin in rats that had been implanted with matrices that did not have any embedded magnets. It should be noted that an electromagnet at room temperature will not rise above $30^{\circ}C$ in the half an hour of field exposure, and this value is less than natural body temperature. Thus, it is not suprising that the system was not perturbed by this temperature change. This confirms the results obtained in vitro where release rates from matrices did not change with an increase in the magnet's surface temperature (section II.3.5).

REFERENCES

[1] Gutman, Y., C.W. Gattschalk, and W.T. Lassiter, Micropuncture Study of Inulin Adsorption in the Rat Kidney, Science 147:753-754, 1965

[2] Brown, L., C. Wei ,and R. Langer, In Vitro and In Vivo Release of Macromolecules from Polymeric Drug Delivery Systems, J. Pharm. Sci., 72:1181-1185, (1983)

[3] Murray, J.B., L. Brown and R. Langer, Controlled Release of Microquantities of Macromolecules, Cancer Drug Delivery, 1(2)119-123 (1984)

[4] Murray J.B., L. Brown, R. Langer and M. Klagsburn, A Micro Sustained Release System for Epidermal Growth Factor, In Vitro, 19(10);743-748, (1983)

[5] Brown, L. and E. Edelman, unpublished results

CHAPTER VIII: BIOCOMPATIBILITY

VIII.1 Introduction

The feasibility of using a magnetically modulated delivery system *in vivo* was demonstrated in the previous chapter. Aside from technical problems, issues of biocompatibility must be considered. This chapter deals with the biocompatibility problems that are presented by each element of the system. The polymer matrix, with the embedded magnets, was studied to insure that it did not elicit an immune response. Studies are reported that show that drug can be delivered from such matrices in a bioactive manner. The effect of the DC magnetic field imposed by the embedded magnet and the effects of the externally applied AC field are also dealt with. Finally, issues surrounding the bioavailability of the magnetic field are presented to show that implanted matrices can indeed be acted on by the applied fields and should not induce harmful heating effects on the surrounding tissue.

VIII.2 Biocompatibility of Polymer Implants

The biocompatibility of five different polymers that were proposed for use in polymeric delivery systems was studied with a rabbit cornea model[1,2]. Alcohol washed ethylene-vinyl acetate copolymer used in this work and poly(hydroxyethyl methacrylate) showed no evidence of inflammation. In contrast, polyacrylamide or poly(vinyl pyrrolidone) pellets caused inflammation, marked disruption of the corneal collagen superstructure, severe edema, and infiltration by new blood vessels and inflammatory cells.

In a separate paper [3] four polymeric slabs containing a magnetized steel bead were implanted into the rabbit corneas. After two weeks the corneas were still clear and there was no evidence of edema, cellular infiltrate, or neovascularization by subsequent histological examination. The samsrium cobalt magnets were not observed to corrode in vitro or in vivo during the course of experiments that lasted up to two months. This was probably the result of a number of concomitant protective features. The magnets were coated with gold or nickel, and enveloped with EVAc polymer material. These layers shielded them from the low molecular weight salt solutions. In addition, despite the fact that low molecular weight compounds should permeate EVAc, the hydrophobicity of the poymer material limits the permeability of these compounds. Long term studies are required to verify these results.

The discussion presented in chapter I regarding the in vivo uses of EVAc drug delivery devices is a more than adequate testament to the ability of the system to deliver drugs with intact bioactivity.

VIII.3 Physiologic Effects of Exposure to Magnetic Fields

VIII.3.1 Cells and Animals A number of Soviet scientists [4,5] exposed rat liver cells to fields of 300-900 G pulsating at 7 kHz and found an inhibition in activity of oxidation-reduction and dehydrogenase enzymes, along with damage to mitochondrial membranes. Recent reports in the journal Science cited modification of cellular transcription [6], and enhanced DNA

synthesis [7], for weak fields(10^{-6} to 10^{-4} T) oscillating at 15 to 10^{3} Hz. Mice exposed to a 50 Hz magnetic field of 200 G for 6.5 hours had a marked increase in resistance to infection either for one exposure or 15 repeated daily exposures[8]. Histological specimens from guinea pigs exposed to the same field conditions for periods of 1 or 24 days disclosed evidence of mild hemorrhaging or emphysema in the lungs, testicular edema, as well as impaired peripheral circulation [9] . All of these conditiond were reversed when the field was withdrawn. Other studies have shown lymphoblastic proliferation in albino rats. Finally, rats exposed to fields in excess of 4200 G for longer than 4 days, developed disorganized and narrowed adrenal cortical zona fasciculata, a decrease in the number of megakarocytes in the bone marrow, and an increased spleen size, and number of liver tissue mitoses [10].

A large number of animals are capable of sensing magnetic fields for navigation (birds [11], honeybees [12]) and to detect prey or avoid predators [fish 13,14]. Human beings are less sensitive to these fields and the results of experiments designed to determine the degree to which they can detect magnetic fields are equivocal, at best [15,16]. Interestingly, 100 G fields oscillating between 10 and 100 Hz caused flashes of light and magnetophosphenes within the visual fields of subjects. The maximum effect occured at or about 20 Hz [17].

VIII.3.2 Humans Most of the reports on humans stem from research in the Soviet Union on the exposure of industrial workers to transmission lines and power stations. Differences in technique and the delay in receiving the information after translation make it difficult to evaluate this information

accurately. Changes were reported in the worker's vascular tone, sensory nerves, hyperhydrosis, and EEG recordings. "Prominent shifts in CNS activity" were noted along with hypotension secondary to sinus bradycardia [18,19]. They also described a relative leukopenia and, remarkably, a shortened erythrocyte sedimentation rate. Many of these symptoms, however, are nonspecific and can be attributed to a variety of noncontrolled factors.

In contrast, more rigorous studies of U.S. Navy Seafarer/Sanguine project workers revealed no medical, psychomotor or behavioral abnormalities [20], at 45-75 Hz fields that spanned the lower ranges from 0.01 to 0.15 G. A question of an elevation of serum lipids in Navy pilots at this frequency was raised but discarded [21].

The American embassy in Moscow was subjected to microwave signals to obstruct radiowave surveillance, at levels above USSR saftey standards but below USA safety standards. Reports of an increased incidence of serious disease, especially leukemia, in personnel manning this embassy arose but were dismissed as unfounded. No evidence was found that offered an association of electromagnetic radiation with leukemia or other forms of cancer [22-24].

VIII.3.3 Therapeutic Potential of Magnetic Fields A number of therapeutic uses have been proposed for magnetic fields. Potential applications of "magneto-therapeutics" include tumor growth inhibition [25-27], improvement of thrombophlebitis [28],and hastening of bone healing [29]. Fields of 10-100 G were studied for their osteogenic capability, over a range of frequencies from 15 to 10^6 Hz. Yet, there are also reports that

attempt to discredit these techniques. It was shown, for example, that the blunting of tumor growth could be the result of natural host immune response and not the result of the magnetic field itself [30], and that magnetic fields could delay wound healing and fibroblast proliferation [31].

VIII.3.4 Field Exposure Standards One available means of determining overall concern with exposure to these fields is to assess the limitations placed on exposure. If anything, these limitations represent the more conservative viewpoint regarding potential harm. In the United States there are no governmental standards pertaining to the exposure to magnetic fields. At the Stanford Linear Accelerator Center, the laboratory directors have developed a set of regulations limiting exposure to the whole body, head, arms, or hands. This is provided in the table I. In the Soviet Union a similar set of standards has been developed for relatively strong magnetic fields. These regulations specify maximum field strengths, as well as maximum field gradients of inhomogeneous fields to the whole body or hands.

TABLE VIII-I

MAGNETIC FIELD EXPOSURE STANDARDS

	Extended Periods (hours)	Short Periods (hours)
Whole Body or Head	200 G (DC)	2 000 G (DC)
Arms or Hands	2 000 G	20 000 G

	Field	Field Gradient
Whole Body	300 G (DC)	5-20 G/cm (DC)
Hands	700 G	10-20 G/cm

VIII.3.5 Conclusion It appears that long term exposure to high strength, high frequency fields might be detrimental. At frequencies less than 100 Hz little physical harm was demonstrated. A concrete statement, however, cannot now be made regarding the potential health hazards of electromagnetic fields for this area of research is rapidly evolving. The magnetically modulated system uses two types of magnetic fields. DC fields from the embedded permanent magnets and AC fields from applied stimulus. The permanent magnets have magnetic moments of about 1100 G and the magnets are minute. There might be effect on tissue immediately surrounding the magnets. The alternating magnetic fields are less than 100 Hz and 1000 G. The fields are applied for a short period of time, to a small area and fall off rapidly with distance. The net strength of the fields and duration of exposure is far lower than the recommended limits for both the U.S. and the U.S.S.R. . Nonetheless, this system, like many others, awaits the availability of more rigorous studies regarding the potential health hazards of magnetic field exposure.

VIII.4 Effect on Implanted Matrices by Environmental Magnetic Fields

Aside from effects on an organism embedded with permanent magnets and exposed to oscillating magnet fields, there is also the possibility that environmental fields might inadvertently trigger the implanted matrix. Natural geomagnetic fields have been measured to be about 10^{-8} Gauss [30] at 60 Hz. Fields in the general vicinity of electrical appliances have been shown to be as low as 10^{-3} G and as high as 25 G [33]. Transmission lines carry 4,000 amps at 765 kV, but the strength of the fields about and beneath

these lines is only on the order of 0.25-10 G [34,35], and human beings cannot sense the fields from transmission lines. Therefore, it is highly unlikely that such low strength fields will have an affect on the implanted magnets. Nuclear magnetic reasonance imaging devices may pose a potential danger, however. Fields from these devices are in the frequency of interest and at megaGauss strengths.

VIII.5 Bioavailability of the Applied Fields

Electromagnetic waves and quasistatic magnetic fields may be rapidly attenuated in a conducting media. Magnetic fields induce currents that exclude the applied field. These currents increase with frequency, such that at very high frequencies there is significant shielding. It is important to determine the extent of shielding of the 60 Hz magnetic fields that might be applied to a polymer implant. This is termed the bioavailability of the field.

The extent of attenuation is the ratio of the imposed field to the applied field. This ratio can be appreciated by comparing the characteristic time associated with the attenuation to the time reponse of the system. In a sense this can be seen as a "magnetic Reynolds number" [36]. If the system to which the magnetic field is applied responds faster than the time needed to attenuate the field there should be little important interference with the stimulus. In a magnetic field excited system oscillating at a frequency ω, the attenuation ratio, R, can be written in terms of the frequency, the electric conductivity of the media, σ, the

magnetic permeability of the media, μ, and the dimensions of the media, l.

$$R = \frac{\text{dissipation time}}{\text{period excitation}} = \omega\sigma\mu l^2 \qquad (1)$$

Alternatively, R can be thought of as the square of the ratio of the characteristic length in the system to the depth to which an applied field can penetrate. This penetration distance has been termed the "skin depth" [37] and can be derived from equation (1), as

$$\delta = \sqrt{\frac{2}{\omega\sigma\mu}}$$

As depicted in table II a 60 Hz field can be expected to penetrate 6.5×10^6 m into EVAc material, and 65 m into an average human. The magnetic field will therefore not be attenuated by induced currents before the full effect is exerted.

VIII.6 Induced Heating

Induced currents not only attenuate magnetic fields but lead to ohmic heating of the conducting medium. The amount of power generated from the heat can be computed for the magnet fields described above. The analysis is presented in appendix E and for the materials used here, is approximately 10^{-15} to 10^{-4} watts; a trivial value.

VIII.7 Conclusion

The different elements of the proposed magnetically modulated drug delivery system present different potential biocompatibility problems. Previous studies have shown that the EVAc material is inert *in vivo* and capable of delivering a variety of substances in their bioactive form. Samarium cobalt magnets embedded in these matrices have not yet been observed to elicit any additional inflammatory response. A preliminary search of the literature dealing with the biohazards of magnetic fields revealed a confusing and rapidly evolving picture. There now appears to be little potential danger at the field strengths and frequencies proposed in the drug delivery system, but further studies must be performed for an uneuivocal answer. There should be no chance of extraneous modulation of drug delivery from environmental fields. The magnets will not dissipate significant heat to the surrounding tissue, and will be subjected to the full extent of the field, without attenuation.

REFERENCES

[1] Gimbrone, M.A. Jr. et. al., Tumor Growth and Neovascularization, J . Natl. Cancer. Inst. 42:413-427, (1974)

[2] Langer, R., H. Brem, and D. Tapper, Biocompatibility of Polymeric Drug Delivery Systems for Macromolecules, J. Biomed. Mat. Res., 15:267-277 (1981)

[3] Hsieh, D., R. Langer and J. Folkman, Magnetic Modulation of Release of Macromolecules from Polymers, Proc. Natl. Acad. Sci. USA, 78:1863-1867 (1981)

[4] Shislo, M.A. et. al., Influence of Magnetic Fields on Enzymes, Tissue Respiration and Some Aspects of Metabolism in an Intact Organism, in "Influence of Magnetic Fields on Biological Objects", translated from Russian and available from the NTIS as JPRS 63038(1974).

[5] Yashina L.H., The Effects of a Low-Frequency Pulsed Magnetic Field on the Activity of Oxidation-Radiation Enzymes in the Liver of Albino Rats (An Historical Survey), Gigyena Truda I prfessional'nye Zabolvaniya, (1972) Available from NTIS as Translations on the Effects of Magnetic Fields, JPRS 6286 (1974).

[6] Goodman, R., C.A.L. Bassett, and A.S.Henderson, Pulsing Electromagneic Fields Induce Cellular Transcription, Science, 220:1283-1285

[7] Liboff, A.R., T. Williams, D.M. Strong, and R. Wistar, Time-Varying Magnetic Fields:Effect on DNA Synthesis, Science, 223:818-820

[8] Odinstov, N.Y., The effect of a Magnetic Field on the Natural Resistance of White Mice to Listeria Infection, Voprosy Epidemiologii Mikrobiologii 1 Immunologii, (1965), Translated from Russian and available from NTIS as JPRS 62865(1974).

[9] Toropstev, I.V. et. al., Pathologoanatomic Characteristics of Changes in Experimental Animals under the Influence of Magnetic Fields, in "Influence of Magnetic Fields on Biological Objects "translated from Russian and available from the NTIS as JPRS 63038(1974)

[10] Barnothy, M.F. and I. Sumegi, Effects of the Magnetic Field on Internal Organs and Endocrine System of Mice, Plenum Press, New York, 1969, pages 103, in "Biological Effects of Magnetic Fields", Vol. 2, Barnothy, M. ed.

[11] Durfee, W.K. et. al., Extremely Low Frequency Electric and Magnetic Fields in Domestic Birds, University of Rhode Island, Kingston, R.I.

[12] Lindauer, M. and H. Martin, The Earth's Magnetic Field Affects the Orientation of Honey Bees in the Gravity Field. Zeits. ver. Physiologie. 60:219, (1968)

[13] Clement-Metral, J.D., Direct Observation of the Rotation in a Constant Magnetic Field of Highly Organized Lamellar Structures, FEBS Letters 50:257, (1975)

[14] Rommel, S.A. and J.D. McCleave, Oceanic Electric Fields: Perception by American Eels?, Science 176:1233, (1972)

[15] Milburn, B.B., "Very Low Frequency Electromagnetic Fields and Behavior", PhD thesis, U.C.L.A., (1974)

[16] Tucker, R.D. and O.H. Schmitt, Tests for Human Perception of 60 Hz Moderate Strenth Magnetic Fields, IEEE Trans. on Biomed. Eng. BME-25(6):509-518, Nov., (1978)

[17] Barlow, H.B., H.E. Kohn, and E.G. Walsh, Visual Sensations Aroused by Magnetic Fields, J. Physiol. 148:372, (1947)

[18] Vyalov, A.M. et. al. On the Problems of the Effect of Constant and Variable Magnetic Fields on the Human Organism, Voprosy Profpatologii(Problems of Occupational Pathology), 1964. Available from NTIS as Translations on the Effects of Magnetic Fields, JPRS 36912 (1966).

[19] Vyalov, A.M., Clinico-Hygenic and Experimental Data on the Effects of Magnetic Fields under Industrial Conditions, in "Influence of Magnetic Fields on Biological Objects", translated from Russian and available from the NTIS as JPRS 63038 (1974).

[20] Krumpe, P.E. and M.S. Tockman, Evaluation of the Health of Personnel Working near Project Sanguine Beta Test Facility from 1971 to 1972.

[21] Beischer, D.E., Survival of Animals in Magnetic Fields of 140, 000 Oe. Plenum Press, New York, 1964, page 201. in "Biological Effects of Magnetic Fields: Vol. 1", Barnothy, M. ed.

[22] Milham, S. Jr., Mortality from Leukemia in Workers Exposed to Electrical and Magnetic Fields, N. Eng. J. Med. 307:249, 22 July, (1982)

[23] Dwyer, J.M. and D.B. Leeper, A Current Literature Report on the Carcinogenic Properties of Ionizing and Nonionizing Radiation. II. Microwave and Radiofrequency Radiation.

[24] Milham, S. Jr., Mortality from Leukemia in Workers Exposed to Electrical and Magnetic fields, N. Eng. J. Med., 307:249 (1982)

[25] Uklova, M.A. and Kvakina, Y.B. Effect of Magnetic Fields on Experimental Tumors (Direct and Through the Nervous System), in "Influence of Magnetic Fields on Biological Objects" translated from Russian and available from the NTIS as JPRS 63038(1974).

[26] D'Sousa, L. et. al., The effects of a Magnetic Field on DNA Synthesis by Ascites Sarcoma 37 Cells, Plenum Press, New York, 1969, page 53, in "Biological Effects of Magnetic Fields: Vol. 2", Barnothy, M.ed.

[27] Becker, R.O., Biological Effects of Magnetic Fields:A Survey, Med. Electron. Biol. Eng. 1:293, (1963)

[28] Edlinskiy, I.B. et. al., Changes in Some Blood Trace Elements in Patient and Acute Thrombophlebitis of the Lower Extremities under the Influence of a Constant Magnetic Field, Voprosy Kurotologii, Fizioterapii I Lechebnoy Fizicheskoy Kul'tury, 1969. Translated from Russian and available from NTIS as JPRS 62865(1974).

[29] Degenm I.L. et. al., Consolidation of Bone Fragments in a Constant Magnetic Field, Ortopedia Travmatologiya I Protezirovaniye, 1971. Translated from Russian and available from NTIS as JPRS 62864(1974).

[30] Barnothy, M.F., ed. "Biological Effects of Magnetic Fields" Plenum Press, New York, 1969.

[31] Gross, W. and L.W. Smith, Wound Healing and Tissue Regeneration. Plenum Press, New York, 1964, page 140, in "Biological Effects of Magnetic Fields: Vol. 1", Barnothy, M. ed.

[32] Konig, H.L., ELF and VLF Signal Properties: Physical Characteristics, Plenum Press, New York, p. 4 in "ELF and VLF Electromagnetic Field Effects", (1974)

[33] Miller, M.W. Effect of Extremely Low Frequency Electric and Magnetic Fields on Roots of Vicia Faba: Final Report for Project Sanguine.

[34] Sheppard, A.S. and M. Eisenbud, "Biological Effects of Electric and Magnetic Fields of Extremely Low Frequency", New York University Press, New York, (1977)

[35] Deno, D., Common Record Hearings on Health and Public Safety of 765 kV Transmission Lines, Testimony before Public Service Commission of the State of New York in cases 26529 and 26559.

[36] Hughes, W.F. and F.J.Young, "The Electromagnetodynamics of Fluids", Wiley, NY, P. 154 (1966)

[37] Woodson, H.H. and J.R. Melcher, "Electromechanical Dynamics: Part II: Fields, Forces and Motion", chapter 7, Wiley & Sons, NY (1968)

IX. SUMMARY OF PAST WORK AND SUGGESTIONS FOR FUTURE RESEARCH

IX.1 Introduction

The models developed in the past chapters explained the role of the volume of matrix acted on by the magnet and the influence of the amplitude and frequency of the applied magnetic field. These models, however, were by necessity specific and at times qualitative. A more quantitative model needs to be developed if modulated drug release is to become a predictable science. Further research must be done to fill in the voids. In this chapter an attempt will be made to outline the important parts of any potential model and to detail what experiments remain to be performed in order to develop a rigorous model of modulated release.

The magnetic modulated system can be broken down into four component parts. The first two, the embedded magnet and the applied field, make up a 'magnetic interaction' group. The second group of two revolves around the polymer matrix and includes the drug as well as the polymer material. The entire system exists in some defined environment, be it buffered solution *in vitro* or subcutaneous fluid *in vivo*. Each of the components individually influence drug release and acts on other components as well. The system is depicted as a pyramid in figure 1. The points at the base of the pyramid represent the individual components and the lines that connect them represent the intercomponent interactions. The circle surrounding the pyramid is the environment surrounding the matrix. Any model dealing with the system will need to view the system in

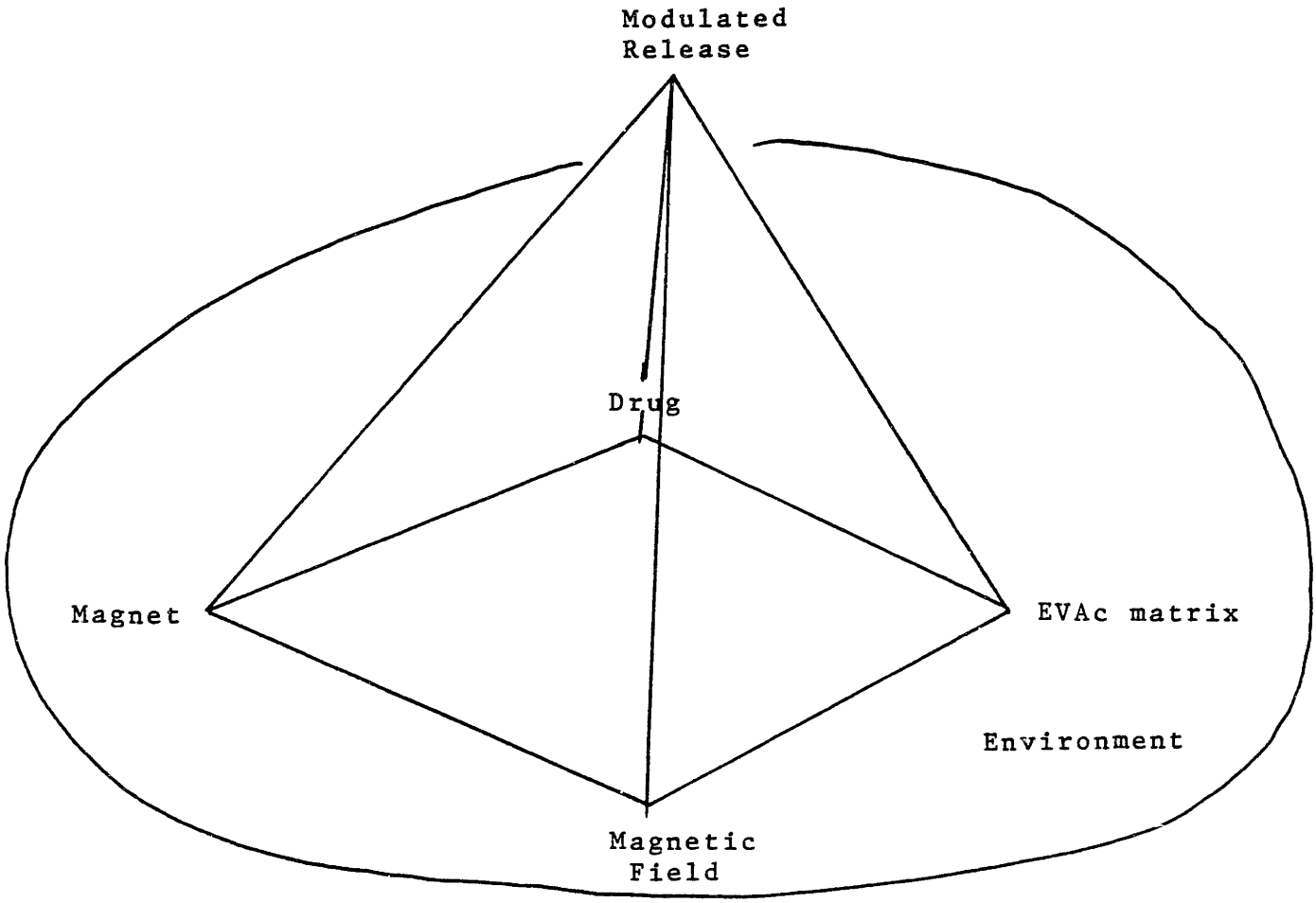

Figure 1: Schematic representation of the magnetically modulated system. The vertices of the pyramid represent the four key elements of the system; the matrix embedded magnet and the applied oscillating magnetic field, which act on the combined matrix unit composed of the polymer material and the dispersed drug. The interactions between each of these components are the lines that connect the vertices. The circle about the pyramid depicts the environment in which the matrix resides, be it phosphate buffer _in vitro_, or subcutaneous fluid _in vivo_. The lines of the pyramid converge to yield modulated or enhanced release.

a fashion not unlike this pyramid. In the discussion that follows suggestions for research that would futher elucidate these areas will be presented after a short summary of the facts and observations accumulated to date. The individual properties of each of the components that should or have already been shown to affect drug release will be discussed first and then the interactions between the components will be detailed.

IX.2 Discussion

IX.2.1 Embedded Magnet Some of the properties of the embedded magnet which contributed to modulated release were examined in chapter IV. Modulation increased with increasing magnet size, increasing magnetic pole strength, and with anisotropic magnet shapes. Preliminary evidence, not reported in that chapter, indicated that release increased when the number of magnetic spheres in a flat slab EVAc-BSA matrix were increased. Matrices were cast as large slabs and embedded with magnetic spheres as described in section II.2.2 . Smaller samples, 1.0 x 1.0 x 0.2 cm^3, were cut from the large slab to contain up to nine magnetic spheres. The rate of BSA release from matrices embedded with nine magnetic spheres increased 4.8 fold when exposed to an 1800 G, 9.5 Hz magnetic field (rotating permanent magnets) for two hours of each day over a three week period. The increase from identical matrices containing only one sphere was far less, approximately 1.6 fold. Comparison of matrices of identical size with more than one samarium cobalt magnet was not possible because of the magnetic interactions between the high strength magnets. Thus, for more magnets to be placed in a single matrix the size of the matrix had to be enlarged. Flat slab matrices, also 1.0 x 1.0 x 0.2 cm^3, were fabricated

with one torroidal $SmCo_5$ magnet, and other matrices were made with the same particle size and loading, but at twice the length to accomodate two magnets (section II.2.2). The different samples were exposed to over 50, 10 minute pulses of 500 G, 60 Hz electromagnetic fields, over the course of two weeks. BSA release was increased 2.5 fold above baseline in both cases, though the relative baseline and peak release rates were higher for the longer matrices as expected. These two experiments provide further evidence for a volume of influence model. If magnets can be brought close enough together to act on a given volume of matrix the net effect on that matrix will be increased, but if the volume is increased as the number of magnets is increased, no additional modulation can be achieved.

Modification of the fabrication technique might allow for more than one high strength magnet to be embedded in the polymer-drug matrices. Nonmagnetized samarium cobalt objects could be placed in the matrix and then magnetized. This is possible, but the ultimate strength of the magnet will only be a fraction of the magnetic strength achieved if the objects were magnetized prior to being embedded in the matrix. The loss of strength stems from the way in which the samarium cobalt magnets are made. Fine powdered particles of the $SmCo_5$ metal are sintered into a large block. The entire block is then magnetized and smaller magnets of certain shapes drilled out of the block. After drilling the magnets are magnetized a second time to their final and full strength. If the first magnetization is eliminated, and the second is delayed until the magnet is embedded in the matrix, the net magnetic moment of the magnet will be far lower than what can be achieved if it were handled in the standard

fashion. An alternative scheme is the utilization of magnetic fields to position the magnets in the matrices at the time of fabrication. A magnetic field, stronger than the field generated by one of the magnets, might be applied around the glass mold in which the matrices are cast. This field should determine how the magnets will be positioned in the matrix, for it will supercede the attraction between the magnets and cause the magnets to align themselves with the applied field. A constant, uniform field will not be appropriate, for it will draw the magnets to the bottom of the mold and not let them rest in the middle of the matrix. This can be avoided by only applying the field after a part of the matrix has had time to harden, or by using fields similar to those used to contain and accelerate magnetic plasmas [1]. These fields have components in many directions and if designed properly can 'hold' the magnets at a specified height and orientation.

The biocompatibility of the these magnets has only been investigated in a cursory manner. The magnetic spheres elicited no inflammatory response when implanted in a rabbit's cornea [2] and the $SmCo_5$ magnets embedded in the matrix also appear to be inert in vivo (section VIII.2). This is probably because of the nickel and gold coatings that were applied to the magnets and protect the magnet from corrosion by the low molecular weight salt buffers and subcutaneous fluid. Futhermore, despite the fact that EVAc material is highly permeable to low molecular weight compounds, fluid entry is limited by the exreme hydrophobicity of the copolymer material. More long term follow-up is required, however, especially with the rare earth magnets.

IX.2.2 Applied Magnetic Field The experiments in chapter III showed that modulation increased with increasing frequency of field oscillation from 5 to 60 Hz, and increasing field amplitude from 200 to 900 G. Release remained elevated for the duration of field exposure.

The electromagnet offered vast improvements over the mechanical devices with rotating permanent magnets, yet the system can still be made smaller, more efficient, and capable of delivering fields over a wider range of frequencies. The electromagnet used in this work was constrained to 60 Hz alone. A system could be built were fields could be generated over a range of frequencies. This might include the use of an audio oscillator attached to an audio power amplifier to send a high power, variable frequency signal to an electromagnetic coil. The magnetic field that would be produced would oscillate at the frequency of the input signal, at a field strength proportional to the power of the input. Alternatively, an alternating current generator might be used to drive a variable speed motor. Again, the frequency and amplitude of the field would be determined by the input from the signal generator. Both of these systems would allow for studies at very high frequencies to determine whether the extent of modulation drops off as the frequency is increased. This drop off is suggested from the deformation studies and discussion in chapter V, and from the microscopic model presented in chapter VI.

IX.2.3 Magnet - Field Interactions An entire field of electromagnetics is devoted to the study of the interactions between magnets and oscillating magnetic fields [1]. The equations that govern these interactions need not be summarized. Experiments in section II.3.5

illustrated that release modulation was increased when the pole vector of the embedded magnet was aligned with the applied field, or in another sense, when the force on the magnet exerted by the field was maximized.

The alignment of the magnet in vitro or in vivo might be detected by a device attached to the magnetic field generator. The device would find the orientation of the magnet, and then manipulate the direction of the field such that it was optimally in line with the magnet. This procedure would maximize the force exerted on the magnet and minimize extraneous or wasted energy. Such a device could be as simple as a gaussmeter that scanned the matrix implantation site. The meter will record a maximum field generated from the magnet when the meter's probe is aligned with the pole vector of the magnet. Once this maximum is achieved the device could note and lock on to the position and set the direction of the applied field.

IX.2.4 Dispersed Drug Previous research has defined the change in release profile from sustained release matrices dispersed with a specific drug at different concentrations and shapes, and for different drugs. For example, the rate of drug release was increased for higher solubility drugs [3]. All of the matrices examined in this thesis were made with BSA, a highly soluble protein of approximately 68,500 molecular weight. The modulation of less soluble and lower molecular weight compounds must be studied and understood if substances such as insulin are to be modulated. If enhanced release is independent of diffusion the solubility of the drug will be minimally important in determining the extent of release, and low solubility drugs will modulate to the same extent as high

solubility drugs. Yet, the microscopic model of chapter VI predicts that the Schmidt number of the solution of drug will play an important role in the eventual affect. This number represents the ratio of the protein solution's velocity profile to its spatial concentration gradient. Low molecular weight compounds will already be diffusing at fast rates and will require high frequency or large amplitude stimulii for pulsed flow to exceed diffusion. In contrast, when diffusion-limited flow is slow, the enhancement of flow by an oscillating stimulus will have that much greater relative effect. Insulin and BSA have Schmidt numbers that are of the same order, 10^4 [4,5], and therefore will be expected to produce similar results by this model. Before extensive experiments with magnets are investigated physical deformation of the matrices, as described in chapter V, might be used to see if the release of other compounds can be enhanced.

IX.2.5 Polymer Matrix The rate of drug release from a flat slab EVAc matrix decreases with time. Early in the course of drug release there is minimal matrix between the stored drug and the environment, and little impairment to diffusion. As release progresses the drug deeper in the matrix must diffuse through more matrix to reach the environment, and release rates are slowed. Zero-order release from a polymer matrix was achieved when the amount of drug available for release increased as the distance the drug had to diffuse increased [6]. This was accomplished by coating hemispherical or disk shaped matrices with a impermeable coating, and then constraining release from an aperture drilled into this coating. Modulated release has been achieved from these matrices, but it appears that the dynamics of the increased release may be slightly different than in the nonlayered case. Disc shaped matrices were fabricated with one

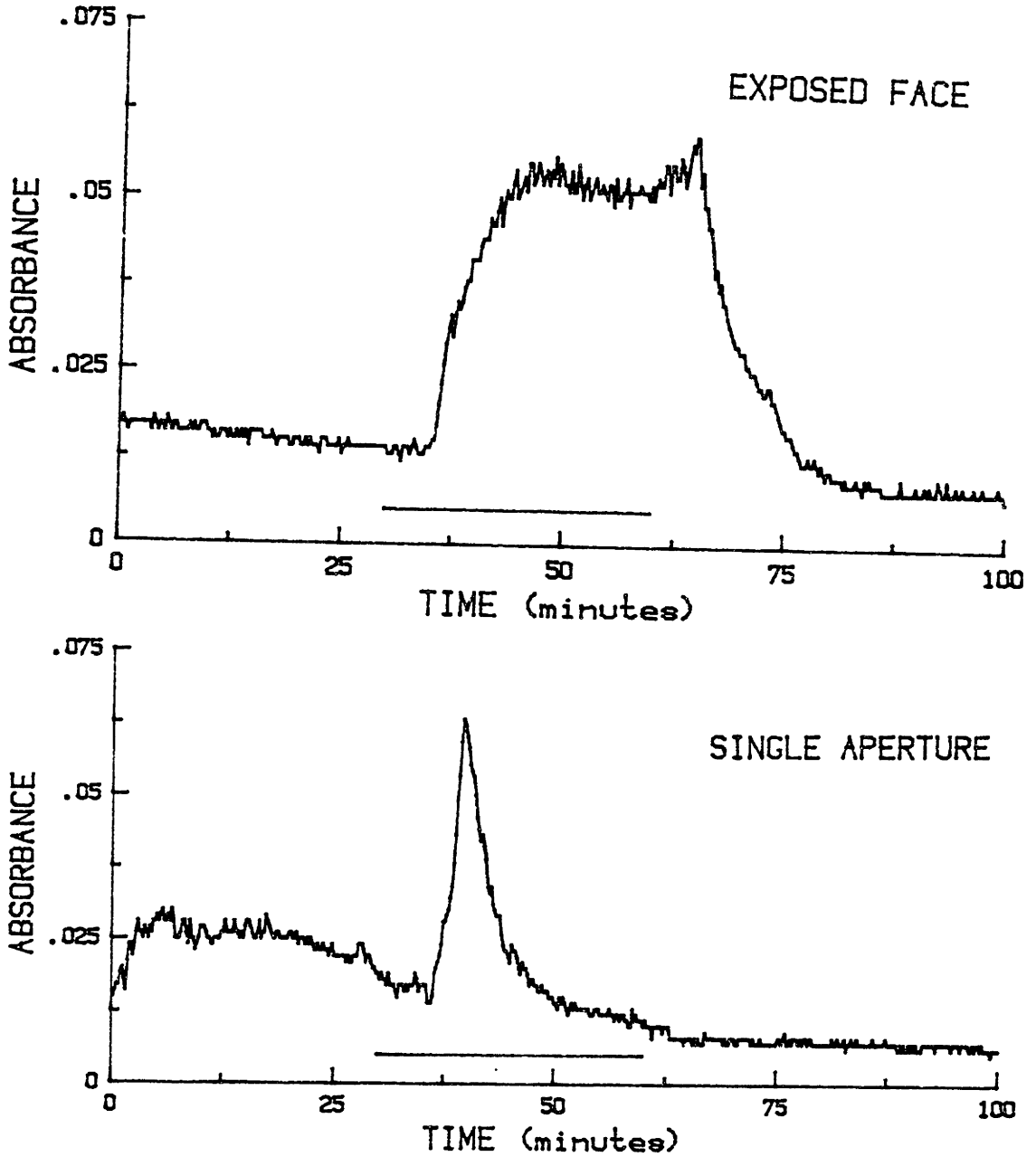

Figure 2: Continuous recording of BSA release from two different EVAc-BSA matrices exposed to a 10 Hz, 1800 G magnetic field for 10 minutes. Panel a depicts the sustained elevated release that is achieved from a matrix with all faces exposed for release. In contrast, a matrix coated with an impermeable layer and constrained to release BSA through a hole in this coating, exhibited a pulse of increased release, and then a return to baseline even before the field was withdrawn.

torroidal samarium cobalt magnet (section II.2.2) and exposed to 10 minute pulses of 500 G, 60 Hz electromagnetic fields. Matrices were left uncoated or layered with EVAc and an apeture drilled in this coating. The release of BSA was followed dynamically and in real time with a flow through spectrophotometer (section III.2) . Figure 2 shows that while release from a matrix with all faces entirely exposed was elevated for the duration of field exposure, the single aperture matrices delivered a spike of release and no additional drug during the remainder of field exposure. Future experiments might examine the mechanism behind this phenomenon. A spike or pulse is the time derivative of a step and a hole is, in a sense, the spatial derivative of a plane. A potential model might incorporate the transient increased release from many holes in different locations and distances from the magnet, to achieve the integrated step release from the plane. In addition, it seems that the position of the hole is important. Modulated release from coated matrices with holes drilled through the part of the coating that was above the center of the magnet was far greater than from matrices with holes far from the magnet. This might offer futher support for the volume of influence model. If the hole was outside of the volume of matrix acted on by the magnet, little modulated release might be expected. On the other hand, matrices with an aperture right over the magnet might display significant increases in BSA release with exposure to oscillating fields.

IX.2.6 Drug-matrix interactions It has been known for some time that the morphology of the matrix contributed to the sustained release, and that drug dispersed in the matrix formed a tortuous network of drug pockets, which were connected by small pores [7]. The size of the pockets

was determined by the particle size of the drug, and the concentration or loading of the drug determined the number of pockets. Thus, the net amount of drug released from the matrices increased with increasing drug particle size, and increasing drug loading [8]. At low particle sizes and loadings a portion of the drug was permanently trapped in the matrix in pockets that never communicated with the environment [8]. The tortuosity of the matrix and the existence of the small channels connecting the larger pockets of drug was used to account for prolonged release from EVAc matrices [9]. In matrices embedded with magnets and exposed to magnetic fields, trapped drug was freed, and the pockets adjacent to the magnet were broken open (section II.2.4.ii).

The particle size of the protein used in the experiments in this thesis was kept at a narrow range, 150-180 microns, and only one loading, 33%, was studied. Preliminary data indicated that there was no statistically distinquishable difference between modulation from matrices with 25,33,50 % loadings of BSA. The use of different particle size ranges also did not seem to affect modulated release. Further experiments along these lines are needed, but what this might suggest is that the morphological affects on the matrix occur early in the course of the experiments, and are probably directed more at the connecting pores than the drug pockets. These pockets are significant determinants of sustained release and are less affected by the size and properties of the dispersed drug than the larger pockets.

IX.2.7 Magnet-matrix interactions The studies described in chapter V showed that enhanced release from EVAc-BSA matrices could be obtained when

the matrices were physically deformed. The response to a mechanical or physical deformation was found to be similar to the response from a matrix embedded with a magnet and exposed to oscillating magnetic fields. If the mechanism of modulation hinges on the displacement of the magnet within the matrix, and if the extent of this displacement limits the extent of the modulation, then matrices that allow for greater displacement should exhibit greater modulation. Both models described above predict increased release for increased magnet displacement. As the extent of magnet displacement increases, the volume of influence of the magnet will increase. Thus, the sphere of influence model will predict further enhancement of release. The microscopic model of chapter VI relates enhanced release to the square of an amplitude factor. This factor is the ratio of the displacement of the magnet to the radius of the flow-limiting connecting channels. Therefore, as the displacement increases or the channels diminish in size, the amount of modulation should increase substantially.

It is easy to recommend that experiments be performed that would change the elasticity of the polymer matrix, but it will be difficult to change only the elasticity without influencing other properties of the polymer material. The modulus of elasticity of EVAc changed with different ratios of ethylene to vinyl acetate [10]. Yet, so did the solubility of the material in a polar solvent, and its water sorbtivity. At the same time the rate of protein release from EVAc-BSA matrices without any magnets was increased with increasing amounts of vinyl acetate in the EVAc material and decreasing molecular weight of 40% vinyl acetate samples [10]. Careful experimental design must be considered in order to

isolate the elasticity as the single variable being changed in the proposed studies.

The mechanism of enhanced release and the delay in achieving peak modulation were explained in part by the freeing of trapped drug and the time needed to develop an area or gap around the magnet for the magnet to move in (chapter IV). What has not yet been delineated is whether there is a decay in the response with time. If the morphological changes occur after the first few field exposures then modulated release should drop off as the distance between the internal drug and the external environment increases. The potential for response decay is an important possible limitation of clinical application of the system. It will be interesting to see if there is a difference between flat slab matrices and the hemispherical devices, described in section IX.2.3, that would compensate for the increased distance with increasing release surface area.

IX.2.8 Environment The release of BSA from EVAc matrices was minimal when the pH of the environment was approximately the isoionic pH of BSA. Release was independent of the ionic strength of the environment [8]. BSA release from nonmodulated EVAc matrices increased when the release was conducted at higher temperatures, presumably because of accelerated diffusion [8], but the modulated system showed little response to temperature changes (section II.3).

IX.3 CONCLUSION

The models developed in the previous chapters were, of necessity, specific and qualitative. The volume of influence model (chapter IV) explained, in part, the interaction between the matrix and the embedded magnet. The microscopic model (chapter VI) provided some insight into how pulsatile flow could lead to enhanced release, and the dynamic displacement studies (chapter V) showed that this enhanced release could indeed be achieved with deformation of the matrices. The microscopic model also predicted the response to different stimulus frequencies. A more quantitative model needs to be developed if modulated release is to become a predictable science. The pyramid depicted in figure 1 displays the elements of the system that must be considered by any model. Of all of the proposed experiments listed above, the most important and potentially enlightening appear to be the ones devoted to the study of polymer matrices with different modulii of elasticity, field frequencies greater than 60 Hz, and macromolecules with different solubilities. The discussion presented above summarizes what results might be expected or predicted from the models developed in this thesis. Varying the modulus should provide additional data on the matrix-magnet interaction and additional control over the extent of the response. A more pliable material will yield more than a less pliable one, and allow the magnet to exert its effects over a greater volume of the matrix. These investigations go hand-in-hand with further study of the role of the frequency of field oscillation on modulated release. As discussed in section V.4, the response time of the matrix material dictates that at some critical frequency the matrix material will respond optimally to the

movement of the magnet. At frequencies above this value the material will be 'too slow' to respond to each stimulus and the response will be attenuated. The time response will be different for different types of polymer material and, perhaps, for matrices made with the same polymer but different drugs. Thus, further research over the entire range of frequencies is warranted for a variety of matrices. The experiments with other substances must be done to allow for parameters of the drug to be entered into a large scale, integrated model. Many of the drugs that are potential candidates for regulated release have far lower solubilities than BSA. These studies will not only determine whether modulation can occur with substances of a lower solubility than BSA but will also provide valuable insight into the mechanism of modulation. If modulation is solubility independent, then modulation should not be a diffusion mediated or limited process.

REFERENCES

[1] Kraus, J.D, and K.R. Carver, "Electromagnetics", McGraw-Hill Book Company, New York (1973)

[2] Hsieh, D., R. Langer and J. Folkman, Magnetic Modulation of Release of Macromolecules from Polymers, Proc. Natl. Acad. Sci. USA, 78:1863-1867 (1981)

[3] Brown,L., "Controlled Release Polymers: In Vivo Studies with Insulin and other Macromolecules", Sc.D. Thesis in the department of Nutrition and Food Science, M.I.T., Cambridge, MA (1983)

[4] Sober, H.A., ed., "Handbook of Biochemistry, Selected Data for Molecular Biology", p. C-10, The Chemical Rubber Co., Cleveland OH (1968)

[5] McCarthy, M. and D.S. Soong, personal communication, Department of Chemical Engineering, University of California at Berkeley

[6] Hsieh, D., W. Rhine and R. Langer, Zero-Order Controlled Release Polymer Matrices for Micro- and Macromolecules, J. Pharm. Sci., 72:17-22 (1983)

[7] Bawa, R.S., "Controlled Release of Macromolecules from Ethylene-Vinyl Acetate Copolymer Matrices: Microstructure and Kinetic Analysis", M.S. Thesis, Department of Nutrition and Food Science, M.I.T., Cambridge, MA, (1981)

[8] Rhine, W., D. Hsieh, and R. Langer, Polymers for Sustained Macromolecule Release: Procedures to Fabricate Reproducible Delivery Systems and Control Release Kinetics. J. Pharm. Sci., 69:265-270 (1980)

[9] Siegel, R.A., "Macromolecular Drug Release from Porous Implants: Sources of Matrix Tortuosity", Ph.D. Thesis, Department of Electrical Engineering and Computer Science, M.I.T., Cambridge, MA, (1984)

[10] Kunica, E., "Release Kinetics from Various Ethylene-Vinyl Acetate Copolymers", M.S. Thesis, Department of Nutrition and Food Science, M.I.T., Cambridge, MA, (1984)

APPENDICIES

A. ETHYLENE-VINYL ACETATE COPOLYMER

B. 1. BOVINE SERUM ALBUMIN

2. SAMARIUM COBALT

C. DISPLACEMENT OF A SOLID BY A POINT FORCE

D. MAGNETIC SKIN DEPTH

E. INDUCTION HEATING

F. COMPUTER PROGRAMS

G. EXPERIMENTAL DATA

APPENDIX A: ETHYLENE - VINYL ACETATE COPOLYMER

Ethylene-vinyl acetate copolymer (EVAc) is a random, linear copolymer composed of repeating units of ethylene and vinyl acetate (VA). A polymer if ethylene alone is crystalline. This crystallinity is reduced with the addition of increasing molar concentrations of vinyl acetate because of the difference in the atomic radii of the two monomers [1]. VA has a greater atomic radius than ethylene, and when interspersed into a polyethylene chain will prevent crystallinity for a given number of carbon units in its vicinity. Therefore, a copolymer 50% VA by weight, will have no cystallinity. The copolymer used in this thesis was 40% VA; it exists on the borderline between the crystalline and amorphous states [1]. Aside from increasing flexibility, with decreased crystallinity, the addition of vinyl acetate increases the solubility of the copolymer in polar solvents because of the VA polarity.

EVAc emulsions are used as adhesives, sealants, coatings and binders. Table I details some typical physical properties of the pure copolymer materials. The addition of the drug to form a polymer-drug matrix should alter these physical properties. Dynamic material testing was performed with the Dynastat system. This device provides closed-loop control of either load or displacement covering a range of frequencies from DC to 99 Hz. It is described in detail elsewhere [2].

TABLE I: TYPICAL PROPERTIES OF EVAc [3]

Vinyl acetate content, % by weight	40
Inherent viscosity at 30 °C (0.25g/dl toluene)	0.70
Melt Index, g/10 min	57
Residual VAc monomer, % by weight	< 0.3
Odor	slight
Antioxidant, ppm BHT	750
Tensile strength (MPa)	4.5
Elongation at Break, %	1450
Elastic (tensile) modulus, MPa	2.1
Density at 23°C, kg/m^3	965
Bulk Density, kg/m^3	480
Refractive Index, n25/D	1.476
Hardness, Shore A-2 durometer, 10 sec	40
Softening Point, ring and ball, °C	104

When slabs of EVAc material or EVAc matrices containing BSA (150-180 particle size range, 33% loading) were tested on this machine the loss angle and modulus and the storage modulus were determined. They are displayed in figures 1 through 3. The data shows that EVAc is a rubbery material with a storage modulus in the 10^6 Pa range. This is the same range noted in the specifications provided by the manufacturer [3]. When BSA was added to the matrices the modulii obtained in compression and tension were even lower, implying that the matrix was even more pliable than a slab of pure EVAc. Presumably this arises from the porous anture of the network. The lack of significant change with increasing frequency to 100 Hz is important in light of the experiments that showed increasing modulation with increasing frequency of field oscillation. Furthermore, it implies that the material cannot be modelled as a two or three element material with one time constant. Instead, there probably exists a heirarchy of viscoelastic time constants which join in superposition to define the resopnse of the material as a whole.

REFERENCES

[1] Salyer, I.O., and A.S. Kenyon, Structure and Property Relationships in Ethylene-Vinyl Acetate Copolymers, J. Pol. Sci., Part A-1, 9:3083-3103 (1971)

[2] Sternstein, S.S., Transient and Dynamic Characterization of Viscoeleastic Solids, chapter 7 in Polymer Characterization, Carver, ed., Am. Chem. Soc., (1983)

[3] Users' Guide DUPONT ELVACE Acetate/Ethylene Emulsions, Du Pont Co., Polymer Products Department, Ethylene Polymers Division, Wilmington, Delaware 19898

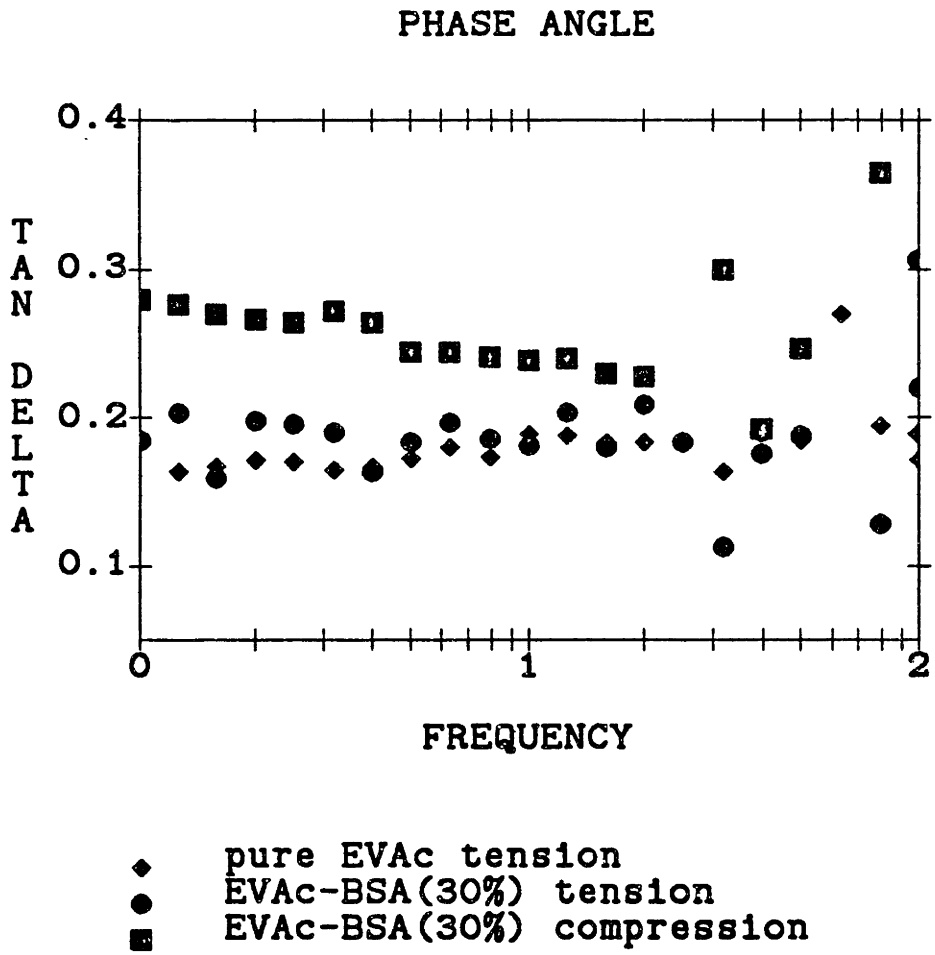

Figure 1: Loss angle of slabs of 100% EVAc and EVAc-BSA matrices (30-33% loading, 150-180 particle size range) tested in compression and tension over a span of frequencies from DC to 99 Hz. Both the abcissa and ordinate are plotted logarithmically, with units that express powers of 10.

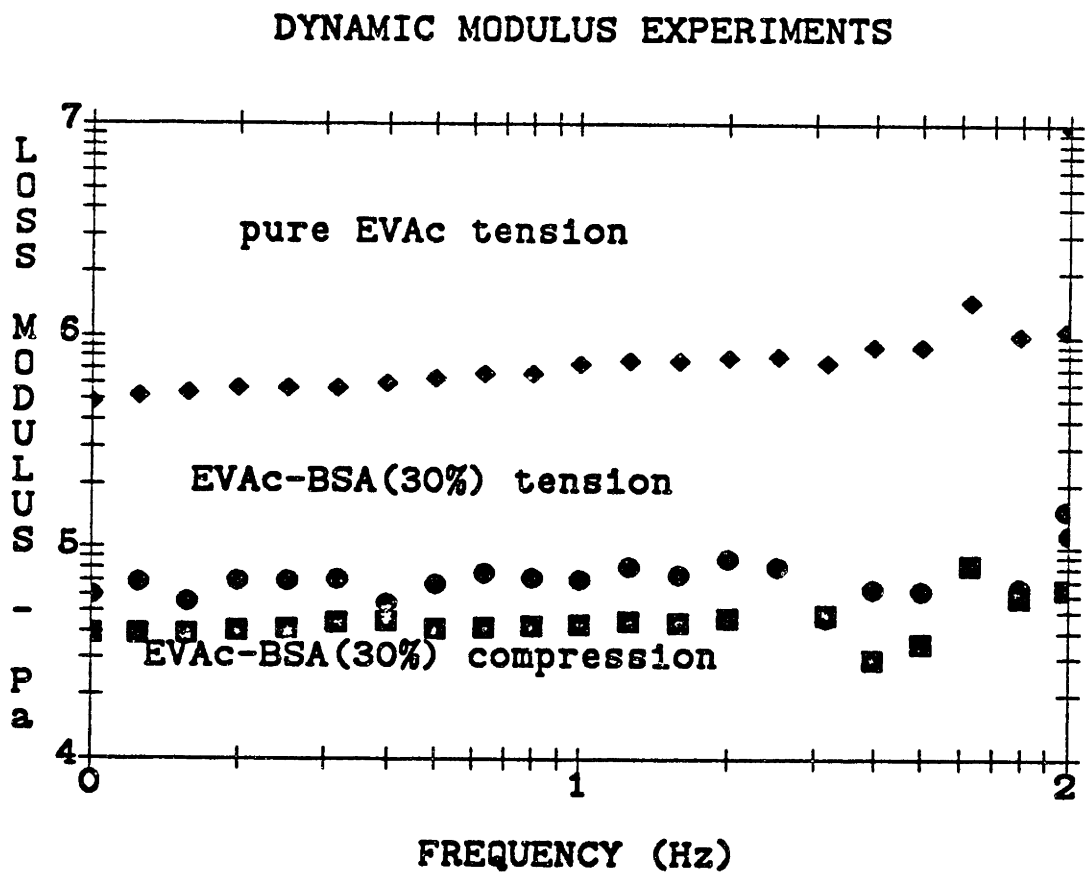

Figure 2: Loss modulus of slabs of 100% EVAc and EVAc-BSA matrices (30-33% loading, 150-180 particle size range) tested in compression and tension over a span of frequencies from DC to 99 Hz. Both the abcissa and ordinate are plotted logarithmically, with units that express powers of 10.

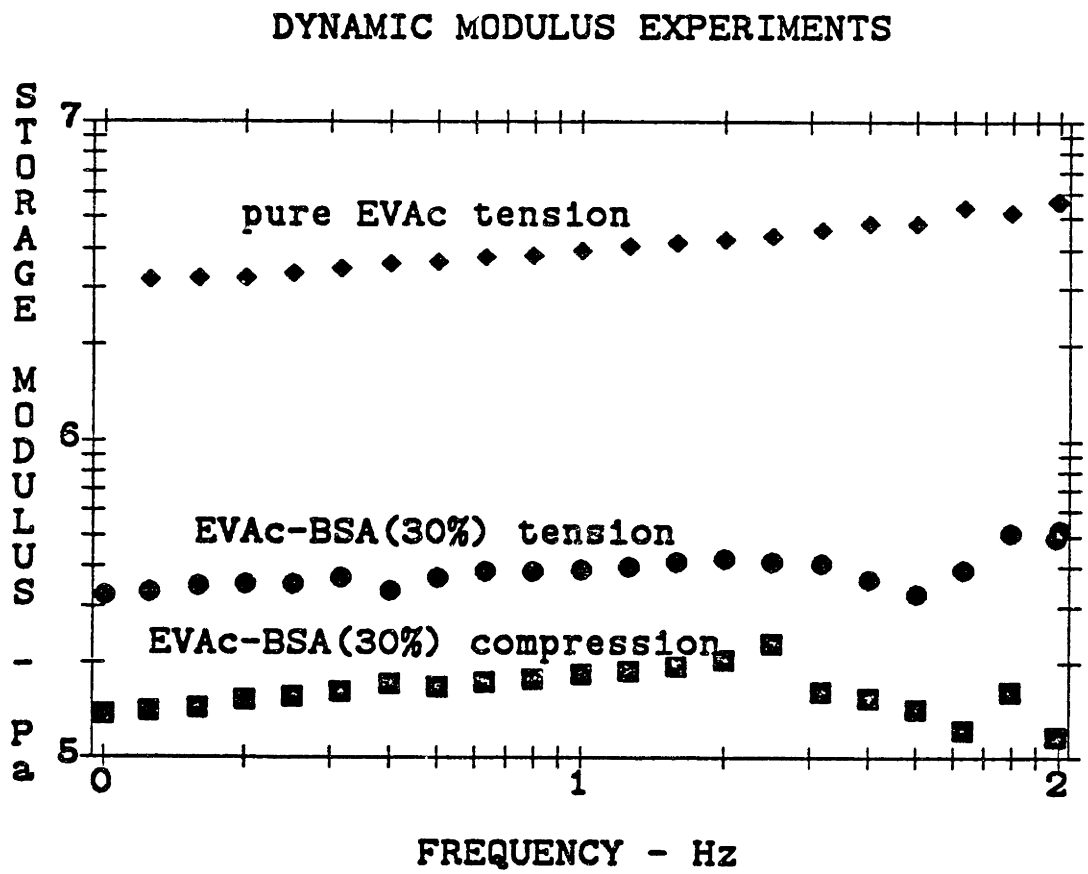

Figure 3: Storage modulus of slabs of 100% EVAc and EVAc-BSA matrices (30-33% loading, 150-180 particle size range) tested in compression and tension over a span of frequencies from DC to 99 Hz. Both the abcissa and ordinate are plotted logarithmically, with units that express powers of 10.

APPENDIX B:

B.1: BOVINE SERUM ALBUMIN

Bovine serum albumin was used as the test macromolecule in this work. It has been used in the past to study the sustained release of macromolecules from polymer matrices [1-9]. The protein is ellipsoid, 10 x 60 ^{o}A in diameter, is approximately 68,500 daltons in molecular weight, has a pI of 4.8-5.2 [2,10,11], and is highly soluble in water. At 37^{o}C it has a water solubility of 0.585 g/cm^{3}, and a diffusion constant of 6-9 x 10^{-7} cm^{2}/sec [10] . It can be assayed spectrophotometrically at 220 and 280 nm [11].

REFERENCES

[1] Rhine, W., D. Hsieh, and R. Langer, Polymers for Sustained Macromolecule Release: Procedures to Fabricate Reproducible Delivery Systems and Control Release Kinetics, J. Pharm. Sci., 69:265-270 (1980)

[2] Bawa, R.S., "Controlled Release of Macromolecules from Ethylene-Vinyl Acetate Copolymer Matrices: Microstructure and Kinetic Analysis", M.S. Thesis, Department of Nutrition and Food Science, M.I.T., Cambridge, MA, (1981)

[3] Hsieh, D., R. Langer and J. Folkman, Magnetic Modulation of Release of Macromolecules from Polymers, Proc. Natl. Acad. Sci. USA, 78:1863-1867 (1981)

[4] Hsieh, D., W. Rhine and R. Langer, Zero-Order Controlled Release Polymer Matrices for Micro- and Macromolecules, J. Pharm. Sci., 72:17-22 (1983)

[5] Langer, R., E. Edelman and D. Hsieh, Magnetically Controlled Polymeric Delivery Systems, Chapter 25, pp 585-596, in "Biocompatible Polymers, Metals, and Composites", M. Szycher ed., Technomic Pub. Co., Inc. (1983)

[6] Miller, E.S, N.A. Peppas and D.N. Winslow, Morphological Changes of Ethylene/Vinyl Acetate-Based Controlled Delivery Systems During Release of Water-Soluble Solutes, J. Membrane Sci., 14:72-92 (1983)

[7] Siegel, R.A., "Macromolecular Drug Release from Porous Implants: Sources of Matrix Tortuosity", Ph.D. Thesis, Department of Electrical Engineering and Computer Science, M.I.T., Cambridge, MA, (1984)

[8] Kunica, E., "Release Kinetics from Various Ethylene-Vinyl Acetate Copolymers", M.S. Thesis, Department of Nutrition and Food Science, M.I.T., Cambridge, MA, (1984)

[9] Edelman, E.R., J. Kost, B. Bobeck, and R. Langer, Regulation of Drug Release from Polymer Matrices using Oscillating Magnetic Fields, J. Biomed. Mat. Res., submitted, (1984)

[10] Kozinski, A.A., and E.N. Lightfoot, Protein Ultrafiltration: A General Example of Boundary Layer Filtration, A.I.Ch.E. J. 18(5)1030-1040 (1972)

[11] Grutzer, W.B., Spectrophotometric Determination of Protein Concentration in the Short Wavelength Ultraviolet, in "Handbook of Chemistry and Molecular Biology, Physical and Chemical Data", G.D. Fasman ed., Vol. II, p. 197, Cleveland: CRC Press

B.2: SAMARIUM COBALT ($SmCo_5$) MAGNETS

Samarium cobalt ($SmCo_5$) is in the family of fine particle magnets with the following metallurgic composition [60-65 % Cobalt]-[rare earth metal]. The material has an electrical resistivity of 50 -cm at 25 ^{o}C, a magnetic permeability of 1.05 - 1.1, and a density of 8 gm/cm^3. The turntable mounted magnets and the embedded magnets were both made from this material. These $SmCo_5$ magnets, called "crucore-18" magnets, have a high remanent field, 8700 G, high coercivity, 8000 Oe, and high energy product, BH_{max}, 18 MG-Oe.

APPENDIX C: DISPLACEMENT OF AN INFINITE SOLID BY A POINT FORCE

The displacement of an infinite solid by a force acting at a point on that solid is derived in this appendix. The equations that define the displacements were used in the discussion of chapter V to explain the different results obtained from deformation of an EVAc matrix across its entire face, and at just one spot on the face.

Timoshenko [1] has shown that when a force, P, is applied at a point in an infinite solid, the stresses, σ, and strains, ε, in that material can be described in cylindrical coordinates as follows:

$$\sigma_r = \frac{P}{8\pi(1-\upsilon)} \left[(1-2\upsilon)z(r^2 + z^2)^{-3/2} - 3r^2z(r^2 + z^2)^{-5/2} \right] \quad (1)$$

$$\sigma_\theta = \frac{P}{8\pi(1-\upsilon)} \left[(1-2\upsilon)z(r^2 + z^2)^{-3/2} \right] \quad (2)$$

$$\sigma_z = -\frac{P}{8\pi(1-\upsilon)} \left[(1-2\upsilon)z(r^2 + z^2)^{-3/2} + 3z^3(r^2 + z^2)^{-5/2} \right] \quad (3)$$

$$\tau_{rz} = \frac{P}{8\pi(1-\upsilon)} \left[(1-2\upsilon)r(r^2 + z^2)^{-3/2} + 3rz^2(r^2 + z^2)^{-5/2} \right] \quad (4)$$

Since EVAc is a very rubbery material Poisson's ratio, υ, can be taken as being equal to 0.5, and the equations reduce to:

$$\sigma_r = -\frac{P}{4\pi}\left[\, 3r^2 z(r^2 + z^2)^{-5/2} \,\right] \tag{5}$$

$$\sigma_\theta = 0 \tag{6}$$

$$\sigma_z = -\frac{P}{4\pi}\left[\, 3z^3(r^2 + z^2)^{-5/2} \,\right] \tag{7}$$

$$\tau_{rz} = -\frac{P}{4\pi}\left[\, 3rz^2(r^2 + z^2)^{-5/2} \,\right] \tag{8}$$

If we define the strains in terms of the stresses, then,

$$\varepsilon_r = \frac{1}{E}\left[\, \sigma_r - \upsilon(\sigma_\theta + \sigma_z) \,\right] \tag{9}$$

$$\varepsilon_\theta = \frac{1}{E}\left[\, \sigma_\theta - \upsilon(\sigma_r + \sigma_z) \,\right] \tag{10}$$

$$\varepsilon_z = \frac{1}{E}\left[\, \sigma_z - \upsilon(\sigma_r + \sigma_\theta) \,\right] \tag{11}$$

where E is the Young's modulus of the material.

The displacement of a material in a given direction can be derived from these strains, for:

$$u = r\, e_\theta, \text{ and} \tag{12}$$

$$w = \int \varepsilon_z \, d_z \tag{13}$$

Substitution of equations 5, 6, and 7 into equation 10, and combination with equation 12 yields,

$$u = \frac{3\,P\,r^2 z + z^3}{4\,\pi\,(r^2 + z^2)^{-5/2}} \tag{14}$$

The derivation of the displacement in the z direction, w, is more complex, and requires integrating the strain ε_z, in that direction. This strain can be expressed as,

$$\varepsilon_z = \frac{1}{E}\,\frac{P}{4\pi}\left[\, 3r^2 z(r^2 + z^2)^{-5/2} - 3z^3(r^2 + z^2)^{-5/2} \,\right] \tag{15}$$

The solution of this integral is best solved using trignometric substitiutions. Let $z = r \tan\theta$, then

$$z^3 = r^3 \tan^3\theta,$$

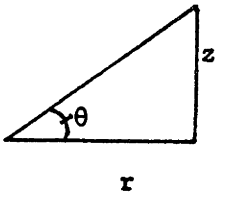

$$r^2 + z^2 = r^2(1 + \tan^2\theta) = r^2 \sec^2\theta, \text{ and}$$

$$dz = r \sec^2\theta \, d\theta.$$

Combining equations 13 and 15 in these terms yields,

$$w = \int \left[\frac{r3 \tan^3\theta \; r \sec^2\theta}{r^5 \sec^5\theta} + \frac{r^4 \tan\theta \sec^2\theta}{r^5 \sec^5\theta} \right] d\theta$$

$$= \int \left[\frac{\tan^3\theta}{r \sec^3\theta} + \sin\theta \cos^2\theta \right] d\theta$$

$$= \frac{\sin\theta (\cos^2\theta + 2)}{3 r} - \frac{\cos^3\theta}{3} \qquad (16)$$

now $\sin\theta = \frac{z}{(r^2 + z^2)^{1/2}}$, and $\cos\theta = \frac{r}{(r^2 + z^2)^{1/2}}$

so equation 16 can be reduced to

$$w = \frac{3P}{4\pi} \frac{r^2 z + z^3}{(r^2 + z^2)^{5/2}} \qquad (17)$$

REFERENCES

[1] Timoshenko, S.P. and J.N. Goodier, "Theory of Elasticity", McGraw-Hill Book Co., New York, 3rd ed., pps. 127-136 (1970)

APPENDIX D: MAGNETIC SKIN DEPTH

Magnetic fields induce circulating surface currents on objects within the field. These currents exclude the field from the object. The strength of the shielding currents increases with increasing frequency. The distinction between high and low frequencies for a given object can be determined from a depth of field penetration or skin depth, δ.

Ohm's law for moving media subjected to an electromagnetic field states that the current density is equal to the electrical conductivity of the media, σ, times the electric field density, E, plus the vector cross product of the velocity of the media and the magnetic field density.

$$\bar{J} = \sigma (\bar{E} + \bar{v} \times \bar{B}) \qquad (1)$$

rearranging (1) to solve for the elecric field density provides

$$\frac{1}{\sigma} \bar{J} - \bar{v} \times \bar{B} = \bar{E} \qquad (2)$$

the curl of this expression is

$$\frac{1}{\sigma} \nabla \times \bar{J} - \nabla \times (\bar{v} \times \bar{B}) = \nabla \times \bar{E} \qquad (3)$$

Equation 3 can be reduced using Faraday's law, $\nabla \times \bar{E} = -\frac{\partial B}{\partial t}$

and Ampere's law, $\bar{J} = \frac{\nabla \times \bar{B}}{\mu}$, such that (3) becomes

$$\frac{1}{\mu\sigma} \nabla \times (\nabla \times \bar{B}) - \nabla \times (\bar{v} \times \bar{B}) = - \frac{\partial B}{\partial t} \qquad (4)$$

the vector identity $\nabla \times (\nabla \times \bar{B}) = \nabla (\nabla \cdot \bar{B}) - \nabla^2 \bar{B}$ can then be used to bring equation 4 to its final form

$$\frac{1}{\mu\sigma} \nabla^2 \bar{B} = \frac{\partial B}{\partial t} \qquad (5)$$

Equation 5 is a diffusion equation, where the diffusion constant D can be expressed as the inverse of $\mu\sigma$. A characteristic diffusion time, τ can be determined.

$$\tau_{mag} \sim \frac{\text{characteristic length}^2}{2/D} = \frac{\delta^2}{2/\mu\sigma} \qquad (6)$$

If the time-varying field is expressed in terms of its frequency of oscillation, ω, equation 6 can be rewritten as

$$\frac{1}{\omega} = \frac{\delta^2 \mu\sigma}{2}$$

or

$$\delta = \sqrt{\frac{2}{\omega\mu\sigma}} \qquad (7)$$

This skin depth determines how far an oscillating magnetic field can penetrate a particular material before being attenuated by the induced surface currents. If the skin depth is on the order of the thichness of the object in the field, the field will be attenuated before it can totally pentrate the object. In the table below some characteristic physical values are given for human skin and arm, and for a slab of ethylene-vinyl acetate copolymer. Skin depths are determined for the frequency range of magnetic fields used in this thesis, and the values compared to typial dimensions of these objects.

	μ $\frac{V\text{-}s}{A\text{-}m}$	σ 1/Ω-m	frequency Hz	skin depth m	thickness m
SKIN	$4\pi \times 10^{-7}$	1	0.5 - 60	710 - 65	0.01
ARM					
EVAc	$4\pi \times 10^{-7}$	10^{-10}	0.5 - 60	7×10^{7} - 6.5×10^{6}	10^{-3}

The skin depths are far greater than the dimensions of a typical limb with an embedded matrix. Thus, the 0.5 to 60 Hz magnetic fields used in this work will penetrate a normal sized human and a slab of EVAc without attenuation.

APPENDIX E: INDUCTION HEATING

The eddy currents induced by the magnetic field not only serve to shield out the field, but also induce heat that is dissipated within surrounding material. This is an important consideration *in vivo*. In this appendix an equation for power dissipation is derived and values computed for a typical human limb and a $SmCo_5$ magnet.

If the limb or magnet are modelled as a long cylindrical shells of radii δ the following analysis can be used to determine the currents induced on these objects by oscillating magnetic fields. This is depicted in figure 1. For an uniform, time-varying applied field $H = i_z H_o \cos \omega t$ one expects an induced electric field as dictated by Farday's equation, which sets up a surface current $K = \delta J$ (1)

This cylindrically symmetrical geometry dictates that the induced field will only possess a θ component., ie. in the direction orthogonal to the field

This current combines with the applied field to establish a net field

$$H = i_z (H_o \cos \omega t + K_\theta(t)) \qquad (2)$$

$$= i_z (H_o \cos \omega t + \delta\sigma E_\theta(t)) \qquad (3)$$

$$\text{if } i_z = i_r \cos \theta - i_\theta \sin \theta \qquad (4)$$

then

$$H = i_\theta (H_o \cos \omega t + \delta\sigma E_\theta(t)) \sin \theta \qquad (5)$$

Faraday's law in integral form

$$\int_c E \cdot n \, dl = -\frac{d}{dt} \int_s B \cdot n \, da \qquad (6)$$

yields,

$$2\pi r E\theta = -\frac{d}{dt} B\pi r^2 \qquad (7)$$

Recognizing that $B = \mu_o H$, and combining equations 5 and 7

$$E_\theta = -\frac{r}{2} \mu \left(\frac{\partial H_o}{\partial t} + \sigma\delta \frac{\partial E_\theta}{\partial t} \right) \qquad (9)$$

If $E_\theta = E_\theta e^{j\omega\tau}$, and $H_o = Re\{H_o\} e^{j\omega\tau}$, then

$$\frac{\partial E_\theta}{\partial t} = j\omega E\theta \quad , \quad \frac{\partial H_o}{\partial t} = j\omega Ho$$

and equation 9 can be written as

$$E_\theta = -\frac{r\mu}{2} \left(j\omega Ho + \sigma\delta j\omega E\theta \right) \qquad (10)$$

rearrangment of terms leads to

$$E_\theta \left(1 + \frac{r}{2} \mu_o \sigma\delta j\omega \right) = -\frac{r}{2} \mu_o j\omega H_o$$

and, since $J = \sigma E$

$$J_\theta = - \frac{r/2 \ \mu o j \omega \sigma \ H_o}{1 + r/2 \ \mu_o \sigma \delta j \omega} \qquad (11)$$

If $A = r/2 \ \sigma \mu \omega$, then

$$J = \frac{-j \ AH_o}{1 + jA\delta} \ \frac{1 - A\delta}{1 + A\delta} = - \frac{A^2 \delta \ H_o - j \ AH_o}{1 + (A\delta)^2}$$

$$J = \frac{A^4 \delta^2 H_o^2 + (AH_o)^2}{1 + (A\delta)^2} = AHo \ \frac{1 + (A\delta)^2}{1 + (A\delta)^2} = \frac{AH_o}{1 + (A\delta)^2}$$

$$J^2 = \frac{(AH_o)^2}{1 + (A\delta)^2} \qquad (12)$$

The power dissipated from this current is

$$\langle P_d \rangle = \frac{1}{2} \int \frac{J^2}{\sigma} dv = \frac{2\pi r \ \delta l}{\sigma} \ \frac{(AH_o)^2}{(1 + A\delta)^2}$$

$$= \pi \ r \delta l \left[\frac{\omega \mu o r}{2} \right]^2 \qquad (13)$$

The power dissipation can be calculated for a typical arm, and even the magnet.

	r m	δ m	l m	μ V s/A-m	σ Ω -m)$^{-1}$	< P_d > watts
magnet	0.003	0.0016	0.0014	1	2×10^{4}	8.3×10^{-15}
arm	0.05	0.1	0.1	$4\pi\times10^{-7}$	1	3.1×10^{-4}

Thus, negligible heat is generated, and little power dissipated by this system.

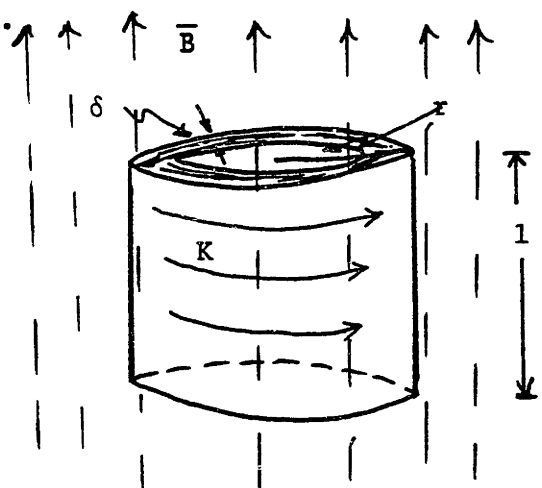

Figure 1: The long thin cylinder is used to approximate a human limb. Surface currents, K, are induced by fields, $\bar{B}$, applied to the cylinder. These surrents shield the cylinder from the fields, in turn.

APPENDIX F: COMPUTER PROGRAMS

NER.FOR	FORTRAN	analyzes kinetics of macromolecule release from EVAc matrices
VOL.FOR	FORTRAN	computes volume of activation for magnet embedded matrices
MJD.FOR	FORTRAN	microscopic model of enhanced release
POUENCH.RPL	RS1	analyzes release kinetics of radiolabelled macromolecule release from EVAc matrices

NER.FOR

```
C PROGRAM NER: POYMER MATRIX-PROTEIN RELEASE ANALYSIS
C  At each point in time this program computes
C RLSMG: amount of BSA released  (mg)
C RMPH:  the arte of BSA release (mg/hr)
C WARAY: the percent of total BSA released during this interval
C TOTAR: the cumulative BSA released at that time (mg)
C TOTWA: the cumulative percent released at that time
C PRPH:  % released per hour in that interval
C  Plotting files can then be generated for x,y data comparison

      CHARACTER INFIL*15,ANFIL*15,yn*1,pltfil*15
      REAL SUM(20),SUMSQ(20),AV(20),SD(20),PCDEV(20),OD(1000)
      REAL DJT(1000),TPS(1000),THLF(1000),ARRAY(25,1000)
      REAL VOL(1000),TOTWA(1000),TOTAR(1000),RLSMG,SUM2(20)
      REAL VAR(20),WEIGH(1000),RR(1000), PLOT(0:6,-2:10)
      LOGICAL out
      DATA TOTAR/1000*0./,TOTWA/1000*0./,RR/1000*1./

      CALL OPENFILE (3,'OLD',' Input file name?     ',INFIL)
      CALL OPENFILE (1,'NEW',' Output file name?    ',ANFIL)
      out=1
      TYPE *,'Would you like a plot file to be generated?'
      READ (5,1) L,yn
1     FORMAT (Q,A1)
      IF (YN. NE .'Y'. AND .YN. NE .'y') GOTO 11
      CALL OPENFILE (2,'new',' Plotting file name? ',pltfil)
      TYPE *,'For the X coord,'
      CALL PARSELECT(psx1,psy1)
      TYPE *,'For the Y coord,'
      CALL PARSELECT(psx2,psy2)
      TYPE *,'O.k.  Will do.'

10    FORMAT (I3)
11    READ (3,10) JTM
      READ (3,10) IPL
      WRITE (1,12) JTM
12    FORMAT (I3,5X,'= # OF TIMEPOINTS')
      WRITE (1,13) IPL
13    FORMAT (I3,5X,'= # OF SAMPLES')
C WRITE #TIME POINTS AND SAMPLE INTO ANALYSIS FILE

      READ (3,70) RAC
70    FORMAT (F8.6)
      WRITE (1,75) RAC
75    FORMAT (F8.6,'= PROTEIN FRACTION OF WT.')

      READ (3,25)
      WRITE (1,15)
15    FORMAT (/,' COEFFICIENT MATRIX')
20    FORMAT (10F8.4)
21    FORMAT (10F8.3)
```

```
      DO 30 L=1,JTM
25      FORMAT (/)
        READ (3,20) (ARRAY (K,L), K=1,IPL)
        WRITE (1,20) (ARRAY (K,L), K=1,IPL)
30    CONTINUE

      READ (3,25)
      WRITE (1,35)
35    FORMAT (/,' WEIGHTS')
      READ (3,20) (weigh(k), k=1,ipl)
      WRITE (1,21) (weigh(k), k=1,ipl)
c     weigh(k) = weigh(k)*1000.
C     WEIGHT ENTERED IN MILLIGMS NOW CONVERTED TO MICROGMS

      READ (3,25)
45    FORMAT (/,' VOL      CUML T  OD WLEN')
      WRITE (1,45)

      DO 60 1=1,jtm
        READ (3,20) vol(1),tps(1),od(1)
        IF (od(1). EQ .0) od(1) = 220
        WRITE (1,21) vol(1),tps(1),od(1)
        thlf(1)=tps(1)**0.5
C     THLF IS THE SQUARE ROOT OF CUMULATIVE TIME
        IF (L-1) 54,54,55
54      djt(1)=tps(1)
C     SET THE FIRST TIMEPERIOD TO THE TIME AT FIRST TIMEPOINT
        GOTO 56
55      djt(1)=tps(1)-tps(1-1)
C     THE TIMEPERIOD IS COMPUTED BY SUBTRACTING PREVIOUS TIMEPT FROM CURRENT
56      CONTINUE
60    CONTINUE

400   DO 4000 jjt=1,jtm

        IF (out) WRITE(1,410) jjt,tps(jjt),djt(jjt),thlf(jjt)
410   FORMAT(/,' TIMEPT#:',I2,' AT:',F7.2,' HRS. ,DURATIONS',F7.2
       1  ' SQRT(CUM.TIME):',F6.2)
        PLOT(0,1) = real(jjt)
        PLOT(0,2) = tps(jjt)
        PLOT(0,3) = thlf(jjt)

        IF (out) WRITE(1,410)
        IF (out) WRITE(1,415)
415   FORMAT(3X,'RLS(MG)',2X,' RR(MG/HR)',2X,' %RLS',4X,'TOT RLS',
       1  3X,'TOT%RLSD',1X,' %RLS/HR')
C **** PUT IN TITLES
C FOR EACH TIMEPOINT ANALYZE DATA & COMPUTE STATISTICS
C INITIALIZE STAT VECTORS
        DO 1000 IN=1,6
          sum(in) = 0.
          sumsq(in) = 0.
1000        CONTINUE
```

```
      ismp = ipl
      jti = jjt-1

      DO 2000 iip=1,ipl
        IF (OD(JJT).EQ.100) rlsmg=array(iip,jjt)*vol(jjt)
C THIS IS FOR NUis CASES SUCH AS IN RADIOACTIVE EXPTS
        IF (OD(JJT).EQ.220) rlsmg=(array(iip,jjt)/11.15)*vol(jjt)
        IF (OD(JJT).EQ.280) rlsmg=(array(iip,jjt)/0.634)*vol(jjt)

C***** COMPUTE ANALYSIS

        IF (rlsmg. EQ .0) ismp = ismp-1

        sum(1) = sum(1) + RLSMG
        sumsq(1) = sumsq(1) + RLSMG*RLSMG

        rmph = RLSMG/djt(jjt)
        sum(2) = sum(2) + rmph
        sumsq(2) = sumsq(2) + rmph*rmph
C rmph is the release rate in mg/hr

        waray = 100.*RLSMG/(weigh(iip)*rac)
        sum(3) = sum(3) + waray
        sumsq(3) = sumsq(3) +waray*waray
C waray is the % of total released this timepoint

        totar(iip) = totar(iip) + RLSMG
        sum(4) = sum(4) + totar(iip)
        sumsq(4) = sumsq(4) + totar(iip)*totar(iip)
C totar is the cumulative amount released in mg

        totwa(iip) = totwa(iip) + waray
        sum(5) = sum(5) + totwa(iip)
        sumsq(5) =sumsq (5) + totwa(iip)*totwa(iip)
C totwa is the cumulative % released

        prph = waray/djt(jjt)
        sum(6) = sum(6) + prph
        sumsq(6) = sumsq(6) + prph*prph
C prph is the % released/hr this timept

        IF (rmph. EQ .0.) rmph = 0.0001

    IF (out) WRITE(1,210) rlsmg,rmph,waray,totar(iip),totwa(iip),prph
210 FORMAT(6F10.4)
        PLOT(1,iip) = rlsmg
        PLOT(2,iip) = rmph
        PLOT(3,iip) = waray
        PLOT(4,iip) = totar(iip)
        PLOT(5,iip) = totwa(iip)
        PLOT(6,iip) = prph

2000       CONTINUE
```

```
      IF (out) WRITE(1,420)
420   FORMAT(/,14X,' AVE:',6X,' SD:',8X,' %AV:')

C ****** COMPUTE STATISTICS
      DO 3000 is=1,6
        IF (ismp. EQ .0) GOTO 3010
        av(is) = sum(is)/ismp
        IF (av(is). EQ .0.) av(is) = 1.0

        sum2(is) = (sum(is)*sum(is))/ismp
        var(is) = (sumsq(is) - sum2(is))/(ismp-1)
        sd(is) = abs(var(is))**0.5

        pcdev(is) = 100.*sd(is)/av(is)
        GOTO 339

3010    av(is) = 0.
        var(is) = 0.
        pcdev(is) = 0.

339     IF (out) WRITE(1,340) is,AV(is),SD(is),PCDEV(is)
340     FORMAT(I4,3X,3F12.4)
        PLOT(is,-2) = AV(is)
        PLOT(is,-1) = SD(is)
        PLOT(is,0)  =  PCDEV(is)

3000       CONTINUE

      IF (yn. NE .'y'. AND .yn. NE .'Y') GOTO 4000
      WRITE(2,*) PLOT(psx1,psy1),',',PLOT(psx2,psy2)

4000     CONTINUE

    CLOSE(3)
    CLOSE(1)
C CLOSE INPUT AND OUTPUT FILES
    IF (yn. NE .'y'. AND .yn. NE .'Y') GOTO 5000
    CLOSE (2)
    TYPE *,'Would you like another plot file generated?'
    READ (5,1) L,yn
    if (yn. NE .'y'. AND .yn. NE .'Y') GOTO 5000
    CALL OPENFILE (2,'new',' Plotting file name? ',pltfil)
    TYPE *,'For the X coord,'
         CALL PARSELECT (psx1,psy1)
    TYPE *,'For the Y coord,'
         CALL PARSELECT (psx2,psy2)
    TYPE *,'O.k.  Will do.'
    out=0
    GOTO 400

5000     WRITE(5,999) ANFIL
999 FORMAT(2X,' ANALYSIS COMPLETED & PLACED IN THE FILE NAMED ',A15)

    END
```

```
      SUBROUTINE OPENFILE (UNT,TYP,QUEST,NAME)
      CHARACTER QUEST*20,TYP*3,NAME*15
      INTEGER UNT

      TYPE 22,QUEST
22    FORMAT (A20)
      READ (5,111) L,NAME
111   FORMAT (Q,A15)

      OPEN (UNIT=UNT,FILE=NAME,TYPE=TYP)
      END

      SUBROUTINE PARSELECT (x,y)
      TYPE *,'0 Time'
      TYPE *,'1 Release (milligrams)'
      TYPE *,'2 Release Rate (mg/hr)'
      TYPE *,'3 % Release'
      TYPE *,'4 Total Released'
      TYPE *,'5 Total % Released'
      TYPE *,'6 % Released/hour'

2     TYPE *,'Please select the number of the parameter.'
      ACCEPT *,x
      IF (x. LT .0.0. OR .x. GT .6.0) GOTO 2
      IF (x. EQ .0.) GOTO 10
      TYPE *,'Sample numbers'
      TYPE *,'-2      Average of samples'
      TYPE *,'-1      Standard Dev. of samples'
      TYPE *,'0 % Average'
      TYPE *,'N Number of particular sample'

4     TYPE *,'Select a number please.'
      ACCEPT *,y
      IF (y. LT .-2.0. OR. y. GT .9.0) GOTO 4
      RETURN

10    TYPE *,'1 Timepoint number'
      TYPE *,'2 Cumulative time'
      TYPE *,'3 Sqrt(Ctime)'
      TYPE *,'Select a number please.'
      ACCEPT *,y
      IF ((y. LT .1.0). OR .(y. GT .3.0)) GOTO 10

      RETURN
      END
```

VOL.FOR

```
C PROGRAM: VOLUME OF ACTIVATION
    CHARACTER OT*15
         REAL r,s,a,b,t
C r radius of cylindrical matrix
C s radius of sphere of activation
C a magnet offset from matrix center
C b magnet distance from matrix bottom
C t theta:orientation of the magnet,
C        with respect to the horizontal

         jp=0
C jp is the number of the polymer matrix now being considered

   10    n=0
         i=356278579          ! i is the random number generator seed

         TYPE *,'Enter r,s,a,b,t'
    READ (5,20) r,s,a,b,t
   20    FORMAT (5F10.4)

        DO 100 j=1,160000
             x=ran(i)
             y=ran(i)
            z=ran(i)
C center at .5,.5, 2s is the diameter
             IF(z. GT .(2*s-b+.5)) GOTO 100
C above cylinder top
            IF(z. LT .(.5-b)) GOTO 100
C below cylinder bottom
            IF(SQRT((x-.5+a)**2+(y-.5)**2). GT .r) GOTO 100
C outside cylinder radius
            IF(SQRT((x-.5)**2+(y-.5)**2+(z-.5)**2). GT .s) GOTO 100
C outside sphere radius
            n=n+1
C update point counter if the point was within the sphere and the matrix
  100    CONTINUE

        v=(FLOAT(n)/160000.)*COSD(t)
C v is the volume of magnet activation
C and since the imaginary box surrounding the matrix is
C of unit dimensions the volume is simply the fraction of points
C generated that fell within the intersection of the sphere and the
cylinder
C cos(t) takes into account attenuation of the applied field
C with magnet orientation

         jp=jp+1    ! update the matrix counter
         TYPE *,jp,v
         GOTO 10 ! start again for another polymer matrix
    END
```

MJD.FOR

```
C  Harris and Goren enhanced release model
C  J Bessel Function

     CHARACTER FIL*15
         REAL ZERO,ONE
          COMPLEX ALP,ALR,AP,AR,BETA,BJ,BT,j
          COMPLEX RAT,RATIO,RD1,RD2,RD,RN1,RN2,RN,RNM

     CALL OPENFILE (1,'NEW',' Output file name?     ',FIL)

  5       TYPE *,'Enter maximum bead displacement, pore radius(microns),
     1   and number of iterations (all as integers):'
          READ(5,13) IAMP,IPORE,II
          WRITE(1,13) IAMP,IPORE,II

          D  = 6.1 * 10.**-7
C  diffusivity of substance (cm2/sec)

          FKV= 1.013*.01
C  fluid kinematic viscosity = viscosity(gm/cm-sec)/density(g/cc)
C  density = 1.00287 g/cc
          Sc = FKV / D
C  Schmidt number = FKV/D

          ZERO = 0.0
          ONE  = 1.0

11   FORMAT(2I10)
12   FORMAT(F10.5)
13   FORMAT(3I10)
14   FORMAT(2F10.5)

          DO 200 I = 1,4
               IF (I. eq. 1) FR = 5.0
               IF (I. eq. 2) FR = 6.67
               IF (I. eq. 3) FR = 9.5
               IF (I. eq. 4) FR = 11.0
               IF (I. eq. 5) FR = 60.0
               OMEGA = 2. * 3.14159265 * FR

          N=0
          SUM=0.
```

```
    DO 100 IP = 1,IPORE
              Rp=IP*10.**-4
            DO 100 IA=1,IAMP,II
              Dp=IA*10.**-4
C Convert to cm

              Aa=Dp/Rp
C  dimensionless amplitude factor

              Re = omega*Rp*Rp/FKV
C  Re is an oscillating Reynolds number
              Pe = omega*Rp*Rp/D
C  Pe is the Peclet number=Reynolds number * Schmidt number

              AP   = CMPLX(0.,-Re)
              ALP  = CSQRT(AP)
              AR   = CMPLX(0.,Re)
              ALR  = CSQRT(AR)
              BT   = CMPLX(0.,-Pe)
              BETA = CSQRT(BT)

              CALL BESER(ZERO,BETA,BJ)
              RN1 = 4. * BJ
              CALL BESER(ONE,BETA,BJ)
              RN1 = RN1 / (BETA * BJ)
              REALR = REAL(RN1)+1.
              ANSW  = (REALR*Aa*Aa) + 1.

              SUM = SUM + ANSW
              N= N+1
100 CONTINUE

         AVE = SUM /N
         TYPE *,FR,AVE
         WRITE (1,14) FR,AVE
200 CONTINUE

         GOTO 5

    END
```

```
      SUBROUTINE OPENFILE (UNT,TYP,QUEST,NAME)
      CHARACTER QUEST*20,TYP*3,NAME*15
      INTEGER UNT

      TYPE 21,QUEST
21    FORMAT (A20)
      READ (5,22) L,NAME
22    FORMAT (Q,A15)

      OPEN (UNIT=UNT,FILE=NAME,TYPE=TYP)

           RETURN
      END

C  J Bessel Function of order ORD on argument ARG
      SUBROUTINE BESER (ORD,ARG,BJ)
           COMPLEX ARG,BJ,TERM,TER1,TER2
           REAL K,ORD

           RKF  = 1.
           RKPF = 1.
C  set first term of the expansion
           IF (ORD. LT .0.5) BJ  = CMPLX(1.,0.)
           IF (ORD. GT .0.5) BJ  = ARG/2.

C 21 terms in the expansion
           DO 333 KJ = 1,20
                K = REAL(KJ)
                RKF  = K * RKF
                RKPF = (K + ORD) * RKPF
                TER1 = (-1.)**KJ
                TER2 = (ARG/2.)**(2.*K+ORD)
                TERM = (TER1 * TER2) / (RKF*RKPF)
C               TERM = (((-1.)**K) * (ARG/2.)**(2.*K + ORD)) / (RKF * RKPF)
                BJ   = BJ + TERM
 333       CONTINUE

          RETURN
           END
```

PQUENCH.RPL

```
procedure;

/* This RS1 programming language procedure computes the ng released of a
radioactivally labelled substance.  The quench curve is determined if
desired and the ESR stored with the cpms and ng released in one table */

    IF YESANSWER("Do you want to keep the old quench curve?")
         THEN GOTO LA;

    DELETE GRAPH 'GQUENCH';

    DTE = GETDATE('Enter the date of the test',FALSE,'21-AUG-79');
    ET = DTE - '21-AUG-79';
    ETY = ET/356;
/* ETY IS THE TIME(in years) ELAPSED SINCE AUGUST 21, 1979 */
    TYPE ETY,' years have elapsed since the standards were set';
    THLF = .693*ETY/12.35;
    ATTEN = 91000 * EXP(-THLF);

    DIS TQUENCH;
    SET COL 2 OF TQUENCH TO COL 2/ATTEN;
/* COL 0 of TQUENCH contains the vial labels
   COL 1             ESRs
   COL 2             CPMs
   COL 2 will then be replaced with the EFFICIENCY*/

    'TQUENCH'[0,2] = 'eff';
    DIS TQUENCH;

    MAKE GRAPH 'GQUENCH' FROM TABLE 'TQUENCH';
    CALL PUBLIC $FITLINE('GQUENCH',1);
/* Fit a line to the esr-efficiency graph */
```

```
LA: SLOPE = GETNUMBER("Enter the slope:");
    INTERCEPT = GETNUMBER("Enter the intercept:");
    T = GETTABLE("Enter the name of the table that contains the data:");

    IF YESANSWER('Do you want to enter the backround?',TRUE)
         THEN DO;
              BKRND = GETNUMBER('Enter the background CPMs:');
              SET COL 1 OF TABLE(T) TO COL 1 - BKRND;
              END;
         ELSE SET COL 1 OF TABLE(T) TO COL 1-ROW 1 of COL 1 of table(T);
/* SUBTRACT THE BACKROUND FROM THE CPMS  */

    SET COL 3 OF TABLE(T) TO COL 1 OF TABLE(T)/
                        (INTERCEPT+(COL 2 OF TABLE(T)*SLOPE));
/* DETERMINE THE DPMs   */
    SET COL 1 OF TABLE(T) TO COL 3 OF TABLE(T);
    SET COL 1 OF ROW 0 OF TABLE(T) TO 'DPM';

    SPA = GETNUMBER('Enter specific activity:',FALSE,'2E7');
    SET COL 3 OF TABLE(T) TO COL 1*1E6/SPA;
    SET COL 3 OF ROW 0 OF TABLE(T) TO 'ng ';
    SET FORMAT OF COL 1 OF TABLE(T) TO 'G(8,2)';
    SET FORMAT OF COL 3 OF TABLE(T) TO 'G(8,2)';
    DIS TABLE(T);

/* COL 0 OF T contains the TIMEs
   COL 1              CPMs (will be deleted & replaced with the DPMs)
   COL 2              ESRs
   COL 3       will contain the ng released*/

end;
```

APPENDIX G: EXPERIMENTAL DATA

Hall effect measured B field

Input Voltage (Volts)	Surface Field (Gauss)
140.00	650
128.80	600
120.00	550
119.00	550
110.60	500
109.20	500
100.80	450
98.00	450
90.00	400

Distance from Surface (cm)	Magnetic Field (Gauss)
0	650
2.5	600
5.0	550
7.5	500
10.0	450
12.5	400
15.0	350
17.5	325
20.0	300
25.0	250
27.5	225
30.0	210

See section II.2.2

Extent of Modulation from Controls

T hrs	MG no	sem	NM no	sem	NM yes	sem
24	0.65	0.014	0.60	0.028	0.93	0.269
48	0.86	0.042	0.77	0.042	0.88	0.141
72	1.15	0.035	1.07	0.049	0.95	0.085
96	1.02	0.042	1.14	0.049	1.13	0.191
120	1.02	0.014	1.20	0.163	1.10	0.148
144	1.08	0.014	1.11	0.106	1.04	0.092
168	1.01	0.014	0.91	0.042	1.11	0.184
172	0.89	0.014	0.81	0.078	1.08	0.064
196	0.98	0.085	0.94	0.014	1.06	0.057

MG = 1.4 mm magnetic spheres embedded in EVAc-BSA(33%) matrices
NM = 1.4 mm nonmagnetic spheres embedded in the matrices

no = no applied field, modulation simply ratio of release rates over successive periods of time
yes = 1800 G, 9.5 Hz magnetic field applied for 6 hours, and release rates in this time compared to adjacent 6 hour periods of rest

sem = standard error about the mean

Experiments described in section II.3.2

NO FIELD APPLIED	Cumulative Percent Release	
TIME (hours)	no spheres (n=6)	embedded spheres (n=6)
6	0.70	1.05
24	2.54	3.28
30	3.15	3.95
48	5.26	6.04
51	5.93	6.74
54	6.57	7.36
120	13.11	14.02
123	13.67	14.64
126	14.31	15.29
144	16.13	16.66
150	16.81	17.23
168	18.54	18.43
173	19.09	18.90
192	20.88	20.46
198	21.37	21.07
216	22.81	22.48
222	23.37	23.07
312	31.29	29.46
318	31.96	30.16
336	33.22	31.42
342	33.85	31.93
360	35.20	33.24
366	35.71	33.86
384	36.97	35.10
390	37.40	35.54
480	42.26	40.31
487	42.89	40.91
558	45.31	43.19
564	45.79	43.71
654	50.56	48.03
661	51.12	48.56
732	53.18	50.56
739	53.57	50.89
780	55.55	52.93
786	55.88	53.29
876	57.65	56.44
900	58.61	57.52
924	59.61	58.61
948	60.53	59.54
1010	62.75	61.76
1034	63.59	62.72
1058	64.41	63.56
1106	65.61	64.86
1181	67.51	66.81
1205	68.26	67.63
1229	68.98	68.42
1253	69.67	69.02

Data from experiments described in section II.2.5

Release Rates (ng/hour) (average ± standard error)

TIME (hours)	5 Hz	6.67 Hz	9.5 Hz	11 Hz
63.92	10.00 ± 0.61	18.40 ± 0.05	9.80 ± 0.46	9.80 ± 0.23
65.92	15.70 ± 1.50	12.80 ± 0.24	55.40 ± 4.34	38.50 ± 3.41
87.08	8.60 ± 0.88	8.10 ± 1.11	12.00 ± 0.95	12.10 ± 0.54
89.08	12.40 ± 0.58	10.70 ± 0.01	37.70 ± 0.85	44.10 ± 1.77
177.08	6.20 ± 0.36	5.60 ± 0.58	6.20 ± 0.30	5.60 ± 0.37
179.08	13.50 ± 1.00	10.80 ± 0.69	33.40 ± 4.18	42.85 ± 1.92
200.58	5.00 ± 0.26	5.00 ± 1.01	6.80 ± 0.90	8.70 ± 0.73
202.58	10.00 ± 0.48	13.90 ± 1.40	32.70 ± 2.09	37.10 ± 4.94
224.58	4.80 ± 0.28	5.30 ± 0.80	6.10 ± 0.82	7.40 ± 0.72
226.08	11.50 ± 0.96	29.80 ± 2.48	29.90 ± 3.46	32.00 ± 3.29
248.08	4.30 ± 0.37	4.90 ± 0.76	5.70 ± 0.13	8.10 ± 0.15
250.08	11.00 ± 1.01	16.50 ± 1.52	28.10 ± 3.28	34.10 ± 2.94
338.16	7.20 ± 0.04	7.10 ± 0.05	7.10 ± 0.06	7.10 ± 0.06
340.16	28.00 ± 1.21	32.30 ± 0.65	30.00 ± 2.17	41.00 ± 2.19
362.16	4.60 ± 0.36	5.50 ± 0.25	5.70 ± 0.35	6.50 ± 0.37
364.16	23.40 ± 0.54	17.50 ± 1.61	22.40 ± 1.41	28.30 ± 2.32
386.16	12.40 ± 1.11	5.30 ± 0.19	6.00 ± 0.24	4.90 ± 0.32
388.16	25.20 ± 1.17	18.70 ± 1.11	26.00 ± 1.52	25.00 ± 1.89
410.16	8.60 ± 0.52	5.30 ± 0.21	6.40 ± 0.35	5.80 ± 0.33
412.16	23.10 ± 1.01	22.60 ± 1.27	26.10 ± 1.33	25.30 ± 1.24

Data corresponds to experiments described in section III.3.5

Extent of Modulation (average ± standard error)

TIME (hours)	5 Hz	6.67 Hz	9.5 Hz	11 Hz
63.92	1.00 ± 0.061	1.00 ± 0.003	1.00 ± 0.047	1.00 ± 0.024
65.92	1.57 ± 0.160	1.58 ± 0.030	5.66 ± 0.289	3.85 ± 0.349
87.08	1.70 ± 0.155	1.45 ± 0.198	5.10 ± 0.315	3.53 ± 0.379
89.08	1.42 ± 0.089	1.56 ± 0.002	3.93 ± 0.223	4.09 ± 0.672
177.08	1.52 ± 0.176	1.92 ± 0.200	4.17 ± 0.215	5.76 ± 0.685
179.08	1.79 ± 0.155	2.04 ± 0.130	5.79 ± 0.573	9.03 ± 0.889
200.58	2.40 ± 0.101	2.47 ± 0.499	5.24 ± 0.825	7.08 ± 0.887
202.58	2.40 ± 0.115	2.91 ± 0.204	5.20 ± 0.983	5.44 ± 0.552
224.58	2.10 ± 0.023	2.76 ± 0.193	5.36 ± 0.878	5.08 ± 0.276
226.08	2.30 ± 0.123	2.49 ± 0.177	5.51 ± 1.079	5.60 ± 0.341
248.08	2.50 ± 0.108	2.43 ± 0.146	5.21 ± 0.821	5.78 ± 0.477
250.08	2.53 ± 0.059	3.00 ± 0.187	5.10 ± 0.631	5.81 ± 0.536
338.16	1.90 ± 0.122	3.44 ± 0.022	4.38 ± 0.521	4.76 ± 0.280
340.16	2.70 ± 0.136	5.13 ± 0.699	4.07 ± 0.355	5.39 ± 0.578
362.16	4.77 ± 0.173	4.31 ± 0.704	4.74 ± 0.456	6.10 ± 0.299
364.16	2.76 ± 0.064	4.02 ± 0.382	4.72 ± 0.428	6.00 ± 0.368
386.16	1.96 ± 0.175	3.21 ± 0.191	3.85 ± 0.210	6.78 ± 0.710
388.16	2.40 ± 0.111	3.40 ± 0.194	4.07 ± 0.251	6.18 ± 0.860
410.16	2.81 ± 0.171	3.55 ± 0.294	4.28 ± 0.339	5.95 ± 0.396
412.16	2.69 ± 0.118	3.95 ± 0.285	4.16 ± 0.333	4.53 ± 0.344

Data corresponds to experiments described in section III.3.5

MODULATION vs FIELD AMPLITUDE

G vitro	vitro o	vitro p	G vivo	vivo o	vivo p
230	2.5	1.82	495	1.80	2.34
240	3.0	2.12	516	3.90	3.52
295	3.6	3.77	523	3.84	3.91
310	4.0	4.22	530	5.20	4.31
325	4.8	4.67	537	4.38	4.70
370	5.1	6.02	570	6.44	6.56
390	7.4	6.62	575	6.75	6.84
440	7.8	8.12	590	7.34	7.69
550	10.5	11.42	600	8.52	8.25
650	16.0	14.42			

G = Field Amplitude (Gauss)
vitro = in vitro vivo = in vivo
o = observed
p = predicted from linear regression to data

Data corresponds to experiments described in sections III.3.4 and VIII.3.3

MAGNETIC SPHERE PROTRUSION FROM MATRIX SURFACE

PROTRUSION (mm)	MODULATION
1.70	1.30
1.78	1.60
1.86	1.64
1.87	1.78
1.91	1.91
1.95	2.05
1.99	3.29
2.00	7.14
2.01	11.00

Data corresponds to the experiment described in section IV.2.1.ii

Cumulative Percent Release (mg) (average ± standard error)

Time (hours)	control (n=8)	sem	experimental (n=10)	sem
40.13	37.755	5.405	40.055	3.765
47.13	42.720	1.425	60.810	9.485
64.13	49.390	1.490	77.300	0.690
71.13	49.610	0.170	78.070	0.600
138.38	50.695	0.285	79.300	0.030
145.71	51.150	0.355	80.370	0.040
145.71	51.980	0.040	81.190	0.060
160.12	52.715	0.015	82.210	0.150
167.12	53.550	0.065	83.100	0.000
184.12	54.280	0.010	84.005	0.005
189.12	55.155	0.055	84.850	0.055
208.12	55.560	0.245	85.578	0.098
215.12	56.245	0.025	86.243	0.035
232.12	56.670	0.305	87.145	0.118
239.12	57.750	0.270	88.385	0.060
304.12	58.100	0.250	89.270	0.085
311.12	58.350	0.050	90.835	0.605
328.12	58.485	0.035	91.860	0.325
335.12	58.820	0.135	93.400	0.690
352.12	58.980	0.030	93.560	0.010
376.12	59.340	0.000	93.850	0.170
383.12	59.480	0.030	94.120	0.040
400.12	59.795	0.055	94.610	0.030
407.12	59.915	0.020	94.900	0.020
472.12	61.065	0.160	95.970	0.520
479.12	61.240	0.015	96.390	0.060
496.12	61.580	0.040	96.680	0.140
503.12	61.735	0.015	97.010	0.030
520.12	62.060	0.025	97.295	0.135
527.12	62.170	0.010	97.590	0.035
544.12	62.495	0.015	97.815	0.125
551.12			97.950	0.015
568.12			98.075	0.085
575.12			98.240	0.005
640.12			98.625	0.225
647.12			98.845	0.030
664.12			98.880	0.015
671.12			99.005	0.005
688.12			99.075	0.000
695.12			99.195	0.010

control group not subjected to any magnetic fields
experimental group subjected to 1800 G, 11 Hz fields
data corresponds to experiments described in section IV.2.2.ii

MAGNET #	DIST FROM CENTER(cm)	DIST FROM BOTTOM(cm)	ANGLE(deg)	ADJUSTED VOLUME(ccx100)	OBSERVED MODULATION
CYLINDERS					
1	0.06	0.20	89	0.08	4.25
2	0.01	0.21	31	4.32	8.62
3	0.03	0.21	23	4.50	9.19
7	0.06	0.29	14	4.24	7.19
9	0.05	0.36	16	3.60	5.04
TORROIDS					
4	0.07	0.30	28	9.14	5.98
5	0.01	0.22	18	10.19	9.09
6	0.04	0.25	8	10.56	6.64
10	0.02	0.22	2	10.59	11.25
12	0.04	0.25	5	10.62	11.39

Data corresponds to experiments conducted in section IV.2.3.i

EXTENT of MODULATION

D_s = 50 microns
F_d^s = 60 Hz

D_d (microns)	MATRIX VOLUME (mm^3) 123	209	604
25	2.81		7.13
50	7.15	16.00	17.30
75	14.50	23.75	36.50
100	34.00	41.30	99.70

D_s = 50 microns
D_d^s = 75 microns

Frequency (Hz)	DEFORMATION PLANE	POINT
5	8.70	4.02
10	15.35	
15		6.00
30	21.70	6.45
45		7.53
60	21.90	8.05

D_s = Satic Displacement
D_d^s = Dynamic Displacement
F_d^d = Frequency of Dynamic Dispalcement

Experiments described in section V.2

MICROSCOPIC MODEL - chapter VI

PREDICTED MODULATION vs FREQUENCY (Hz) & RADIUS (u)

channel radii (u)	FREQUENCY (Hz) 5.00	6.67	9.50	11.00	15.00	30.00	45.00	60.00
1	1.21	1.37	1.74	2.00	2.84	8.14	16.29	26.44
1 - 3	1.91	2.54	3.84	4.61	6.75	14.54	21.33	27.42
1 - 5	2.65	3.49	4.91	5.62	7.42	13.01	17.49	21.39
1 - 7	2.99	3.76	4.94	5.52	6.92	11.12	14.42	
1 - 9	3.05	3.73	4.68	5.15				
1 - 11	2.99	3.55	4.37	4.77				
1 - 13	2.89	3.37	4.08	4.42				
1 - 15	2.77	3.20	3.83	4.12				
1 - 17	2.66	3.04	3.60					

164,000 dpm [^{3}H]-inulin injected at 45 minutes

time (minutes)	ng/min	Fraction Left
15	15.65	99.80
30	10.96	99.65
45	96.14	98.39
60	31.86	97.98
75	853.96	86.81
90	1002.43	73.70
105	938.72	61.42
120	900.40	49.64
135	417.00	44.19
150	371.53	39.33
165	384.97	34.29
180	262.10	30.87
195	282.36	27.17
210	176.98	24.86
225	152.68	22.86
240	165.72	20.69
255	159.33	18.61
270	75.75	17.62
285	108.59	16.20
300	112.84	14.72
315	95.13	13.48
330	84.20	12.38
345	85.86	11.26

Data corresponds to the experiment described in section VIII.3.1

DYNAMIC MODULUS EXPERIMENTS (Appendix A)

SLAB of 100% EVAc - no BSA: COMPRESSION

Frequency (Hz)	delta	E'(Pa)	E''(Pa)
1.25	0.16360	3181000	520000
1.58	0.16650	3238000	539000
1.99	0.17170	3230000	571000
2.51	0.17050	3340000	569700
3.16	0.16480	3460000	570000
3.98	0.16660	3580000	595000
5.01	0.17300	3618000	630000
6.30	0.17980	3740000	670000
7.94	0.17420	3814000	664000
10.00	0.18880	3936000	743000
12.58	0.18790	4088000	768000
15.84	0.18400	4182000	769000
19.95	0.18400	4289000	790000
25.11	0.18300	4390000	804000
31.62	0.16370	4570000	748000
39.81	0.18780	4790000	900000
50.11	0.18498	4810000	890000
63.09	0.26950	5417000	1460000
79.43	0.19410	5193000	1008000
99.00	0.18930	5664000	1070000
99.99	0.17090	5630000	9626000

DYNAMIC MODULUS EXPERIMENTS (Appendix A)

EVAc-BSA(30%) : TENSION

Frequency (Hz)	delta	E'(Pa)	E''(Pa)
1.00	0.1844	325400	60000
1.25	0.2035	333600	67900
1.58	0.1590	346340	55200
1.99	0.1980	352400	69900
2.51	0.1960	352300	69080
3.16	0.1905	370300	70500
3.98	0.1638	335900	55000
5.01	0.1836	368750	67700
6.30	0.1966	388000	76400
7.94	0.1856	388900	72200
10.00	0.1817	391600	71200
12.58	0.2030	401400	81400
15.84	0.1800	412500	74300
19.95	0.2090	423000	88500
25.11	0.1840	414000	81300
31.62	0.1134	410000	46500
39.81	0.1760	365000	64100
50.11	0.1880	330000	62300
63.09	-2.2400	390000	
79.43	0.1280	509000	65300
99.00	0.3060	494000	151000
99.99	0.2200	522000	115000

DYNAMIC MODULUS EXPERIMENTS (Appendix A)

EVAc-BSA(30%) : COMPRESSION

Frequency (Hz)	delta	E'(Pa)	E''(Pa)
1.00	0.280000	137000	38870
1.25	0.276000	140600	38850
1.58	0.270000	143900	38870
1.99	0.265970	151800	40370
2.51	0.264700	155000	41090
3.16	0.272000	161600	43900
3.98	0.264000	170000	44900
5.01	0.244660	167700	41000
6.30	0.244280	172500	42100
7.94	0.241400	177700	42900
10.00	0.238750	182770	43640
12.58	0.239500	187500	44900
15.84	0.229800	193600	44500
19.95	0.227800	204200	46500
25.11	0.000482	228400	
31.62	0.300000	161300	48550
39.81	0.192500	153500	29550
50.11	0.246760	141900	35000
63.09	0.680000	122400	83400
79.43	0.364400	161300	58800
99.00	0.543600	116500	63350